Characterizing the dual role of Headcase in hemocyte progenitor maintenance in *Drosophila melanogaster*

Ph.D. Dissertation

Bayan Kharrat

Supervisor: Viktor Honti, Ph.D.

Doctoral School of Biology

University of Szeged, Faculty of Science and Informatics

Drosophila Blood Cell Differentiation Group,

Institute of Genetics,

HUN-REN Biological Research Centre, Szeged

Szeged, 2024

Table of contents

List of abbreviations

4EBP: Eukaryotic translation initiation factor 4E binding protein

Adgf-A: Adenosine deaminase-related growth factor A

AGM: aorta-gonad-mesonephros

AML: acute myeloid leukemia

AMPs: antimicrobial peptides

Antp: Antennapedia

AP-2a: Adaptor protein complex 2, alpha subunit

Bc: Black cells

BDSC: Bloomington *Drosophila* Stock Center

BiFC: bimolecular fluorescence complementation

BMP: Bone morphogenetic protein

Bnl: Branchless

BR: brain

Bsk: Basket

Cam: Calmodulin

Cat: Catalase

CC: crystal cell

CCT1: Chaperonin containing TCP1 subunit 1

cDNA: Complementary DNA

CHIZ: Combined Hematopoietic Intermediate Zone

CNS: central nervous system

Col: Collier

CxD: Crossover Suppressor Dichaete

CyO: *Curly of Oster*

CZ: cortical zone

Dad: Daughters against dpp

DAPI: 4′,6-Diamidino-2-Phenylindole, Dihydrochloride

DILPs: *Drosophila* insulin-like peptides

Dlp: Dally-like protein

DN: dominant-negative

DNA: deoxyribonucleic acid

Dome: Domeless

Dpp: Decapentaplegic

DSHB: Developmental Studies Hybridoma Bank

DsRed: Discosoma sp. red fluorescent protein

DTT: Dithiothreitol

DV: dorsal vessel

E-cad: E-cadherin

ECM: extracellular matrix

EGFR: Epidermal Growth Factor Receptor

eIF5B: eukaryotic Translation Initiation Factor 5B

eRF3: eukaryotic Translation Release Factor 3

FBS: fetal bovine serum

FGF: Fibroblast Growth Factor

Foxo: Forkhead box O

GABA: Gamma-Aminobutyric Acid

GATA-: GATA-binding factor-

Gcm: Glial cells missing

GFP: green fluorescent protein

GST: Glutathione S-Transferase

HA: Hemagglutinin

Hdc: Headcase

HECA: Headcase protein homolog

Hh: Hedgehog

His: Histidine

Hml: Hemolectin

Hnt: Hindsight

hpi: hours post infestation

HRP: Horseradish Peroxidase

HSC: hematopoietic stem cell

Hsc70-4: Heat shock protein cognate 4

IMD: immune deficiency pathway

IVTT: in vitro transcription-translation

IZ: intermediate zone

JAK/STAT: Janus Kinase/Signal Transducer and Activator of Transcription

JNK: Jun N-Terminal Kinase

kDa: kilodalton

Kr: Kruppel

L1: Atilla

LC-MS/MS: Liquid chromatography-tandem mass spectrometry

Lz: Lozenge

MFI: mean fluorescence intensity

MPP: multipotent progenitor

Msn: Misshapen

mTOR: mammalian target of rapamycin

mTORC1: mTOR complex 1

Myc: Master Regulator of Cell Cycle Entry and Proliferative Metabolism

MZ: medullary zone

N: Notch

N-cad: Neural cadherin

NimC1: Nimrod C1

ns: non-significant

PBS: Phosphate-Buffered Saline

PDGF: platelet-derived growth factor

PFA: paraformaldehyde

Pi3K: Phosphatidylinositol 3-kinase 92E

PIP2: Phosphatidylinositol 4,5-bisphosphate

PIP3: Phosphatidylinositol (3,4,5)-trisphosphate

PL: plasmatocyte

PL: plasmatocyte

PMSF: phenylmethylsulfonyl fluoride

pNPP: para-Nitrophenylphosphate

PNS: peripheral nervous system

PO: Phenoloxidase

PPO: Prophenoloxidase

PSC: posterior signaling center

Ptc: Patched

Pten: Phosphatase and tensin homolog

PTU: N-Phenylthiourea

Pvf: PDGF- and VEGF-related factor

Pvr: PDGF- and VEGF-receptor related

Pxn: Peroxidasin

Rheb: Ras homolog enriched in brain

RNAi: ribonucleic acid interference

Robo: Roundabout

ROS: reactive oxygen species

RP-HPLC: reversed-phase high performance liquid chromatography

Rpn11: Regulatory particle non-ATPase 11

RUNX: Runt-related transcription factor

S2R+: Schneider S2 cells

S6k: Ribosomal protein S6 kinase

Sb: *Stubble*

Sco: Scutoid

SDS-PAGE: sodium dodecyl-sulfate polyacrylamide gel electrophoresis

Ser: Serrate

Shh: Sonic hedgehog

Sli: Slit

SM6b: S*econd Multiple 6b*

Sp: Sternopleural

Spi: Spitz

Srp: Serpent

Stat92E: Signal-transducer and activator of transcription protein at 92E

Tb: *Tubby*

Tep4: Thioester-containing protein 4

TGF-β: Transforming Growth Factor-β

Tkv: Thickveins

TM3: *Third Multiple 3*

TM6: *Third Multiple 6*

Tsc1/2: Tuberous sclerosis complex 1/2

UAS: Upstream Activating Sequence

Unk: Unkempt

Upd: Unpaired

UTR: Untranslated Region

v: *vermilion*

VDRC: Vienna Drosophila Resource Center

VEGF: vascular endothelial growth factor

Wg: Wingless

Wnt: Wingless-related integration site

y: *yellow*

YFP: yellow fluorescent protein

Zpg: Zero population growth

β-PS integrin: β subunit of the integrin dimer

1. Introduction

1.1. *Drosophila melanogaster* as a model for hematopoiesis

According to evolutionists, blood cells most probably appeared first in choanoflagellates, the unicellular ancestors of animals (Nagahata et al. 2022). Phagocytes are the earliest blood cells to appear in evolution as they can be observed in diploblastic sponges, in which their role is to collect nutrients and distribute them to the rest of the animal (De Sutter & Buscema 1977; De Sutter & Van De Vyver 1977). Since then, phagocytes have evolved in a monophyletic way while adapting to the needs of each evolutionary group. For example, in higher animals, phagocytes do not play a role in nutrition, but they have evolved to identify and phagocyte foreign pathogens and apoptotic cells (Millar & Ratcliffe 1989).

Other types of differentiated blood cells are first observed with the evolution of pseudocoelom in pseudocoelomate animals like flatworms, and more significant diversification is seen in triploblastic coelomates like annelids or segmented worms, in which red blood cells that transfer oxygen, and leukocytes that function as immune cells capable of differentiating self from non-self are observed (Cooper 1976; Vetvicka & Sima 2009). According to our current knowledge, all invertebrates including *Drosophila* contain only the myeloid lineage, the players of the innate immune system that respond in a fast and effective but not very specific way (Williams 2007). However, in addition to that, vertebrates contain the lymphoid lineage, providing an adaptive immune system that is capable of an advanced antigen-specific response. These two systems cooperate and affect each other in vertebrates, for this reason using *Drosophila* as a model for investigating hematopoiesis (the process of blood cell formation) provides an opportunity to study the innate immune cells without the modulating effect of adaptive immune cells (Hoebe et al. 2004).

Many parallels can be observed between *Drosophila* and mammalian hematopoiesis. For example, in both systems, hematopoiesis occurs in two waves, a primitive and a definitive one (Holz et al. 2003; Jagannathan-Bogdan & Zon 2013). The mammalian primitive wave takes place in the early embryonic stages, in which erythrocytes and macrophages are produced from erythroid progenitors in the yolk sac. These cells are transitory, and they are not able to replicate, and their main function is to help in delivering oxygen efficiently to all cells of the rapidly growing embryo (Orkin & Zon 2008). The definitive wave occurs later when hematopoietic stem cells (HSCs) are formed in the

aorta-gonad-mesonephros (AGM) cells of the embryo, and they differentiate to give all blood cell types in the organism. Although HSCs arise in the embryo, they later move to the fetal liver and spleen, then to the bone marrow, which becomes the only location for HSCs after birth (Cumano & Godin 2007). In *Drosophila*, the first embryonic wave occurs in the head mesoderm and produces hemocytes (the blood cells of *Drosophila*) that occupy the circulation and sessile compartment in the embryo, larval stages, and adulthood (Tepass et al. 1994; Holz et al. 2003; Honti et al. 2010; Ghosh et al. 2015). The second hematopoietic wave starts in the dorsal mesoderm and yields the dorsal vessel (the heart–aorta that controls the hemolymph flow) and the lymph gland (the larval hematopoietic organ) (Rugendorff et al. 1994).

Another similarity between the two systems is the presence of hematopoietic compartments populated by blood cells arising from precursor cells and supplying the animal with hemocytes according to its needs (Lanot et al. 2001; Jagannathan-Bogdan & Zon 2013). This process is tightly controlled by a complex network of signaling pathways that is highly conserved between *Drosophila* and mammals, and in which any fault can lead to blood cell disorders or cancers (Smith 1990; Y. Tokusumi et al. 2012).

All the shared characteristics listed above, in addition to the presence of a wide variety of tools that allows the manipulation of any gene of interest, and the availability of antibodies and transgenic reporters that enables the monitoring of blood cell development and differentiation, make *Drosophila* an excellent model for hematopoietic research (Goto et al. 2003; Kurucz et al. 2007; Honti et al. 2009; T. Tokusumi, Shoue, et al. 2009; Anderl et al. 2016).

1.2. Hematopoiesis in the *Drosophila* embryo

One of the first and most important regulators of the first hematopoietic wave in the *Drosophila* embryo is Serpent (Srp) (Abel et al. 1993; Sam et al. 1996; Brückner et al. 2004). The expression of this factor in the head mesoderm cells in embryonic stage 5 directs their differentiation into hemocytes **(Fig 1A)**. This is supported by the fact that *srp* mutant embryos lack any kind of mature hemocytes in later stages and that expressing *srp* in the trunk mesoderm, even in mutants that lack a head mesoderm, generate hemocytes at the cost of other mesodermal tissues (Rehorn et al. 1996; Spahn et al. 2014).

At the end of stage 5, the majority of Srp+ precursors start expressing Glial cells missing (Gcm) and Gcm2, two factors that are essential for their differentiation into plasmatocytes (Bernardoni et

al. 1997; Alfonso & Jones 2002), while a small percentage express Lozenge (Lz) instead of Gcm factors which would direct their differentiation into crystal cells (Lebestky et al. 2000).

Until embryonic stage 11, hemocytes are small and round with a similar shape to prohemocytes (Tepass et al. 1994). However, during stage 11, most of these prohemocytes start to migrate throughout the embryo and differentiate into migratory plasmatocytes and non-migratory crystal cells **(Fig 1B)**. During this process, prohemocytes differentiating into plasmatocytes change their morphology through developing high cell polarity and Actin-rich cellular protrusions, and they gain phagocytic abilities which they use to eliminate apoptotic cells during embryonic development (Tepass et al. 1994; Wood et al. 2006). On the other hand, crystal cell function is unclear during embryogenesis. Plasmatocyte migration continues until late stage 14, where they become evenly distributed throughout the embryo and after that they continue to circulate around the embryo, in addition to forming clusters around the head, foregut, and hindgut (Tepass et al. 1994). Crystal cell clusters appear around the proventriculus at the end of embryonic stages during stage 17, derived from Srp^{+} Lz^{+} Gcm^{-} hemocytes **(Fig 1C)** (Lebestky et al. 2000).

Interestingly, molecular circuits controlling the first embryonic wave in *Drosophila* share a lot of common factors with that of humans. One example of this is Srp, which belongs to the GATA family, from which three members GATA-1, -2, and -3 are involved in hematopoiesis (Orkin & Zon 2008). GATA-1 and -2 which are required for blood progenitor specification during primitive erythropoiesis (Fujiwara et al. 2004). Another example is Lz, which is a member of the RUNX family, from which RUNX1 (AML1), is necessary for the first steps of blood formation and many other later hematopoietic processes (Lebestky et al. 2000; Dzierzak & Speck 2008). Collectively, hemocytes originating from the head mesoderm during the first embryonic wave form two hematopoietic compartments in the larval stage: the circulation and the sessile compartment (Shrestha & Gateff 1982; Lanot et al. 2001).

On the contrary, the second wave of embryonic hematopoiesis starts at embryonic stage 13, when precursors of the lymph gland and pericardial cells appear in the cardiogenic mesoderm. Later, these cells start to move dorsally and cluster around the dorsal vessel, ultimately forming a pair lobed chain of the lymph gland lobes and the pericardial cells surrounding the dorsal vessel (Rugendorff et al. 1994; Holz et al. 2003). Clonal analysis proves the existence of a hemangioblast-like precursors, which can divide asymmetrically to give a dorsal vessel precursor and a lymph gland precursor (Mandal et al. 2004). This is very similar to the hemangioblast precursors in the

AGM mesenchyme in vertebrates, which give rise to both blood and vascular cells (Medvinsky & Dzierzak 1996), and further show the high level of homology between *Drosophila* and vertebrate hematopoiesis.

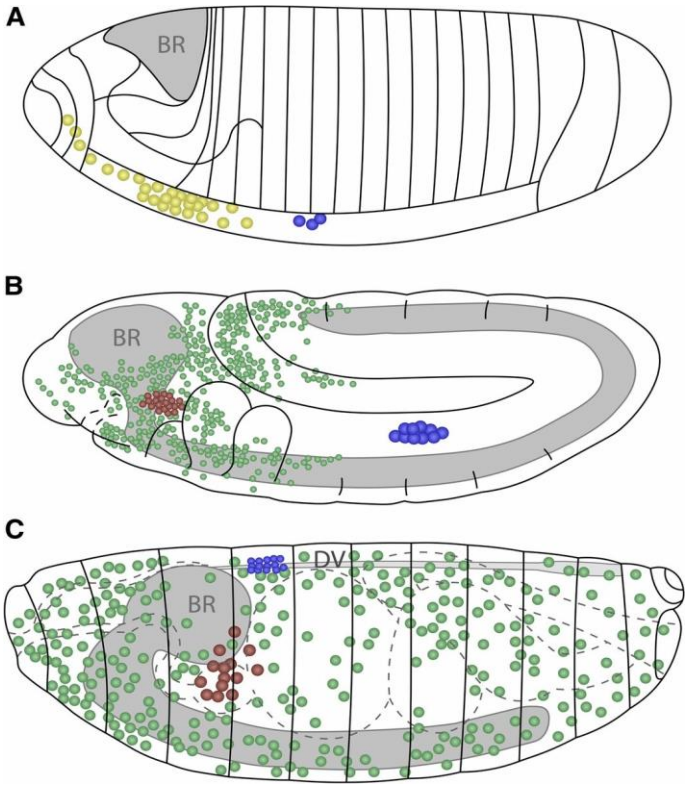

Fig 1. Embryonic hematopoiesis. (A) An illustration of a stage 5 embryo. Circulating and sessile hemocyte precursors (yellow) originate from the head mesoderm, while lymph gland precursors (blue) derive from the dorsal mesoderm. (B) An illustration of a stage 11 embryo. Embryonic prohemocytes move around and differentiate into plasmatocytes (green) and crystal cells (red), whereas lymph gland precursors divide and can be observed in the trunk. (C) An illustration of a stage 17 embryo. Plasmatocytes at this stage circulate around the embryo, while crystal cells cluster at the proventriculus. During dorsal closure, the lymph gland precursors migrate dorsally and surround the dorsal vessel (DV). BR: (brain, gray). Adapted from (Banerjee et al. 2019).

1.3. Hematopoiesis in the *Drosophila* larva

Hemocytes originating from the head mesoderm during the first embryonic wave either circulate in the hemolymph of the larva or leave the circulation and attach to the epidermis to form what is known as the sessile compartment, while hemocytes derived from the dorsal mesoderm during the second hematopoietic wave form the hematopoietic organ, the lymph gland **(Fig 2)** (El Shatoury 1955; Shrestha & Gateff 1982; Lanot et al. 2001; Honti et al. 2010; Makhijani et al. 2011). All

three compartments can produce the three mature hemocyte types: plasmatocytes, crystal cells, and lamellocytes, which can be distinguished based on the morphology, function, and expression of distinct cellular markers (T. M. Rizki 1978; Evans et al. 2003; Honti et al. 2010, 2014; Letourneau et al. 2016; Csordás et al. 2021).

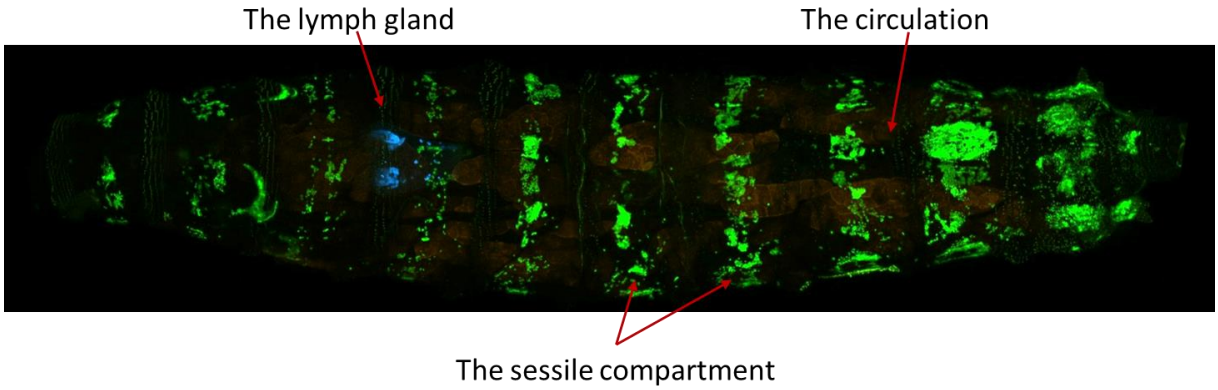

Fig 2. The larval hematopoietic compartments. An image showing the three hematopoietic compartments in the *Drosophila* larva as they appear through the cuticle of a larva where a hemocyte specific driver (*Hemolectin* or *Hml*) is driving GFP expression. The lymph gland color was modified to blue. Captured by Dr. Gábor Csordás.

Until recently, researchers assumed that the circulation and sessile compartment consist of only mature hemocytes (T. M. Rizki 1978; Márkus et al. 2009; Leitão & Sucena 2015; Letourneau et al. 2016). However, the latest single-cell sequencing studies show that these two compartments contain dividing cells and plasmatocytes and crystal cells in different maturation stages (Cattenoz et al. 2020; Cho et al. 2020; Tattikota et al. 2020).

Since parasitic wasps can infest *Drosophila* only in the larval stage, one of the main events that larval hemocytes participate in is the encapsulation of the wasp egg. This is done by the cooperation of the three cell types, where plasmatocytes and lamellocytes form a multi-layered capsule around the egg, and crystal cells release their content of phenol oxidase which initiates a cascade of reactions that produce free radicals that help in destroying the wasp egg, and melanin that melanizes the egg and prevents the parasitic wasp from developing (Nappi et al. 1995; Dudzic et al. 2015; Anderl et al. 2016).

1.3.1. The circulation

The regular contractions of the heart tube ensure the continuous circulation of the hemolymph within the body cavity while pumping it from the tail to the head (Tao & Schulz 2007). In naive larvae, only two types of hemocytes can be found in the circulating hemolymph, phagocyting plasmatocytes and crystal cells participating in wound healing. Upon immune induction by wasp infestation or wounding or in some tumorous mutants, a third type of hemocytes, the lamellocytes, appear in the circulation (T. M. Rizki 1978; Evans et al. 2003; Letourneau et al. 2016; Csordás et al. 2021). In addition to hemocytes, the hemolymph carries oxygen and nutrients necessary for the larva's growth and development and transports away carbon dioxide and metabolic waste. Moreover, it transfers hormones that regulate various physiological processes, and several important immune factors, such as antimicrobial peptides (AMPs) that exhibit broad-spectrum activity against microorganisms and clotting factors that help in wound healing and pathogen immobilization during immune responses (Jiravanichpaisal et al. 2006; Krzemien, Crozatier, et al. 2010; Krautz et al. 2014).

While the total number of hemocytes varies in the circulation according to the age and environment, it is believed that few hundred hemocytes exist in the embryo (Tepass et al. 1994), a number that increases during larval stages to reach around 5000 in pupae (Lanot et al. 2001; Makhijani et al. 2011), when a high number of hemocytes are needed to clean the apoptotic cells resulting from tissue remodeling and to protect the organism from bacteria that might leak from the intestines during histolysis (Lanot et al. 2001; Regan et al. 2013). In response to immune induction, not only lamellocytes appear in the circulation, but also the number of circulating cells increases (Zettervall et al. 2004; Márkus et al. 2009).

1.3.1.1. Plasmatocytes

Plasmatocytes are small (8–10 μm) round cells, forming around 90-95% of total hemocytes **(Fig 3)**. They function mainly in phagocytosis of pathogens and apoptotic cells, which is critical especially during metamorphosis when the imaginal discs develop into adult tissues (T. M. Rizki 1978; Tepass et al. 1994; Babcock et al. 2008; Pastor-Pareja et al. 2008). In addition, plasmatocytes assist other hemocytes in the early stages of encapsulating the wasp egg (Russo et al. 1996; Charroux & Royet 2009) and tumor cells (Williams et al. 2005; Pastor-Pareja et al. 2008).

Plasmatocytes also secrete extracellular matrix (ECM) proteins, such as collagen and laminin, which are required for tissue morphogenesis and repair (Fessler & Fessler 1989; Martinek et al.

2008; Sanchez-Sanchez et al. 2017). For this reason, embryos that lack plasmatocytes are less viable, and even if they survive to become adults, they have difficulties in tissue repair (Defaye et al. 2009; Van De Bor et al. 2015). Other important factors secreted only from mature plasmatocytes include AMPs, which are produced upon bacterial infections to help the animal fight the invaders (Irving et al. 2005; Kurucz et al. 2007). Many cell surface markers can be used to distinguish plasmatocytes. The two most important ones are Eater and NimC1 (Nimrod C1 or P1 antigen), which are receptors that play a role in phagocytosis. While Eater is expressed by all plasmatocytes including the ones populating the sessile compartment and it is required for their attachment to the cuticle of the larvae, NimC1 is not expressed by embryonic hemocytes (Kocks et al. 2005; Kurucz, Márkus, et al. 2007; Bretscher et al. 2015). According to the early observations by ultrastructural imaging, plasmatocytes are not a homogenous pool of cells and they can be divided into subgroups (Shrestha & Gateff 1982). This was supported by the latest single-cell transcriptomics data, which suggests that these subgroups might have different specialized roles, such as phagocytosis, AMP production or protein storage (Cattenoz et al. 2020; Fu et al. 2020; Tattikota et al. 2020). Moreover, these transcriptomics data supported the previous observations made by researchers that not all plasmatocytes are terminally differentiated cells, and that these cells can give rise to the other two mature hemocytes present in the larva, crystal cells and lamellocytes (Honti et al. 2010, 2014; Stofanko et al. 2010; Leitão & Sucena 2015; Cattenoz et al. 2020; Fu et al. 2020; Tattikota et al. 2020).

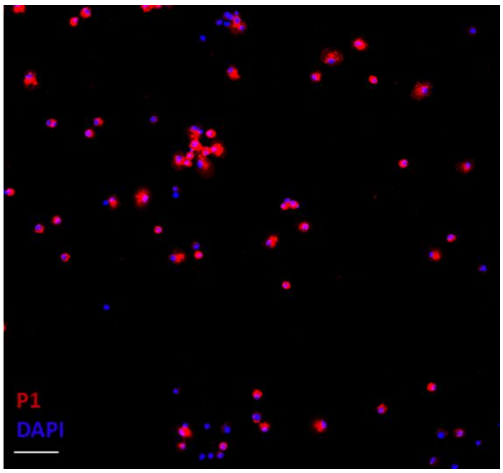

Fig 3. Plasmatocytes in the larval hemolmph. Plasmatocytes are stained with NimC1 (P1) antibody (red), nuclei are stained with DAPI (blue). Scale bar: 20 μm.

1.3.1.2. Crystal cells

Crystal cells are slightly bigger in size than plasmatocytes (10–12 μm), and they form around 2-5% of total hemocytes **(Fig 4)**. Even though they have a comparable size to plasmatocytes, they can be differentiated from them by the absence of cytoplasmic processes, having lower cytoplasmic density, and the presence of prophenoloxidase (PPO) crystals in their cytoplasm (Shrestha & Gateff 1982). Crystal cells play an important role in wound healing and the larval immune response by releasing PPO. When PPO gets activated, it becomes phenoloxidase (PO) that converts phenols to

melanin, which plays an essential role in wound closure and wasp egg melanization (Tang et al. 2006; Cerenius et al. 2008; Nam et al. 2012). Moreover, reactive oxygen species formed as a byproduct of the melanization process help in killing pathogens. For this reason, larvae deficient in melanization are more susceptible to microbial infection (Nappi et al. 1995; Galko & Krasnow 2004; Nam et al. 2012; Neyen et al. 2015). Crystal cells can be visualized through the cuticle simply by boiling the larva, which activates the melanization cascade in them, and turn them into black color (M. T. M. Rizki 1957; Lanot et al. 2001). However, to mark crystal cells more precisely, a *Black cells* (*Bc*) mutant (a dominant mutation in *PPO1* gene) where all crystal cells become black can be used (Babcock et al. 2008). Antibodies and transgenic reporters for early crystal cell markers, such as Lozenge (Lz) or Hindsight (Hnt), two transcription factors necessary for crystal cell specification, or late markers, such as C1 and PPO are also commonly used (Lebestky et al. 2000; Jung et al. 2005; Gajewski et al. 2007; T. Tokusumi, Shoue, et al. 2009; Terriente-Felix et al. 2013; Evans et al. 2014).

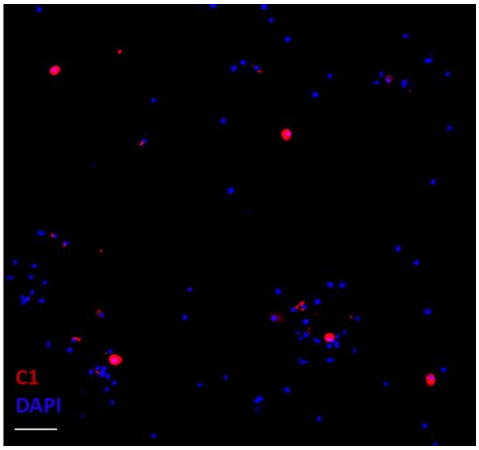

Fig 4. Crystal cells in the larval hemolmph. Crystal cells are stained with C1 antibody (red), nuclei are stained with DAPI (blue). Scale bar: 20 μm.

1.3.1.3. Lamellocytes

Lamellocytes are the largest larval hemocytes (25-40 μm), with irregular edges and many cellular processes (Shrestha & Gateff 1982). Even though these cells do not play a role in phagocytosis, they have more phagocytic organelles and lysosomes than plasmatocytes (Lanot et al. 2001; Kurucz, Váczi, et al. 2007). Lamellocytes are rarely present in naive animals, and they appear only after immune challenges by parasitic wasp, injury or in malignant tumors (Shrestha & Gateff 1982; T. M. Rizki & Rizki 1992; Lanot et al. 2001; Honti et al. 2010). The main function of these cells is to form a multi-layered capsule around the wasp egg and other foreign particles that are too big to be phagocytosed by plasmatocytes **(Fig 5A)** (Nappi et al. 1995; Russo et al. 1996). Other markers are used to distinguish lamellocytes include Misshapen (Msn), a kinase in the Jun N-terminal kinase (JNK) pathway, and Atilla (L1) a protein with an unknown function **(Fig 5B)**. β-PS integrin (β subunit of the integrin dimer) is also expressed at a high level in lamellocytes, and it is

indispensable for the encapsulation of the parasitic wasp egg (Irving et al. 2005; Kurucz et al. 2007; Honti et al. 2009; T. Tokusumi, Sorrentino, et al. 2009; Evans et al. 2014).

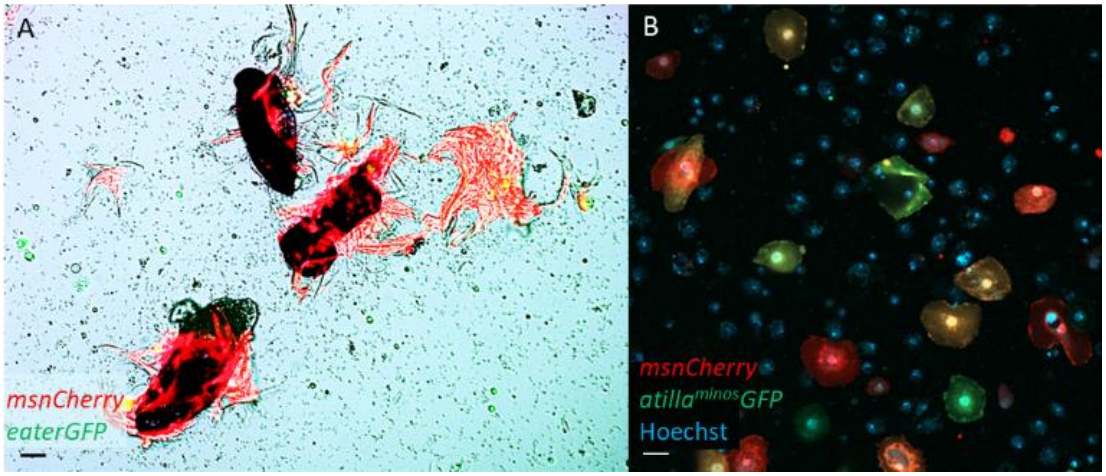

Fig 5. Heterogeneity of lamellocytes in the larval hemolymph. (A) Lamellocytes attached to the surface of a wasp egg in a blood cell culture derived from wasp infested larvae (green: plasmatocytes marked by the *eaterGFP* marker, red: lamellocytes marked by the *msnCherry* marker). (B) Lamellocyte heterogeneity in a blood cell culture derived from wounded larvae (green: *atilla*^{minos}*GFP*, red: *msnCherry*, blue: nuclei). Scale bar: 20 μm. Adapted from (Kúthy-Sutus et al. 2023).

Lamellocytes are not a homogenous cell population, and they can be divided based on their size and expression of cell surface markers into two categories, type I and type II. Type I lamellocytes correlate with the traditional description of lamellocytes as huge cells expressing only lamellocyte markers (e.g., *msn*) without co-expressing any plasmatocyte marker (e.g., *eater*), and differentiating from precursors called lamelloblasts or prelamellocytes. While Type II lamellocytes are smaller in size and originate from the transdifferentiation of plasmatocytes upon immune induction, and express both lamellocyte markers and plasmatocyte markers (Anderl et al. 2016; Szkalisity et al. 2021). However, former lineage tracing experiments showed that plasmatocytes can transdifferentiate into large flat (type I) lamellocytes, which shows that lamellocyte classification is not as simple (Honti et al. 2010). Recent single-cell sequencing data categorized lamellocytes also into two groups based on their expression level of *atilla*, one comprising lamellocytes in an intermediate state and another one containing fully differentiated lamellocytes (Tattikota et al. 2020). Nonetheless, these two clusters do not correlate to the type I/type II classification described in (Anderl et al. 2016), which is maybe due to using a different approach where type II lamellocytes were recognized as plasmatocytes since they express the plasmatocyte

marker eater, as suggested by Csordás et al. (2021) (Anderl et al. 2016; Tattikota et al. 2020; Csordás et al. 2021).

1.3.2. The sessile compartment

The sessile compartment consists of hemocyte clusters residing between the outer epidermal and inner muscle layers in what is called the epidermal-muscular pockets. These hemocytes form patches at the posterior end of the embryo, which later develop into dorsal stripes and the sessile pattern seen in larvae **(Fig 6 A-C)** (Anderl et al. 2016; Tattikota et al. 2020; Csordás et al. 2021). The sessile compartment is in a continuous exchange (dynamic steady-state) with the circulation, with cells that leave the circulation to become sessile hemocytes and cells leaving this compartment to join the circulation. Upon applying mechanical pressure to the larva, the sessile compartment dissociates. However, if the physical stress is gone, sessile hemocytes reassemble again in less than an hour, following the same mechanism involved in their initial formation (Makhijani et al. 2011). Moreover, upon wasp infestation, sessile hemocytes detach and transdifferentiate into lamellocytes to help the larva eliminate the wasp egg (Honti et al. 2010, 2014; Márkus et al. 2009; Vanha-Aho et al. 2015).

Many players are involved in the formation of the sessile pattern like the transmembrane receptor Eater that is necessary for their attachment to the cuticle, and Activin-β/TGF-β (Transforming Growth Factor-β), which is secreted by the peripheral neurons innervating the sessile pockets to direct hemocytes to the site and to enhance their attachment and expansion **(Fig 6C)**. The JNK signaling and Rac1 GTPase are also needed for the homing and adhesion of hemocytes into the sessile compartment (Williams et al. 2006; Makhijani et al. 2011, 2017; Bretscher et al. 2015). While other factors like Rho1 GTPase and the Actin cytoskeleton are necessary for the migration of sessile hemocytes to form their stripped pattern (Makhijani et al. 2011). The sessile compartment is maintained until the end of the larval stages. During pupariation, ecdysone signaling induces the dispersal and activation of sessile hemocytes, which aids in tissue remodeling during metamorphosis (Regan et al. 2013).

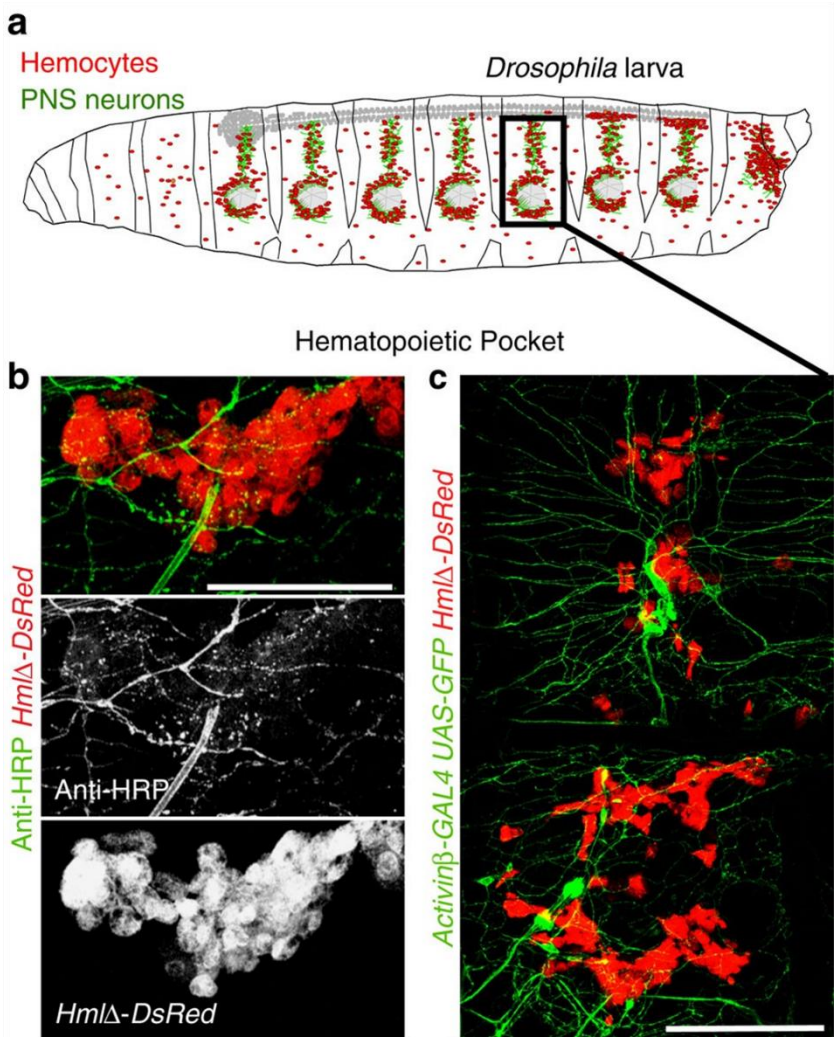

Fig 6. The larval sessile compartment. (**A**) An illustration of the sessile compartment in a *Drosophila* larva (PNS: peripheral nervous system, red: hemocytes, green: neurons). (**B)** A close-up of a hematopoietic pocket showing peripheral neurons extending to sessile hemocytes (red: hemocytes expressing *HmlΔ-DsRed*, green: neurons marked by Anti-HRP). (**C**) The expression of Activin-β by the neuronal extensions to the sessile compartment (red: hemocytes expressing *HmlΔ-DsRed*, green: Activin-β marked by *Activinβ-GAL4; UAS-GFP*). Scale bar: 100 μm. Adapted from (Makhijani et al. 2017).

1.3.3. The lymph gland

The lymph gland is a multi-lobed organ alongside the dorsal vessel of the larva. While the secondary and tertiary lobes are smaller in size and consist only of hemocyte progenitors, the primary (anterior) lobes are larger and can be divided into three main zones based on their distinct morphological and functional characteristics: the medullary zone (MZ) harboring hemocyte precursors, the cortical zone (CZ) consisting of mature hemocytes, and the posterior signaling

centre (PSC) or the hematopoietic niche, which sends signals to the hemocyte precursors to regulate their differentiation (Lebestky et al. 2003; Crozatier et al. 2004; Krzemien, Oyallon, et al. 2010; Banerjee et al. 2019; Kharrat et al. 2022). Recently an intermediate Zone (IZ) was described between the MZ and CZ containing progenitors that are more differentiated than MZ cells but less mature than CZ cells **(Fig 7)** (Cho et al. 2020; Girard et al. 2021; Spratford et al. 2021).

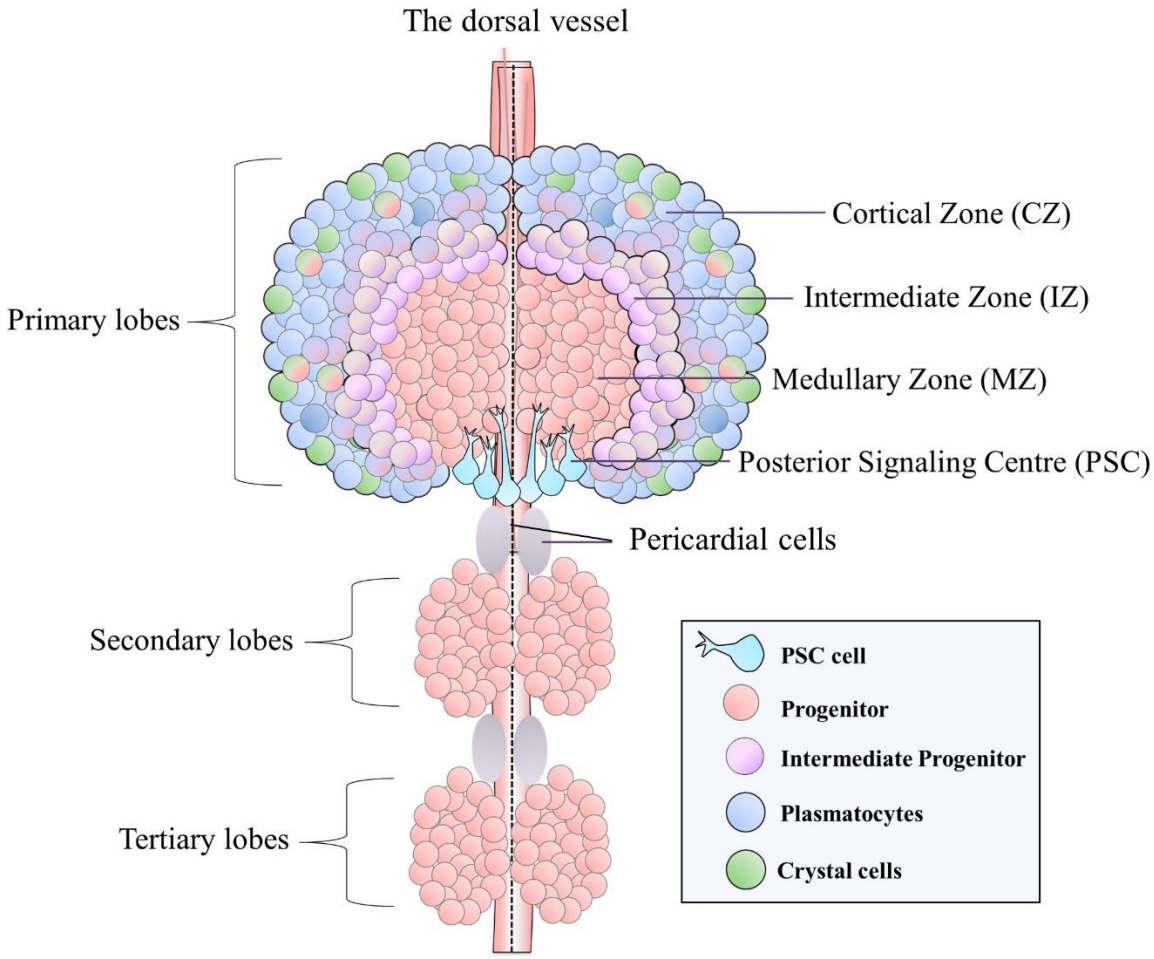

Fig 7. An illustration of the larval lymph gland surrounding the dorsal vessel. The anterior lobes of the lymph gland contain hemocyte progenitors in the MZ, progenitors in an intermediate state in the IZ, differentiated hemocytes in the CZ, and a signaling niche (PSC) that controls progenitor differentiation non-cell-autonomously. In the CZ, only plasmatocytes and crystal cells are observed in naive larvae, while lamellocytes appear in immune induced larvae. Adapted from (Kharrat et al. 2022).

1.3.3.1. The posterior signaling centre (PSC)

The PSC is a group of 20-40 cells at the posterior end of each anterior lobe. In contrast to the rest of the lymph gland cells, which are derived from the first two embryonic thoracic segments, PSC cells originate from Antennapedia (Antp) positive cells in the third thoracic segment. The Antp transcription factor continues to be expressed in the PSC cells to maintain their identity until lymph gland dispersal. The function of PSC cells is to send signals to the hemocyte progenitors in the lymph gland to control their differentiation. This is similar to vertebrate stem cell niches that signal to HSCs to regulate their differentiation, which makes the PSC an excellent hematopoietic niche model in *Drosophila* (Schofield 1978; Lebestky et al. 2003; Crozatier et al. 2004; Mandal et al. 2007).

Together with Antp, the transcription factor Collier (Col) is required for PSC niche maintenance and function **(Fig 8A-8C)**. The PSC is not observed in third instar larvae of *col* mutants, and silencing *col* in the PSC compromises its ability to induce lamellocyte differentiation following wasp infestation (Crozatier et al. 2004). Besides Antp and Col, the PSC cells niche expresses other cell-specific markers such as Dally-like protein (Dlp) and Daughters against dpp (Dad), two components of the Dpp pathway, and Unpaired3 (Upd3), a ligand for the JAK/STAT pathway (Jung et al. 2005; Pennetier et al. 2012).

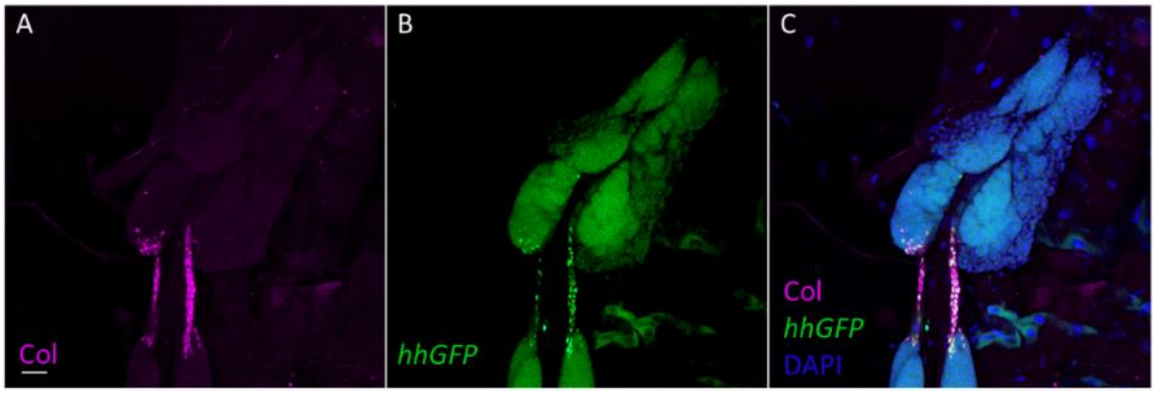

Fig 8. The posterior signaling centre. (A-C.) A confocal image showing the PSC in the lymph gland anterior lobes, expressing the specific markers Col (Magenta) and *hh-GFP* (green). Nuclei are stained by DAPI (blue). Scale bar: 20 μm.

The PSC emits several important signals to the progenitors, such as Decapentaplegic (Dpp) and Hedgehog (Hh) **(Fig 8B-8C)**, two morphogens that upon activating their receptors, Thickveins (Tkv) and Patched (Ptc), respectively, suppress premature differentiation of MZ progenitors (Mandal et al. 2007; Dey et al. 2016). The ligand of the Notch (N) pathway, Serrate (Ser), is also

secreted by the PSC and controls the differentiation of progenitors into crystal cells (Lebestky et al. 2003). While the ligand of the EGFR signaling pathway, Spitz (Spi), secreted from the PSC upon immune induction and oxidative stress is essential for lamellocyte differentiation (Finkel & Holbrook 2000; Kaur et al. 2019). The PSC also communicates with the differentiated hemocytes of the CZ by secreting PDGF- and VEGF-related factor 1 (Pvf1), which activates the Pvf/Pvr pathway in the CZ and ensures equilibrium signaling for progenitor maintenance in the MZ (Mondal et al. 2011).

Similarly to how the number of niche cells in mammals affects stem cell differentiation, the same phenomenon is observed in *Drosophila* (Zhang et al. 2003). Smaller PSC size results in progenitor differentiation, while bigger PSC size causes the expansion of progenitors and a decrease in CZ size. Several factors influence the size of the PSC. Antp and Wingless (Wg) act as positive regulators that increase PSC size through the regulation of the *Myc* gene. Dpp opposes the effect of Wg by downregulating *Myc* (Sinenko et al. 2009; Pennetier et al. 2012). Furthermore, it was discovered that the nutrition of the larva impacts niche size - activating the insulin pathway in the niche increases its size, while knocking it down decreases it (Benmimoun et al. 2012).

Interestingly, besides the PSC, new reports have described an additional cardiac niche (Morin-Poulard et al. 2016; Destalminil-Letourneau et al. 2021). Up until now, two signals were found to be secreted from this niche. The first one is the EGF-like protein Slit, which controls the size of the PSC niche and in turn progenitor maintenance through the Dpp pathway (Morin-Poulard et al. 2016). The other one is the FGF ligand Branchless (Bnl), which helps in keeping normal intracellular calcium levels in the progenitors (Destalminil-Letourneau et al. 2021). This shows similarity to mammalian stem cell niches, where the vascular system sends signals to the stem cells to control their differentiation (Geutskens et al. 2012; Smith-Berdan et al. 2015).

1.3.3.2. The medullary zone

The MZ of the lymph gland contains hemocyte progenitors, which are the precursors of the differentiated hemocytes located in the CZ. These cells express progenitor-specific markers like Thioester-containing protein 4 (Tep4), a protein with a yet unknown function in the MZ, and Domeless (Dome), the JAK/STAT pathway receptor in *Drosophila*, which is essential for progenitor maintenance **(Fig 9)** (Gao et al. 2009).

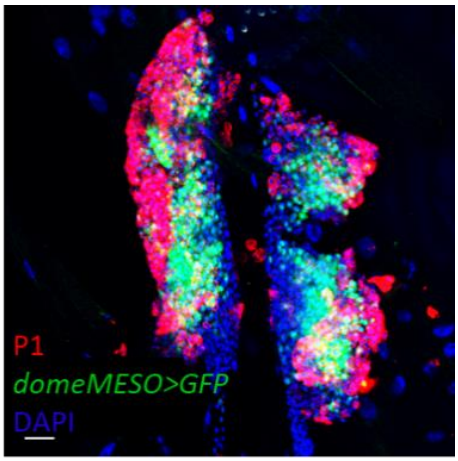

Fig 9. The medullary and cortical zones of the lymph gland. A confocal image showing the MZ in the anterior lobes of a lymph gland marked by the *domeMESO* reporter (green) and the CZ marked by the P1 plasmatocyte marker (red). Nuclei are stained by DAPI (blue). Scale bar: 20 μm.

Interestingly, signaling pathways which were described to play an important role in the PSC niche were also found to be required cell-autonomously in progenitors to suppress their differentiation. Two examples of this are Wg and Col, which when absent, progenitors are prematurely lost (Crozatier et al. 2004; Sinenko et al. 2009; Benmimoun et al. 2015; Oyallon et al. 2016).

Similar to HSCs in mammals, the interaction of progenitors with each other is a necessary signal for their maintenance. Progenitors express the adherens junction protein E-cadherin (E-cad) at a higher level than differentiated hemocytes in the CZ, which keeps them compacted and undifferentiated. Silencing *E-cad* in progenitors causes them to lose their compaction and promotes their differentiation (Gao et al. 2013). Moreover, the flow of calcium signals between the progenitors of the MZ through gap junctions is necessary for their maintenance (Ho et al. 2021). Reactive oxygen species (ROS) also serve as a signal between progenitor cells. Moderate levels of ROS are required for their normal differentiation. Upon immune induction, the elevation of ROS promotes the differentiation of progenitors into lamellocytes through activating the Jun N-terminal kinase (JNK) pathway and lowering E-cad levels (Owusu-Ansah & Banerjee 2009).

MZ progenitors also respond to systemic signals from changes in the animal's environment, such as nutritional changes translated through the Insulin/mTOR pathway. Both starvation and overfeeding can trigger the differentiation of progenitors, suggesting that normal progenitor differentiation requires a balanced diet (Benmimoun et al. 2012; Shim et al. 2012). Moreover, odors in the environment signal to the progenitors through the secretion of the neurotransmitter Gamma-aminobutyric acid (GABA), which in turn controls calcium signaling necessary for progenitor

maintenance (Shim et al. 2013; Madhwal et al. 2020). Interestingly, even the gas composition in the air affects progenitor maintenance in the MZ. Low oxygen or carbon dioxide causes the production of Ser, which promotes the differentiation of progenitors into crystal cells (Cho et al. 2018).

Recent research demonstrated that progenitors in the MZ are not a homogeneous population, and can be divided into three sub-populations. From the core to the cortex these are as the following: core progenitors (cells expressing both Tep4 and Dome), distal progenitors (cells expressing only Dome but not Tep4) and intermediate progenitors (cells expressing both Dome and the CZ marker Hml) (Sinenko et al. 2009; Blanco-Obregon et al. 2020). The later sub-population forms a distinct zone, the intermediate zone (IZ). A Split-Gal4 driver, the *CHIZ-Gal4* was created to mark and manipulate these cells (Cho et al. 2020; Girard et al. 2021; Spratford et al. 2021). It is important to note that Krzemien et al. (2010) originally used the term "intermediate progenitors" to describe a population of mitotic cells that are negative for both MZ and CZ markers, which creates confusion in lymph gland nomenclature.

Interestingly, these 3 subpopulations of the MZ do not only differ in the expression of their cell surface markers but also in their function. For instance, the activity of the N pathway in core progenitors is necessary for their maintenance, but in distal progenitors it promotes their specification into crystal cells (Blanco-Obregon et al. 2020).

1.3.3.3. The cortical zone

Situated in the cortex of the anterior lobe, the CZ contains differentiated hemocytes (plasmatocytes and crystal cells in naive conditions, as well as lamellocytes in case of immune induction) **(Fig 9)** (Jung et al. 2005). The CZ starts to form in mid-second instar larvae and its size continues to grow at the expense of MZ cells until most progenitors are lost at the end of larval stages. Subsequently, the lymph gland breaks down, and all hemocytes are released into the hemolymph to aid in the elimination of apoptotic cells and pathogens, resulting from tissue reconstruction during metamorphosis (Lanot et al. 2001; Jung et al. 2005; Grigorian et al. 2011).

The earliest markers expressed by CZ cells are Hml and Pxn, followed by later markers that are specific for each of the three effector mature hemocyte types (Nelson et al. 1994; Lebestky et al. 2000; Goto et al. 2003; Irving et al. 2005; Kocks et al. 2005; Kurucz, Márkus, et al. 2007; Kurucz et al. 2007; Honti et al. 2009; Binggeli et al. 2014; Bretscher et al. 2015; Dudzic et al. 2015). Interestingly, differentiated hemocytes in the CZ also play a role in the regulation of progenitor

differentiation by sending signals that assist in sustaining the main signaling pathways in MZ progenitors, such as Hh, JNK, Toll and Ras/EGFR (Mondal et al. 2011; Yu et al. 2021).

The basic zonal structure of the lymph gland consisting of niche cells, progenitors and differentiated immune cells became a simplified and attractive model to study hematopoiesis. This can be attributed to both the functional similarities between *Drosophila* and the mammalian hematopoietic niche and the sophisticated approach that *Drosophila* provides to identify and manipulate cells at the molecular level (Jung et al. 2005; Banerjee et al. 2019; Kharrat et al. 2022).

1.4. Hematopoiesis in adult flies

Unlike *Drosophila* embryos and larvae, the hematopoietic system in adult flies is still poorly investigated (Banerjee et al., 2019). The earliest observations of adult hematopoiesis excluded the presence of hematopoietic organs in adults and suggested that hemocytes can be found mainly as sessile hemocytes seen in the abdomen, legs, and halteres (Elrod-Erickson et al. 2000; Lanot et al. 2001). Moreover, these data suggested that adult hemocytes consist of only phagocytic plasmatocytes that are derived from embryonic and larval hemocytes with the absence of progenitor hemocytes or effective hematopoiesis during this stage (Elrod-Erickson et al. 2000; Lanot et al. 2001; Holz et al. 2003). Later, this concept changed when active hematopoietic hubs were identified in the abdomen of adult flies and were shown to contain progenitors derived from the posterior lobes of the larval lymph gland that can differentiate into both plasmatocytes and crystal cells (Ghosh et al. 2015). However, these findings were refined when a recent publication showed that while hemocyte progenitors exist in adults, they derive from the PSC cells and not from lymph gland progenitors. These cells do not proliferate in normal conditions, only in response to immune induction at a low frequency, agreeing with the earliest theory that no significant hematopoiesis occurs in adults (Boulet et al. 2021). Adult hemocytes are reported to continue the expression of their specific larval markers such as Hml and Pxn (plasmatocytes) and Lz (crystal cells) (Elrod-Erickson et al. 2000; Honti et al. 2010, 2014; Ghosh et al. 2015; Boulet et al. 2021). Interestingly, even though lamellocytes do not survive until the adult stage, the lamellocyte marker *msn* is expressed in the majority of adult hemocytes (Boulet et al. 2021). A recent study identified a location for adult hemocytes in the respiratory epithelia and suggested that these cells play an immune role by triggering the secretion of the antimicrobial peptide Drosocin from the surrounding epithelia and the fat body, which helps the animal fight infection **(Fig 10)** (Bosch et al. 2019).

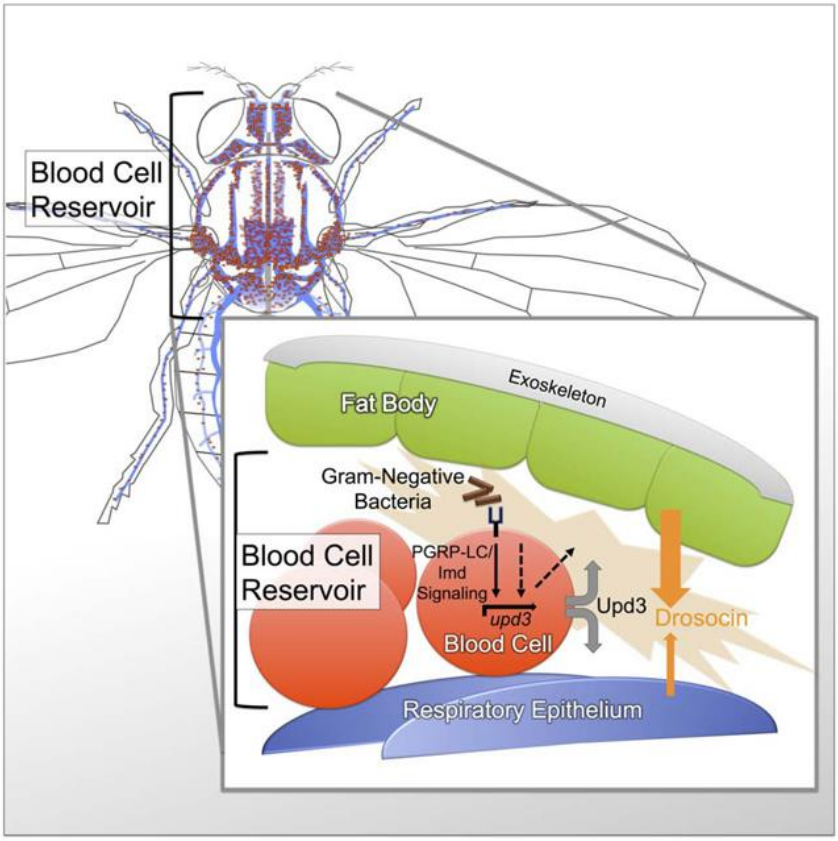

Fig 10. An illustration of the crosstalk signaling between adult hemocytes, fat bodies, and respiratory epithelia. Activation of Imd signaling in hemocytes in response to bacterial infection leads to the secretion of the Jak/Stat ligand Upd3, which activates this pathway in neighboring fat body and respiratory epithelia cells, resulting in Drosocin secretion from these tissues which aids in tackling the illness. Adapted from (Bosch et al. 2019).

1.5. Similarities of hematopoietic regulation between the *Drosophila* lymph gland and mammalian hematopoietic compartments

As mentioned earlier, the structural arrangement of the larval lymph gland shows many similarities to HSC niches in mammals and therefore provides an excellent model to understand the role of the different signaling pathways in hematopoiesis. This model became even more feasible with the development of zone-specific Gal4 drivers that help manipulate signaling pathways in any zone of the lymph gland (Lebestky et al. 2003; Crozatier et al. 2004; Jung et al. 2005; Krzemień et al. 2007; Oyallon et al. 2016).

An example of conserved regulatory pathways is the JAK/STAT pathway, which is required for hematopoietic progenitor maintenance in both fruit flies and mice. Hemocyte progenitors are greatly reduced in the lymph gland in response to JAK/STAT knockdown (Gao et al. 2009), similar

to how HSCs are exhausted in *JAK1* and *JAK2* mutant mice (Akada et al. 2014; Kleppe et al. 2017). Another example is Hh, which maintains hemocyte progenitors in flies, and its orthologue Sonic hedgehog (Shh) expands the hematopoietic progenitor pool in mammals (Bhardwaj et al. 2001; Mandal et al. 2007). Likewise, the Notch pathway in the lymph gland participates in core progenitor maintenance and in the fate determination of plasmatocytes or crystal cells in distal progenitors (Duvic et al. 2002; Terriente-Felix et al. 2013; Blanco-Obregon et al. 2020), a role analogous to its mammalian counterpart, which was described to be involved in HSC self-renewal, differentiation, as well as commitment towards the lymphoid or myeloid lineage (Karanu et al. 2000; Stier et al. 2002; Duncan et al. 2005). Moreover, similarly to how Wg and Dpp signaling control progenitor differentiation in *Drosophila* both cell-autonomously by limiting progenitor differentiation and non-cell-autonomously by controlling the PSC size (Mandal et al. 2007; Sinenko et al. 2009; Pennetier et al. 2012; Dey et al. 2016), their mammalian orthologues Wnt and BMP-4 controls HSC maintenance cell-autonomously and non-cell-autonomously by affecting niche components such as osteoblasts (Bhatia et al. 1999; Reya et al. 2003; Zhang et al. 2003; Duncan et al. 2005).

Another common aspect between HSC and hemocyte progenitor regulation is the importance of cell-cell interaction. For instance, gap junctions in the lymph gland progenitors are required for maintaining normal levels of calcium signaling which is essential for their maintenance (Ho et al. 2021), while in mice they are essential for HSC growth and ability to regenerate after stress (Rosendaal et al. 1997; Presley et al. 2005).

Similar to hemocyte progenitors, mammalian HSCs sense and respond to nutritional signals in the environment; in both entities, higher or lower levels of nutritional input triggers their depletion and premature differentiation (Yilmaz et al. 2006; Zhang et al. 2006; Benmimoun et al. 2012; Shim et al. 2012; Young et al. 2021). Stress signals such as ROS are also sensed by HSCs and hemocyte progenitors, and these signals induce their differentiation by lowering their adhesion molecule levels (Ito et al. 2004; Hosokawa et al. 2006; Owusu-Ansah & Banerjee 2009; Gao et al. 2014). All the above examples highlight the homology and analogy in molecular circuits controlling hematopoiesis between *Drosophila* and mammals and prove further the importance of using *Drosophila* and especially the lymph gland as a tool for investigating this process **(Fig 11)**.

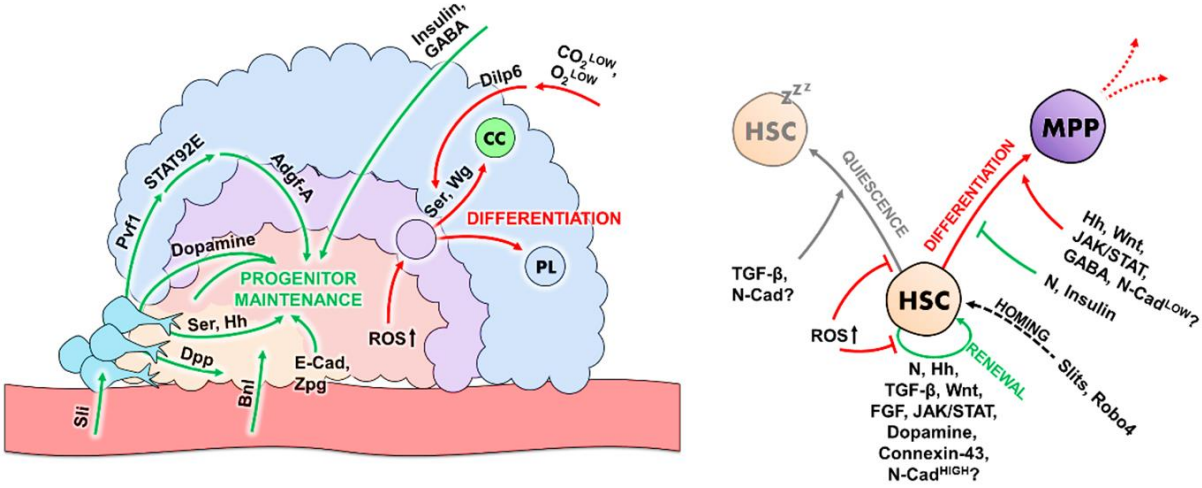

Fig 11. An illustration of the main signaling pathways controlling the differentiation of hemocyte progenitors in the *Drosophila* lymph gland and HSCs in a mammalian HSC niche. Sli: Slit, Stat92E: Signal-transducer and activator of transcription protein at 92E, Adgf-A: Adenosine deaminase-related growth factor A, Zpg: Zero population growth, N-cad: Neural cadherin, CC: crystal cell, PL: plasmatocyte, MPP: multipotent progenitor. Adapted from (Kharrat et al. 2022).

1.6. Headcase as a regulator of hematopoiesis

The *headcase (hdc*) gene was first identified with the help of an enhancer trap insertion in a screen for genes regulated by the bithorax complex (Weaver & White 1995). *hdc* encodes for two cytoplasmic isoforms, a short one (~70 kDa) and a long one (~130 kDa). The long isoform is produced through suppressing the translational termination at the stop codon of the short isoform (Steneberg & Samakovlis 2001). *hdc* expression is first detected at the embryonic stage 13 in the pattern of imaginal primordia, and it continues to be expressed in the larva in all imaginal discs and imaginal precursors of the CNS, intestines, trachea, epidermis, testis, and ovaries. At the end of larval stages, the expression of *hdc* disappears from most tissues and it can be found in adults only in few places such as the brain and the testis (Weaver & White 1995).

Since its isolation, the Hdc protein posed a mystery, because it does not contain any known functional domains, however, numerous important roles have been described for it in many larval tissues. In the imaginal cells, Hdc was shown to block differentiation by regulating the insulin/mTOR pathway **(Fig 12)** (Weaver & White 1995; Avet-Rochex et al. 2014; N. Li et al. 2019; Giannios & Casanova 2021). In the trachea, Hdc was described to function non-cell autonomously in specialized cells called fusion cells to inhibit neighboring cells from acquiring the

branching fate and forming additional branches (Steneberg & Samakovlis 2001). Furthermore, Hdc was found to be required for the maintenance of stem cell niches in the testis and intestines, preventing the loss of hub cells (one of the niche's cellular components) in the former, and the loss of intestinal stem cells and enteroblasts in the latter, via apoptosis (Resende et al. 2013, 2017).

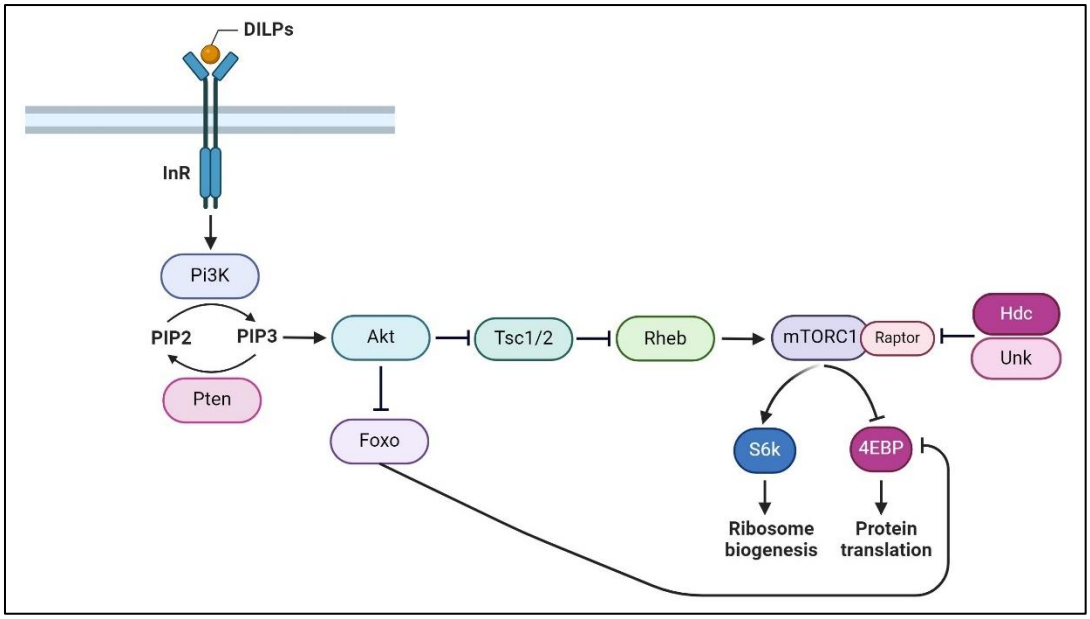

Fig 12. A simplified schematic illustration of the role of Hdc in the insulin/mTOR pathway in the imaginal cells. The activation of the insulin receptor (InR) by *Drosophila* insulin-like peptides (DILPs) activates several downstream signaling pathways, among these is the mTOR pathway. This pathway leads to ribosome biogenesis and protein translation through the activity of S6K and 4EBP transcription factors downstream to mTORC1 complex, which Hdc and its partner Unk were shown to bind to its member Raptor to inhibit its activity. Pi3K: Phosphatidylinositol 3-kinase 92E, PIP3: Phosphatidylinositol (3,4,5)-trisphosphate, PIP2: Phosphatidylinositol 4,5-bisphosphate, Pten: Phosphatase and tensin homolog, Foxo: Forkhead box O, Tsc1/2: Tuberous sclerosis complex 1/2, Rheb: Ras homolog enriched in brain, mTORC1: mTOR complex 1, S6k: Ribosomal protein S6 kinase, 4EBP: Eukaryotic translation initiation factor 4E binding protein (N. Li et al. 2019; Giannios & Casanova 2021; Liguori et al. 2021). Created with BioRender.com.

In the hematopoietic system, *hdc* is expressed only in the lymph gland but not in the circulating or sessile hemocytes in the larva (Weaver & White 1995; Márkus et al. 2009; Varga et al. 2019). Previously, our colleagues found that in *hdc* null mutants and upon knocking down *hdc* in the niche, lamellocytes differentiate in naive larvae without immune induction **(Fig 13A-B)**, suggesting a role for Hdc in hemocyte progenitor maintenance in the hematopoietic niche. This phenotype was rescued by overactivating the Hh or Dpp pathways in the PSC (**Fig 13C)**, indicating that Hdc functions upstream to them in the niche (Varga et al. 2019). However, the mechanism behind

lamellocyte differentiation in these larvae is still unknown, since knocking down *hdc* does not affect the size or identity of the niche.

The role of Hdc in the other domains of the lymph gland (the MZ and the CZ) has not been studied previously. The interaction with its two previously described partners, Unk and Raptor, in regard to hematopoiesis also has not been investigated. Furthermore, no attempts have been made yet to isolate new Hdc interactors in the lymph gland or other tissues. Since the human ortholog of Hdc, HECA, is a tumor suppressor in many tumor models, characterizing the mechanism of Hdc function in the lymph gland would be beneficial not only in the field of *Drosophila* hematopoiesis but it may be crucial for human tumorigenesis studies (Dowejko et al. 2009, 2012).

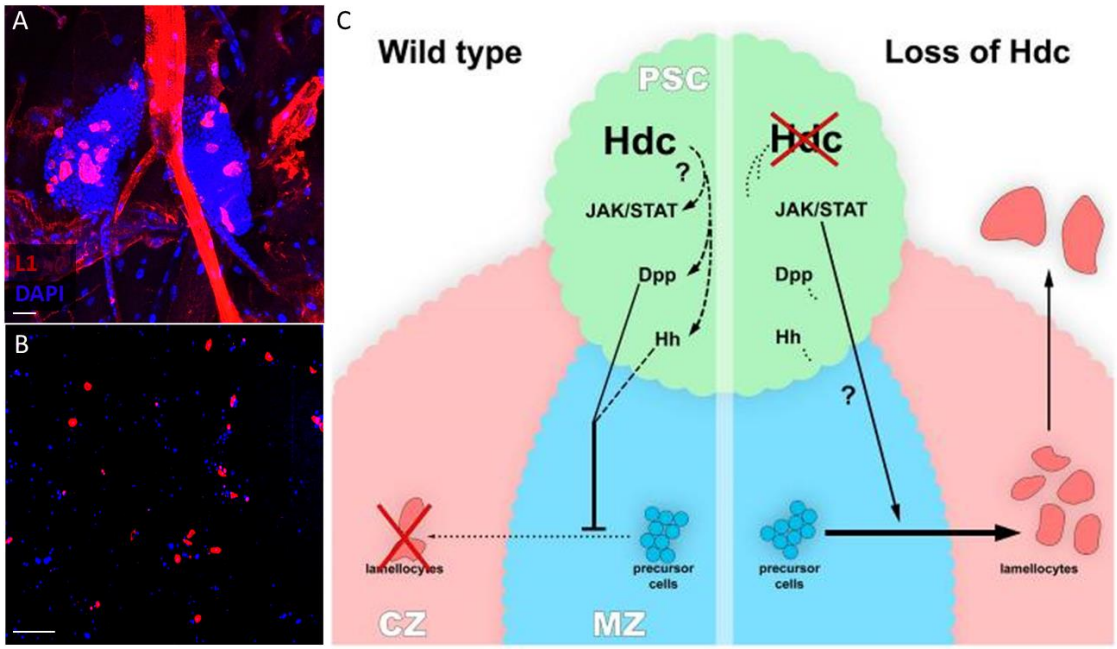

Fig 13. Hdc in the *Drosophila* lymph gland. (A-B) *hdc* silencing in the niche leads to lamellocyte differentiation in the lymph gland (A) and circulation (B). (blue: nuclei visualized with DAPI, red: lamellocytes stained by L1 antibody). Scale bar: 20 μm. (C) A graphical model suggesting that when *hdc* is silenced in the niche, the secretion of two suppressor ligands from the niche, Hh and Dpp, is compromised. This promotes progenitor differentiation into lamellocytes in the lymph gland without immune induction. Based on (Varga et al. 2019).

2. Objectives

Since signaling pathways controlling hemocyte progenitor maintenance in *Drosophila* are highly homologous to those involved in HSC maintenance in vertebrates, the fruit fly provides an excellent model for studying hematopoiesis. Previously, our colleagues identified Hdc as a repressor of blood cell differentiation in the lymph gland hematopoietic niche of the larva. Given that the underlying mechanism of how Hdc maintains the progenitor state of hemocytes is not yet understood, we aimed to investigate the regulatory role of Hdc in the *Drosophila* lymph gland.

Specific aims:

- As literature data suggested a connection between Hdc and the insulin/mTOR pathway, we aimed to investigate whether the hematopoietic role of *hdc* is mediated by insulin/mTOR signaling.
- Previously, it was shown that *hdc*, while compromising PSC function, does not affect the number or identity of PSC cells. Since the insulin/mTOR was shown to play a role in PSC size determination, we aimed to understand why the PSC size remains unaltered in *hdc* larvae.
- Former data suggested that *hdc* expression is downregulated during larval development, possibly to allow for progenitor differentiation at later stages. We asked whether *hdc* expression is also downregulated following immune induction with parasitic wasp, thereby contributing to the differentiation of progenitors to lamellocytes during the immune response.
- We wanted to explore the possibility of a cell-autonomous function of Hdc in the lymph gland hemocyte progenitors and characterize the signaling pathways involved in this role.
- Since only two partners of Hdc (Unk and Raptor) were described previously, we set out to isolate novel interacting partners of Hdc in the lymph gland.

3. Materials and methods

3.1. *Drosophila* stock establishment and maintenance

All *Drosophila* lines used in the study are listed in **S1 Table**. To establish *UAS-hdcRA_STOP/SM6b*, *UAS-hdcRC_STOP/SM6b*, and *UAS-hdcRC_NOSTOP/SM6b* stocks, the respective plasmids were injected into *P{CaryP}attP40* (BDSC_25709), and fly stocks carrying the transgenes on the second chromosome were established as described in (Port et al. 2014) (**Fig 14A).** After this, *UAS-hdcRA_STOP/CyoGFP; hdc$^{\Delta 84}$/TM6Tb* was established by combining *UAS-hdcRA_STOP* and *hdc$^{\Delta 84}$* (**Fig 14B)**. All injections into embryos were done by the Injection Facility of HUN-REN BRC, Szeged, and all stocks and crosses were kept on a standard cornmeal-yeast media at 25 °C.

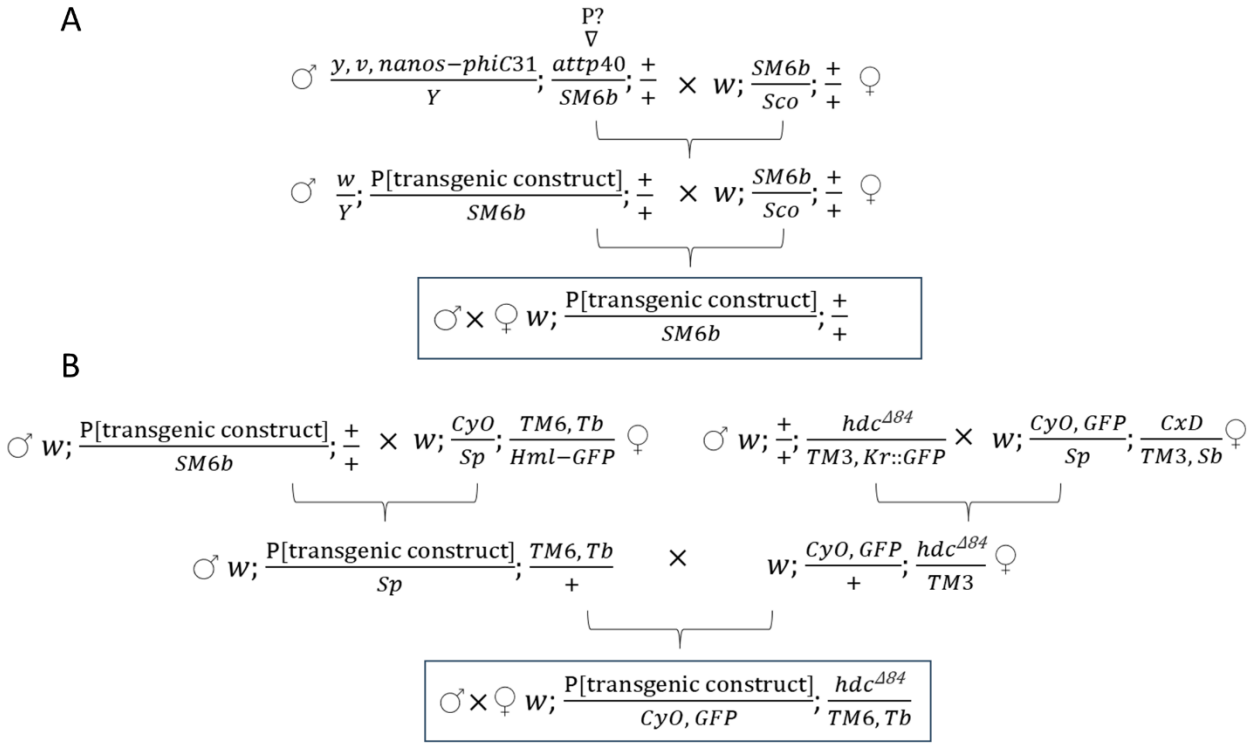

Fig 14. Crossing schemes for establishing transgenic lines. (A) Crossing scheme followed to establish second chromosome insertion lines. The HA-tagged *hdc* transgenic plasmids (UAS-hdcRA_STOP, UAS-hdcRC_STOP or UAS-hdcRC_NOSTOP) containing the *attB* bacterial attachment site were injected into larvae carrying a phage attachment site (*attP40)* on the second chromosome, and the gene encoding for the phiC31 integrase under the control of the *nanos* driver specific for germline cells on the X chromosome (*nanos-phiC31*). Males hatching from the injected larvae which possibly carry the transgenic plasmids in their germline cells (P?) were crossed to second chromosome balancer virgins and then males carrying the

transgenic construct in all their cells as evident by the expression of the *mini white* marker in their eyes were selected from the progeny and crossed individually to second chromosome balancer virgins to create a stable fly line. (B) Crossing scheme followed to establish stocks carrying the transgene encoding for the HA-tagged short isoform of Hdc on the second chromosome (*UAS-hdcRA_STOP*) combined with $hdc^{\Delta 84}$ null allele on the third chromosome. *SM6b* (*Second Multiple 6b*), *CyO* (*Curly of Oster*), *TM6* (*Third Multiple 6*), *TM3* (*Third Multiple 3*), and *CxD* (*Crossover Suppressor Dichaete*) are balancer chromosomes, while *Sco* (*Scutoid*), *Sp* (*Sternopleural*), *Kr::GFP* (*Kruppel* promoter driving *GFP* expression), *Sb* (*Stubble*), and *Tb* (*Tubby*) are dominant markers. *y* (*yellow*) and *v* (*vermilion*) are recessive markers.

3.2. Antibodies and fluorescent dyes

The following primary antibodies were used: mouse anti-L1 (1:10, a kind gift from István Andó) (Kurucz et al., 2007), mouse anti-Col (1:100, a kind gift from Michele Crozatier) (Krzemień et al. 2007), mouse anti-LacZ (1:100, DSHB 40-1a), mouse anti-C1 (HC12F6) (a kind gift from Tina Trenczek), Rabbit anti-HA (1:10000, Abcam, Cat# ab9110), anti-His-HRP (1:10000, Sigma, Cat# A7058-1VL), anti-GST-HRP (1:10000, Merck, Cat# 16-209). Secondary antibodies were: Goat anti-Rabbit HRP (1:10000, Thermo Fisher Scientific, Cat# 31462), Goat anti-Mouse Alexa Fluor™ 568 (1:1000, Thermo Fisher Scientific, Cat# A-11004), Goat anti-Mouse Alexa Fluor™ Plus 488 (1:1000, Thermo Fisher Scientific, Cat#. A32723), Rabbit anti-Mouse Alexa Fluor™ 647 (1:1000, Thermo Fisher Scientific, Cat# A-21239). Nuclei were visualized with DAPI (Sigma-Aldrich, Cat# D9542).

3.3. DNA constructs

To create HA-tagged *hdc* constructs (UAS-hdcRA_STOP, UAS-hdcRC_STOP, and UAS-hdcRC_NOSTOP), cDNA of *hdc* (LD44381) was obtained from the *Drosophila* Genomics Resource Center (DGRC) Gold Collection, and amplified with PCR (Phusion DNA polymerase) using the following primer pairs: hdcRA_STOP_fwd and hdcRA_STOP_rev, hdcRC_STOP_fwd and hdcRC_STOP_rev, and hdcRC_NOSTOP_1_fwd, hdcRC_NOSTOP_1_rev, and hdcRC_NOSTOP_2_fwd and hdcRC_NOSTOP_2_rev, respectively **(S2 Table)**. The pTHW vector (DGRC #1099) was amplified on the other hand with pTHW_fwd and pTHW_rev **(S2 Table)**, and the amplified cDNA segments were cloned together with the amplified plasmid using Gibson assembly (HiFi DNA Assembly master mix, NEB, cat# E2621L), according to the manufacturer's protocol, and the mixture was then transformed into 2T1 *E. coli* chemically competent bacteria, and positive colonies were confirmed by enzymetic digestion and then Sanger-sequencing.

Assembled constructs of *hdc* enhancers and *hdc* tagged isoforms were purified by HiSpeed Plasmid Midi Kit (Qiagen, cat# 12643) according to the manufacturer's instructions, and diluted in injection buffer described in (Sullivan et al. 2000) for injection into embryos.

To create the hdc-nYFP, unk-cYFP, and Cam-cYFP constructs, Gateway cloning was used (Walhout *et al.* 2000). In summary, cDNA of *hdc* (LD44381), *unk* (BS27380), and *Cam* (LD02334) were obtained from the *Drosophila* Gold Collection and amplified using the following primer pairs: hdc_cDNAFor and hdc_cDNArev, unk_cDNAFor and unk_cDNArev, and Cam_cDNAFor and Cam_cDNArev respectively **(S2 Table)**. The PCR reactions were done using Q5 Hot Start High-Fidelity DNA Polymerase (New England Biolabs, Cat# M0493S), and PCR products were purified using NucleoSpin Gel and PCR Clean-up (MACHERRY-NAGEL, Cat# 740609.50) according to manufacturer's instructions. cDNAs containing attB recombination sites were then recombined into pDONR221 donor vector using Gateway™ BP Clonase™ II Enzyme mix (Invitrogen™, Cat# 11789020) according to manufacturer's instructions, and the recombination reaction was then transformed into 2T1 competent bacteria. After selecting successful insertions of the cDNAs into donor plasmids by enzymatic digestion and sequencing, the cDNAs were further subcloned using Gateway™ LR Clonase™ II Enzyme mix (Invitrogen™, catalog #11791020) into Split YFP tagging destination vectors (Gohl et al. 2010). *hdc* was labelled at the N-terminal end with the N-terminal fragment of the YFP (nYFP), while *unk* and *Cam* were tagged at the N-terminal ends with the C-terminal fragment of YFP (cYFP).

To create His-tagged Hdc (hdc-His) construct, *hdc* cDNA was obtained from the *Drosophila* gold collection and amplified using the primer pairs: hdccDNA_For and hdccDNA_new_rev **(S2 Table)** and cloned into a His-tagged destination vector (pDEST17) (Thermo Fisher Scientific, Cat# 11803012) using Gateway cloning as mentioned earlier. After that, His-tagged Hdc cDNA was amplified from pDEST17 using the primer pair pDEST17-to-pHY22_For and pDEST17-to-pHY22_rev, and subcloned into pHY22 plasmid using In-Fusion HD Cloning Kit (Takara Bio, Cat# 102518) according to manufacturer's instructions.

To create GST-tagged Cam construct (Cam-GST), the cDNA of Cam was recombined from pDONR221 donor vector into a GST-tagged destination vector (pDEST24) using Gateway™ LR Clonase™ II Enzyme mix as mentioned earlier.

3.4. Immunostaining, imaging and processing of lymph gland samples

Third-stage instar larvae were placed on a rubber pad in 30 µl of Schneider's media (Lonza, Cat# 0000879623), supplemented with PTU (*N*-Phenylthiourea, Sigma-Aldrich, Cat# P7629) and 5% heat-inactivated Fetal Bovine Serum (FBS, Biosera, Cat# FB-1090/500). After fixing the head and tail ends of the larvae, the cuticle was opened carefully with tweezers and fixed with pins. The hemolymph and unwanted organs and debris were then removed by washing and dissection until the lymph gland becomes clearly visible. These preparations were then fixed in 2% paraformaldehyde (PFA, Sigma-Aldrich, Cat# 158127-5G) for 10 minutes, washed with PBS and then placed in a 48-well plate containing 200 µl of blocking solution (0.1% BSA-PBS supplemented with 0.01% Triton X-100 (SERVA Electrophoresis GmbH, Cat# 37238.01)). After blocking for 20 minutes, the preparations were incubated with primary antibody for 1 hour at room temperature or overnight at 4ºC, washed with PBS, and incubated with fluorescent secondary antibody (1:1000) and DAPI (1:400) diluted in the same blocking solution for 45 minutes at room temperature. After washing with PBS, the preparations were mounted in Fluoromount-G™ Mounting Medium (Invitrogen, Cat# 00-4958-02) on plain microscope slides, covered with Menzel Microscope Coverslips (Thermo Fisher Scientific, Cat# 11911998), and examined with Zeiss LSM800 confocal microscope. For each lymph gland, Z-stacks of 10 slices were captured using 20× objective. Images are displayed as the maximum intensity projection of the Z-stacks, after brightness/contrast was adjusted using the ImageJ/Fiji (US National Institutes of Health, Bethesda, MD, USA) image processing software. Images from each experiment and the appropriate control were taken using the same microscope settings. For quantifying lamellocyte (L1 positive cells) differentiation in lymph glands, lymph glands from each genotype were divided into three categories: lymph glands containing 0 lamellocytes, lymph glands containing 5 or fewer lamellocytes (≤5), or lymph glands containing more than 5 lamellocytes (>5), and percentages of these categories were calculated. The size of P1 positive (plasmatocyte) area in an anterior lobe was measured by ImageJ/Fiji, and the percentage to the size of the anterior lobe was then calculated. Crystal cells in lymph glands (C1 positive cells) were counted manually using the multi-point tool in ImageJ/Fiji, and crystal cell index was calculated as the number of crystal cells in the lobe divided on the size of the lobe. For assessing the fluorescence intensity of *hdc>GFP*, *gstDGFP*, or *Thor-LacZ*, the mean fluorescence intensity (MFI) was measured based on the pixel

intensity of a selected area. MFI was shown as a fold change in comparison to the average MFI in the control of each experiment.

3.5. Immunostaining, imaging, and counting of circulating hemocytes

To isolate hemocytes from third stage instar larvae, larvae were dissected in 30 µl of Schneider's media supplemented with 5% FBS and PTU in a 12-well slide (Hendley-Essex, Cat# SM011). Hemocytes were left to attach to the surface of the side for 1 hour at room temperature in a wet chamber. The samples were then fixed in acetone for 6 minutes, blocked for 20 minutes in 0.1% BSA-PBS, and incubated with the primary antibody in a wet chamber for one hour at room temperature or overnight at 4ºC. After washing in PBS, hemocytes were then incubated in a wet chamber for 45 minutes with secondary fluorescent antibody (1:1000) and DAPI (1:400) diluted in the same blocking solution. Finally, after washing samples with PBS, they were mounted as previously mentioned and images of the samples were taken using 10× objective in Zeiss Axio Imager Z1 fluorescence microscope. Nuclei were counted automatically using the 'cellcounter' macro in ImageJ/Fiji software. Lamellocytes (L1 positive cells) were counted manually using the multi-point tool in ImageJ/Fiji, and the percentage of lamellocytes to the nuclei number was calculated. A minimum of 100 nuclei were counted from each larva.

3.6. Wasp Infestation

For the wasp infestation experiment, two crosses containing 10 w^{1118} virgins and 10 *hdc>GFP* (*UAS-mCD8::GFP; hdc*^{19}*-Gal4/TM6Tb)* males each were done and left for 24 hours to mate. The next day, the females of each cross were transferred to a new vial to lay eggs for 4 hours, and 72 hours after egg laying, 25 female *Leptopilina boulardi* G486 parasitic wasps (Carton et al., 1992) were added to one of the two vials and left to infest the larvae for 4 hours at 25 °C, while the other vial was left at 25 °C without infestation to serve as a control. 16 hours post infestation (hpi), Infested larvae were selected based on the melanized injury site caused by the oviposition, and lymph glands were dissected from them or naive uninfested control larvae.

3.7. Western blot

To confirm the functionality of HA-tagged Hdc isoforms, 15 larvae from each of the following genotypes: *UAS-hdcRA_STOP/Actin-Gal4, UAS-mCherry*, *UAS-hdcRC_STOP /Actin-Gal4, UAS-mCherry, UAS-hdcRC_NOSTOP/Actin-Gal4, UAS-mCherry* in addition to the negative control

+/Actin-Gal4, UAS-mCherry were exposed to two freezing cycles in liquid nitrogen, and physically homogenized in 120 µl of 1x Laemmli sample buffer, and then boiled on 95 °C for 5 minutes. 40 µl of each sample was then loaded into a 10% SDS-PAGE gel with 6 µl of the Precision Plus Protein ladder (Bio-Rad, Cat# 1610373). After running, the proteins were blotted onto PVDF membrane (Merck-Millipore, Cat#IPVH00010), blocked in 5% dry milk diluted in 0.1% TBS-TWEEN (Molar Chemicals Kft, Cat# 09400), incubated with primary and secondary antibodies, and then the membrane was developed using Amersham ECL Prime Western Blotting Detection Reagent (Cytiva, Cat# RPN2232) according to manufacturer's instructions.

3.8. The liquid chromatography-tandem mass spectrometry (LC-MS/MS) analysis

For Sample preparation, 25 *Drosophila melanogaster* larvae from the genotype (*UAS-hdcRA_STOP/+; $hdc^{\Delta 84}$/ hdc^{19}-Gal4*) were collected, frozen in liquid nitrogen and ground with TissueLyser (QIAGEN) at 50 Hz, and total proteins were extracted using the manufacturer's Lysis buffer supplemented with 1 mM DTT, 1 mM PMSF, 1x protease inhibitor cocktail (Sigma-Aldrich, Cat#539136), 3 mM pNPP, 1 µM proteasome inhibitor MG132. Total protein extracts (4mg/immunoprecipitate) were then immune-purified using anti-HA (three replicates) or anti-GFP (three replicates, serving as a negative control) antibodies conjugated to 50 nm magnetic beads (MACS Technology, Miltenyi) digested in column with trypsin, and analyzed in a single run on the mass spectrometer (Hubner et al. 2010).

Raw data were converted into peak lists using the in-house PAVA software (Guan et al. 2011) and searched against the UniProt *Drosophila melanogaster* database, including additional proteins identified from a previous Swiss-Prot search (protein score>50) using Protein Prospector search engine (v5.15.1) with the following parameters: enzyme, trypsin with maximum 1 missed cleavage; mass accuracies, 5 ppm for precursor ions and 0.6 Da for fragment ions (both monoisotopic); fixed modification, carbamidomethylation of Cystine residues; variable modifications, acetylation of protein N-termini; Methionine oxidation, cyclization of N-terminal Glutamin residues allowing a maximum of two variable modifications per peptide. Acceptance criteria were: minimum scores: 22 and 15; maximum E values: 0.01 and 0.05 for protein and peptide identifications, respectively. The false discovery rate was calculated using peptide identifications representing randomized proteins (2×number of random IDs/total peptide IDs = 2× number of random IDs divided by peptide IDs).

The relative abundance of each protein in the Hdc-HA samples and control samples was calculated using spectral counting. The individual protein peptide counts were first normalized to the total number of peptide identifications in each sample, then the normalized peptide counts were compared in the two samples. For calculating enrichment between Hdc-HA and the control, edgeR was used (Y. Li & Andrade 2017).

3.9. The Split/YFP experiment

For testing the interaction between Hdc and Cam, hdc-nYFP and Cam-cYFP, hdc-nYFP and unk-cYFP (positive control), and hdc-nYFP and PCID2-cYFP (negative control) constructs were co-transfected respectively with pMT-Gal4 vector (DGRC #1042), in which an inducible metallothionein promoter expresses the Gal4 protein, into S2R+ *Drosophila* cell line using the Effectene Transfection Reagent Kit (Qiagen, cat# 301425) according to the manufacturer's instructions. The cells were maintained at 25 °C in Schneider's media containing 10% FBS and 1% antibiotics (Penicillin-Streptomycin, Gibco, Cat# 15140122). 48 hours after transfection, copper sulfate was added to the cells in a 1 mM final concentration to induce protein expression and it was left for 2 hours. After that, the copper sulfate containing media was replaced with 3 ml of fresh media and the interaction was visualized using Zeiss LSM800 confocal microscope and photos were taken using the 63× OIL immersion objective.

3.10. The pull-down assay

For producing the tagged proteins, the Hdc-His protein was expressed in coupled *in vitro* transcription and translation reaction (IVTT) at 30 °C for 1.5 hours using the TNT Quick Coupled Transcription/Translation System (Promega, Cat# L1170,) according to manufacturer's instructions, while for expressing the Cam-GST protein, six-pack *E. coli* cells were used (Lipinszki *et al.* 2018). Briefly, a single transformed colony was grown in 100 ml standard LB medium at 37 °C until the culture reached an OD600 between 0.6-0.8. After that, 0.5 mM IPTG (Isopropyl β- d-1-thiogalactopyranoside) was added to the culture to induce the expression of Cam-GST, in addition to 1mM of CaCl2 to help stabilize the Cam protein in the culture, and the culture was further left for 3 hours at 37 °C, and the bacterial pellet was then harvested by centrifugation (11.000 *g*, 4 °C, 20 min).

For the pull-down assay experiment, the bacterial pellet containing the Cam protein was first washed with PBS, and then resuspended in a lysis buffer (1M Tris pH 7.4, 1M DTT, 5M NaCl, 1M

CaCl2, 10% glycerol, 1x protease inhibitor cocktail (Roche, cat# 11873580001)) and sonicated 4x2 minutes (40% sonication energy and 60% pulse intensity). After sonication, 1% Triton-X was added to the bacteria suspension and left on ice for 30 minutes to aid further in lysing the bacteria, and the lysate was centrifuged to get rid of cellular debris (11.000 *g*, 4 °C, 20 min). After centrifugation, the supernatant containing the Cam-GST protein was transferred into a new tube and the IVTT reaction containing Hdc-His and Glutathione Beads (GE Healthcare, Cat#17-0756-01) that can bind to GST were added, and the mixture was rotated for 2 hours at 4 °C. Serving as a negative control, the IVTT reaction containing Hdc-His was diluted in PBS containing GST tagged Glutathione Beads and also rotated for 2 hours at 4 °C. After rotation, the two mixtures were then centrifuged (600 *g*, 4 °C, 3 min), washed 2x with PBS, centrifuged again, and the Glutathione beads in the pellet were boiled in 1x Laemmli sample buffer for 5 min at 95 °C and then stored at -20 °C for western blot.

For the western blot experiment, the Proteins were separated on a 10% SDS-PAGE gel and blotted onto PVDF membrane (Merck-Millipore, Cat#IPVH00010), and anti-His-HRP (1:10000, Sigma, Cat# A7058-1VL) and anti-GST-HRP (1:10000, Merck, Cat# 16-209) antibodies were used to detect the epitope tagged proteins.

3.11. Data analysis

All quantitative analyses of data were done using GraphPad Prism 8. Graphs were made using GraphPad Prism 8 and BioRender.com. For data consisting of two groups, two-tailed unpaired student's t-test was used, while for data consisting of more than two groups, analysis of variance (ANOVA) with Tukey's test for multiple comparisons was utilized. Values of $p < 0.05$ were accepted as significant (* $p \leq 0.05$, ** $p \leq 0.01$, *** $p \leq 0.001$, **** $p \leq 0.0001$, ns: non-significant).

4. Results

4.1. Characterizing the role of Hdc in the hematopoietic niche

4.1.1. Hdc negatively regulates the insulin/mTOR pathway in the PSC niche

My colleagues previously demonstrated that silencing of *hdc* in the PSC niche leads to the appearance of lamellocytes, the effector hemocytes that normally differentiate only after immune induction, in naive larvae. This suggests a non-cell-autonomous role for Hdc in progenitor maintenance in the *Drosophila* lymph gland **(Figs 15A and 15B, 16A and 16B, and quantified in 15J and 16J)** (Varga et al. 2019). In a follow up experiment, we knocked down Unk, one of the two only described partners for Hdc in literature (Avet-Rochex *et al.* 2014; N. Li *et al.* 2019), using the PSC-specific driver *col-Gal4* driver (Krzemień *et al.* 2007), and found that it causes a comparable phenotype to *hdc* silencing (**Figs 15C and 16C, and quantified in 15J and 16J)**. Moreover, we observed that silencing of both *hdc* and *unk* together further boosts lamellocyte differentiation in *col>hdcRNAi* animals **(Figs 15D and 16D, and quantified in 15J and 16J)**, suggesting that both proteins interact in the niche to suppress progenitor differentiation.

Given that Hdc and Unk were shown to control the insulin/mTOR signaling in the larval imaginal discs (Loncle & Williams 2012; Avet-Rochex et al. 2014; N. Li et al. 2019; Giannios & Casanova 2021), we wanted to investigate the possibility of the involvement of the insulin/mTOR pathway in the hematopoietic phenotype caused by *hdc* loss-of-function in the niche. This assumption is backed up by former findings showing that activating the insulin/mTOR pathway in the niche via expressing a constitutively active form of the Pi3K kinase (Pi3KCa) or silencing the negative regulator Pten leads to lamellocyte differentiation (Y. Tokusumi et al. 2012; Kaur et al. 2019), as demonstrated in **(Figs 15E and 15F, 16E and 16F, and quantified in 15J and 16J)**.

Agreeing with these observations, we found that inhibiting the insulin/mTOR pathway through knocking down the Akt kinase in the insulin pathway (Tsuchiya et al. 2014), or Raptor, a member of the mTORC1 complex and a partner of Hdc (N. Li et al. 2019) suppresses the appearance of lamellocytes in the lymph gland of *col>hdcRNAi* larvae and their release into the circulation **(Figs 15G and 15H, 16G and 16H, and quantified in 15J and 16J)**. Furthermore, *hdc* overexpression in *col>PtenRNAi* larvae decreases lamellocyte numbers in the lymph gland and circulation of these animals **(Figs 15I and 16I, and quantified in 15J and 16J)**.

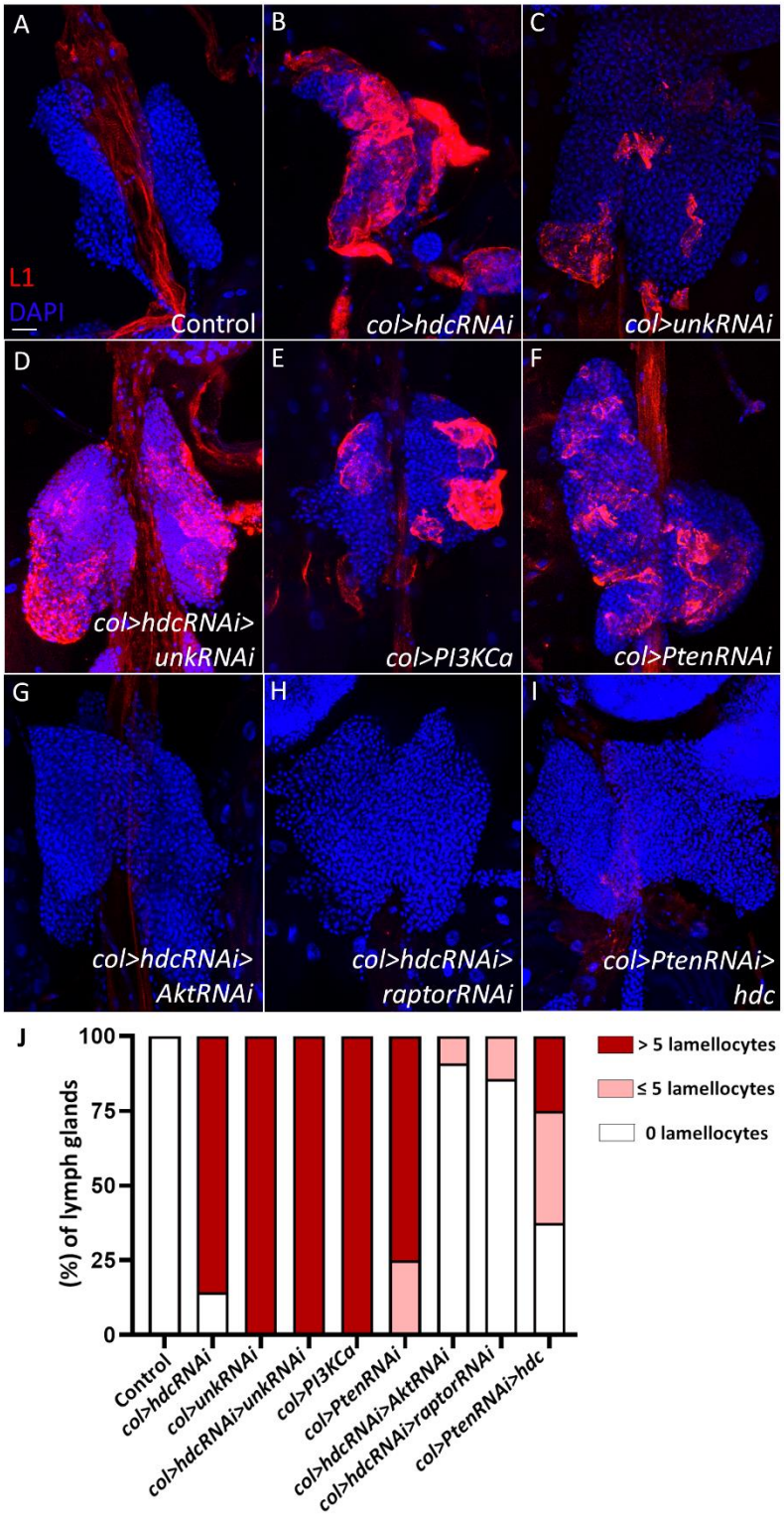

Fig 15. Lymph gland samples from the interaction between *hdc* and the insulin/mTOR pathway in the niche. (A-F) Lamellocytes (red) are absent from control lymph glands (*Pcol85-Gal4/+*) (n = 7) (A), while they are present when *hdc* is silenced in the PSC (*Pcol85-Gal4,UAS-hdcRNAi/+*) (n=7) (B), its partner

unk is silenced (*Pcol85-Gal4/UAS-unkRNAi)* (n = 6) (C), *hdc* and *unk* are silenced together (*Pcol85-Gal4,UAS-hdcRNAi/UAS-unkRNAi*) (n = 9) (D), a constitutively active *Drosophila Pi3K* is expressed (*UAS-Pi3K92E.CAAX/+; Pcol85-Gal4/+*) (n = 8) (E), or the negative insulin pathway regulator *Pten* is silenced (*Pcol85-Gal4/+; UAS-PtenRNAi/+*) (n = 8) (F). (G-H) Lamellocyte differentiation in *col>hdcRNAi* larvae is rescued when simultaneously either *Akt* (*Pcol85-Gal4, UAS-hdcRNAi/+; UAS-AktRNAi/+*) (n = 11) (G) or *raptor* (*Pcol85-Gal4,UAS-hdcRNAi/+; UAS-raptorRNAi/+*) (n=7) are silenced (H). (I) Overexpression of *hdc* rescues lamellocyte differentiation in *col>PtenRNAi* larvae (*Pcol85-Gal4/+; UAS-PtenRNAi/UAS-hdc.S*) (n=8). n refers to the number of lymph glands analyzed. Nuclei are visualized by DAPI (blue). Scale bar: 20 μm. (J) A bar graph showing the percentage of lymph glands from the genotypes presented in panels (A-I) categorized into lymph glands with 0 lamellocytes, lymph glands with 5 or fewer lamellocytes, and lymph glands containing more than 5 lamellocytes.

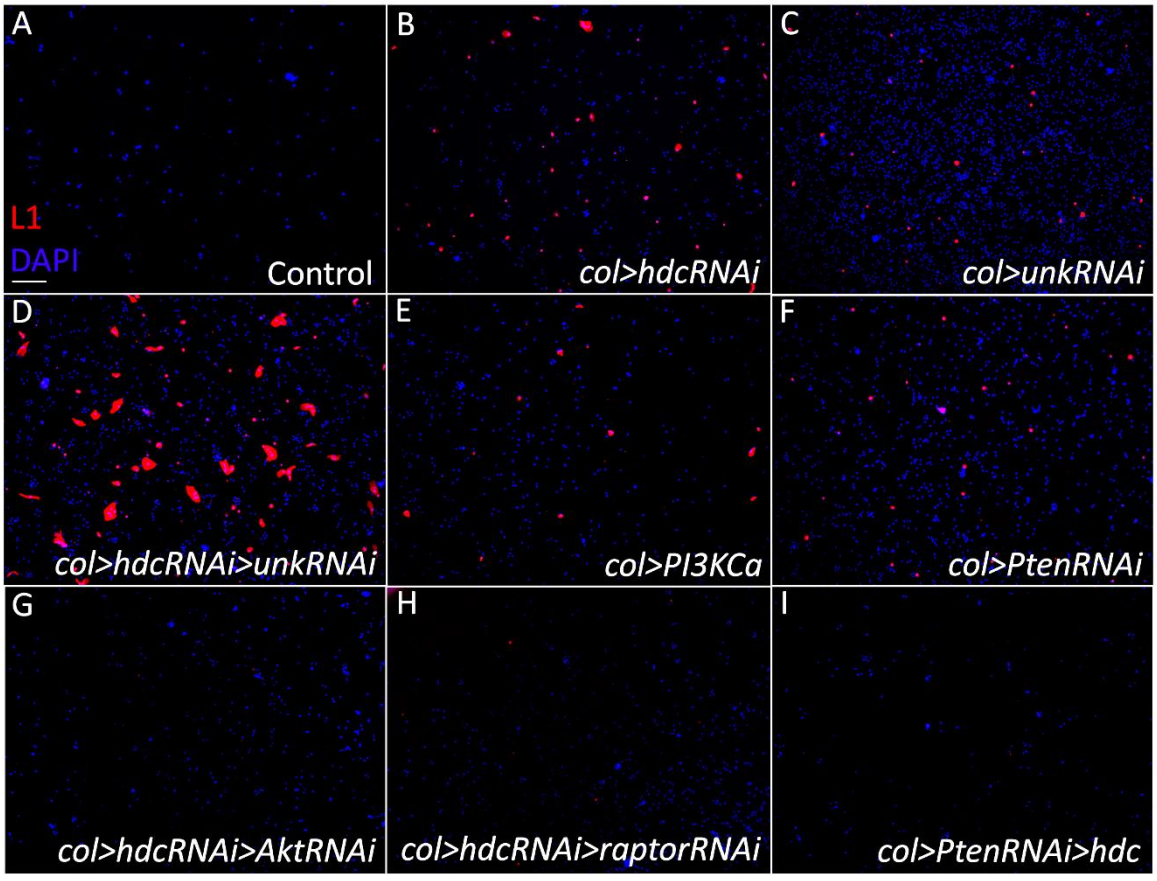

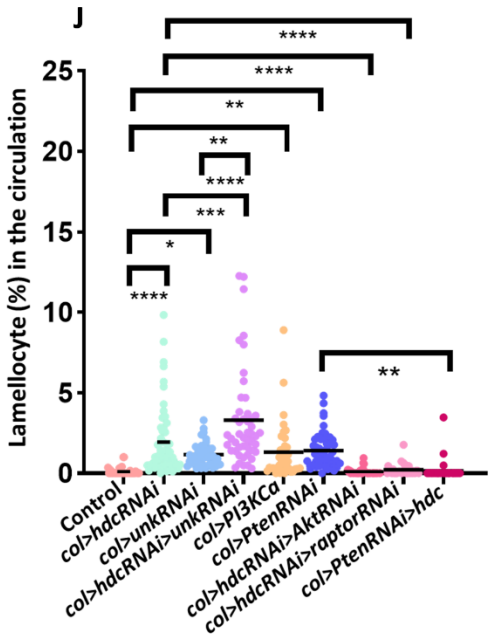

Fig 16. Circulation samples from the interaction between *hdc* and the insulin pathway in the niche. (A-F) Lamellocytes (red) are absent in the circulation of control larvae (*Pcol85-Gal4/+*) (0.08% (n = 43)) (A), but can be detected when *hdc* is silenced in the PSC (*Pcol85-Gal4,UAS-hdcRNAi/+*) (1.9% (n = 53)) (B), its partner *unk* is silenced (*Pcol85-Gal4/UAS-unkRNAi)* (1.1% (n = 44)) (C), both *hdc* and *unk* are silenced together (*Pcol85-Gal4,UAS-hdcRNAi/unkRNAi*) (3.2% (n = 48)) (D), the insulin/mTOR pathway is activated in the PSC by expressing *Pi3KCa* (UAS-*Pi3K92E.CAAX /+; Pcol85-Gal4/+*) (1.3% (n = 39)) (E), or silencing *Pten* (*Pcol85-Gal4/+; UAS-PtenRNAi/+*) (1.4% (n = 51)) (F). (G-H) The number of lamellocytes in the circulation of *col>hdcRNAi* larvae is reduced when simultaneously *Akt* (*Pcol85-Gal4, UAS-hdcRNAi/+; UAS-AktRNAi/+*) (0.08% (n = 41)) (G) or *raptor* (*Pcol85-Gal4, UAS-hdcRNAi/+; UAS-raptorRNAi/+*) (0.2% (n = 34)) is silenced (H). (I) Overexpression of *hdc* reduces lamellocyte numbers in the circulation of *col>PtenRNAi* larvae (*Pcol85-Gal4/+; UAS-PtenRNAi/UAS-hdc.S*) (0.14% (n = 36)). n refers to the number of larvae analyzed. Nuclei are visualized by DAPI (blue). Scale bar:20 μm. (J) A scatter dot plot showing the percentage of lamellocytes in the circulation of larvae from the genotypes presented in panels (A-I). Each dot in the graph represents a single larva. Data were analyzed using ANOVA with Tukey's test for multiple comparisons, * $p \leq 0.05$, ** $p \leq 0.01$, *** $p \leq 0.001$, **** $p \leq 0.0001$.

All these findings together point to the role of Hdc as a negative regulator of the insulin/mTOR pathway in the niche and propose that when Hdc function declines, the insulin/mTOR pathway will be continuously active, which would in turn trigger lamellocyte differentiation in the lymph gland and their subsequent release into the hemolymph.

4.1.2. Hdc depletion causes apoptosis in the hematopoietic niche

PSC size has been reported to increase when the insulin/mTOR pathway is continuously active in the hematopoietic niche (Benmimoun et al. 2012; Y. Tokusumi et al. 2012; Kaur et al. 2019). This was also observed in our experiments when we activated the insulin/mTOR pathway in the niche by overexpressing *Pi3KCa* or silencing *Pten* **(Fig 17A–17C and quantified in 17H)**. Nonetheless, this phenotype is not observed in *col>hdcRNAi* larvae **(Fig 17D and quantified in 17H)** (Varga et al. 2019)**,** which seems to contradict our theory that silencing *hdc* leads to a continuous activation of the insulin/mTOR pathway in the niche.

One possible explanation for this phenomenon is that *hdc* silencing may cause cell death, which conceals the increase in size caused by the constant activity of the insulin/mTOR pathway. To investigate this possibility, we expressed the apoptosis inhibitor *p35* simultaneously while silencing *hdc* in the niche. Indeed, we observed that this restored PSC cell number in *col>hdcRNAi* larvae, without causing any difference in control larvae **(Fig 17E and 17F, and quantified in 17H)**, implying that our hypothesis was correct. Furthermore, we found that depleting Hdc in the niche of *col>PtenRNAi* larvae reduces its size to normal in these animals **(Fig 17G and quantified in 17H)**, demonstrating that cell death due to the loss of *hdc* compensated for the increase in niche size resulting from the insulin/mTOR pathway activation.

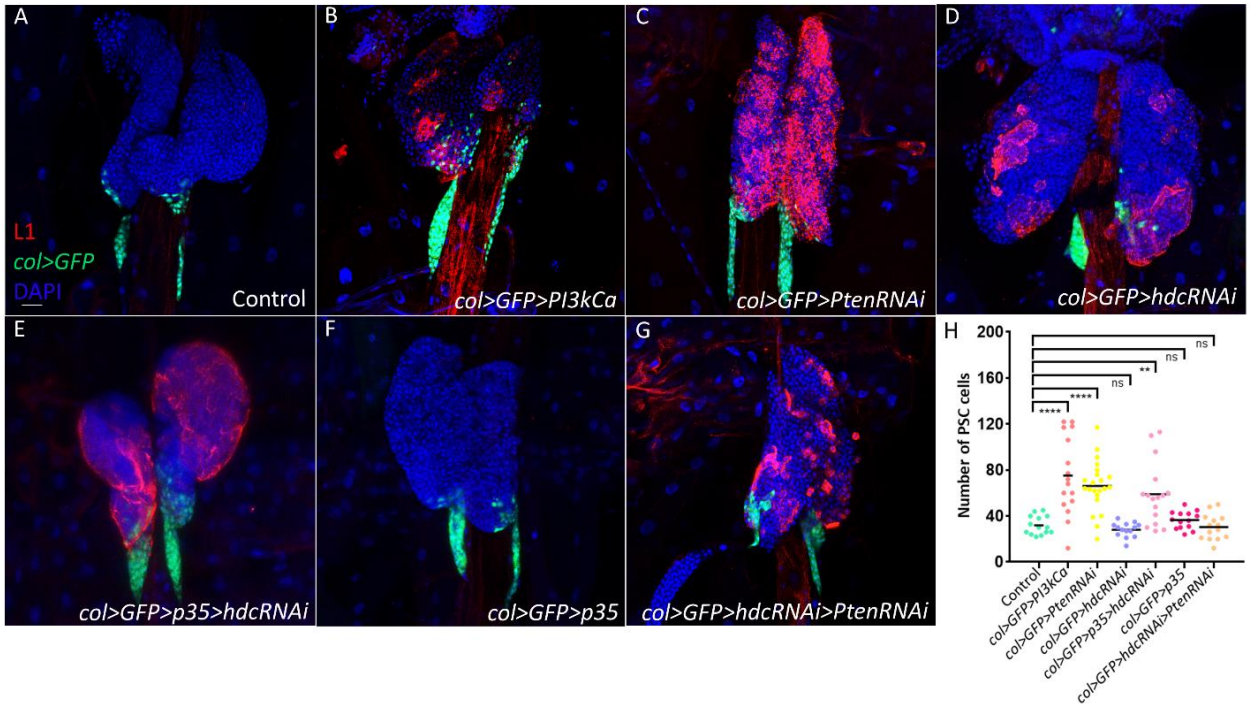

Fig 17. *hdc* silencing causes apoptosis in the hematopoietic niche. (A-C) An enlargement of the PSC is observed when the insulin/mTOR pathway is activated by expressing *Pi3Kca* (UAS-*Pi3K92E.CAAX; Pcol85-Gal4, UAS-GFP/+*) (average number of PSC cells = 75, n = 16) (B) or silencing *Pten* (*Pcol85-Gal4, UAS-GFP/+; UAS-PtenRNAi*) (average number of PSC cells = 66, n = 22) (C) in comparison to the control (*Pcol85-Gal4, UAS-GFP/+*) (average number of PSC cells = 31, n = 14) (A). (D-F) Silencing *hdc* alone does not alter PSC size (*Pcol85-Gal4, hdcRNAi/+; UAS-2xEGFP/+*) (average number of PSC cells = 28, n = 14) (D), while simultaneous overexpression of the apoptosis inhibitor *p35* increases PSC cell numbers (*Pcol85-Gal4,hdcRNAi/+; UAS-2xEGFP/UAS-p35*) (average number of PSC cells = 59, n = 16) (E), a phenotype not observed in case *p35* is overexpressed alone (*Pcol85-Gal4, UAS-GFP/+; UAS-p35/+)* (average number of PSC cells = 36, n = 14) (F). (G) Silencing *hdc* simultaneously with *Pten* reduces PSC size of *col>PtenRNAi* larvae to normal (*Pcol85-Gal4, hdcRNAi/+; UAS-2xEGFP/UAS-PtenRNAi*) (average number of PSC cells = 30, n = 14) (blue: nuclei, green: PSC, red: lamellocytes). n refers to the number of lymph gland lobes analyzed. Scale bar: 20 μm. (H) A scatter dot plot showing PSC cell number in larvae from the genotypes presented in panels (A-G). Each dot in the graph represents a PSC from one lymph gland lobe. Data were analyzed using ANOVA with Tukey's test for multiple comparisons, ** $p \leq 0.01$, **** $p \leq 0.0001$, ns: non-significant.

4.1.3. *hdc* silencing causes ROS accumulation in the niche of the lymph gland, which in turn triggers lamellocyte differentiation

The overactivation of the insulin/mTOR pathway leads to higher levels of protein production, which can overload the cell machinery and create a status of cellular stress (Giannios & Casanova 2021). In the hematopoietic niche of the lymph gland, activation of the insulin/mTOR pathway results in ROS buildup, which acts as a non-cell-autonomous signal that triggers the differentiation of progenitors (Sinenko et al. 2012; Kaur et al. 2019).

To investigate whether *hdc* silencing in the niche results an elevation in ROS levels, we utilized the *gstD-GFP* reporter, a transgenic line where the expression of GFP is driven by the *Glutathione S transferase D1* gene enhancer, which is sensitive to oxidative changes in the cell (Sykiotis & Bohmann 2008). As anticipated, we found that the *gstD-GFP* is upregulated in the niche of *col>hdcRNAi* larvae in comparison to control larvae **(Fig 18A-18B' and quantified in 18C)**. Moreover, another sensor for cellular stress, *Thor-lacZ*, which is directly regulated by the levels of Forkhead box O (Foxo) transcription factor (that gets elevated in response to ROS accumulation) (Jünger et al. 2003; Puig et al. 2003; Teleman et al. 2008; Sinenko et al. 2012) is activated in the niche of these larvae **(Fig 18D-18E' and quantified in 18F)**, proving that the niche is under an oxidative stress status when Hdc is depleted.

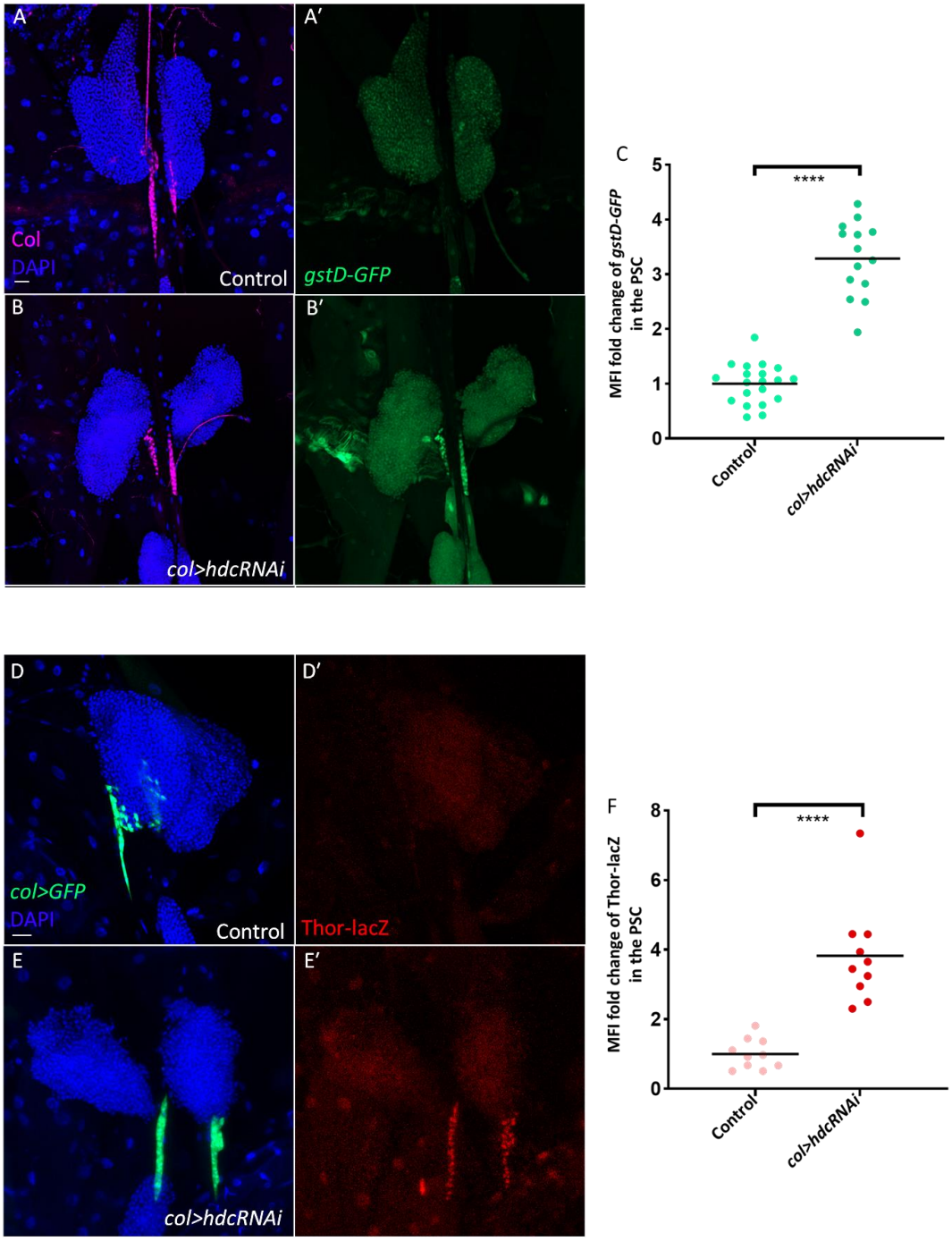

Fig 18. *hdc* silencing in the niche elevates ROS levels in it. (A-B') Silencing *hdc* results in the activation of the *gstD-GFP* reporter in the PSC (*Pcol85-Gal4, UAS-hdcRNAi/gstD-GFP*) (number of lobes =14) (B-B'), in comparison to the control (*Pcol85-Gal4/gstD-GFP*) (number of lobes = 20) (A-A') (blue: nuclei, green: ROS, magenta: Collier). (C) A scatter dot plot showing the fold change (average = 3.2 folds) increase in the mean fluorescence intensity (MFI) of *gstD-GFP* in the PSC of *col>hdcRNAi* (*Pcol85-Gal4, UAS-hdcRNAi/gstD-GFP*) larvae in comparison to the control (*Pcol85-Gal4/gstD-GFP*). Each dot in the graph represents a PSC from one lobe. Data were analyzed using two-tailed unpaired Student's t-test, **** $p \leq$

0.0001. (D-E') Silencing *hdc* induces the transcription of *Thor* as detected by an anti-lacZ staining for the *Thor-lacZ* reporter (*Pcol85-Gal4, UAS-hdcRNAi/Thor-lacZ*) (number of lobes = 10) (E-E') in comparison to the control (*Pcol85-Gal4/Thor-lacZ*) (number of lobes = 10) (D-D') (blue: nuclei, green: PSC, red: Thor-LacZ). (F) A Scatter dot plot showing the fold change (average = 3.8 folds) increase in MFI of Thor-LacZ in the PSC cells of *col>hdcRNAi* (*Pcol85-Gal4, UAS-hdcRNAi/Thor-lacZ*) larvae compared to the control (*Pcol85-Gal4/Thor-lacZ*). Each dot in the graph represents a PSC from one lobe. Data were analyzed using two-tailed unpaired student's t-test, **** $p \leq 0.0001$.

Next, we asked whether ROS buildup in the niche of *col>hdcRNAi* larvae is the reason behind lamellocyte differentiation. To investigate this, we overexpressed the Catalase enzyme that degrades ROS, and the FoxO transcription factor that upregulates the expression of antioxidant enzymes (Finkel & Holbrook 2000; Nemoto & Finkel 2002) in *col>hdcRNAi* larvae. We found that overexpressing either of these factors rescued lamellocyte differentiation in the lymph gland and decreased circulating lamellocyte numbers **(Fig 19A-19C and 19A'-19C' and quantified in 19G and 19G')**. We also observed that knocking down *foxo* simultaneously with *hdc* in the niche increases lamellocyte differentiation **(Fig 19D-19E and 19D'-19E' and quantified in 19G and 19G')**, further evidence that the niche-specific buildup of ROS promotes lamellocyte differentiation upon *hdc* knockdown. Previously, it was shown that high levels of ROS in the niche triggers the secretion of the EGFR pathway ligand Spitz (Spi), which binds to its receptors in the MZ and causes the differentiation of progenitors into lamellocytes (Kaur et al.bsk, 2019; Sinenko et al., 2012). However, in our experiments, silencing *spi* does not rescue lamellocyte differentiation in *col>hdcRNAi* larvae **(Fig 19F and 19F' and quantified in 19G and 19G')**, which indicates the implication of either another EGFR ligand or another non-cell-autonomous mechanism. All the above imply that the activation of the insulin/mTOR pathway in *col>hdcRNAi* larvae causes cellular stress and excess production of ROS, which in turn triggers lamellocyte differentiation non-cell-autonomously.

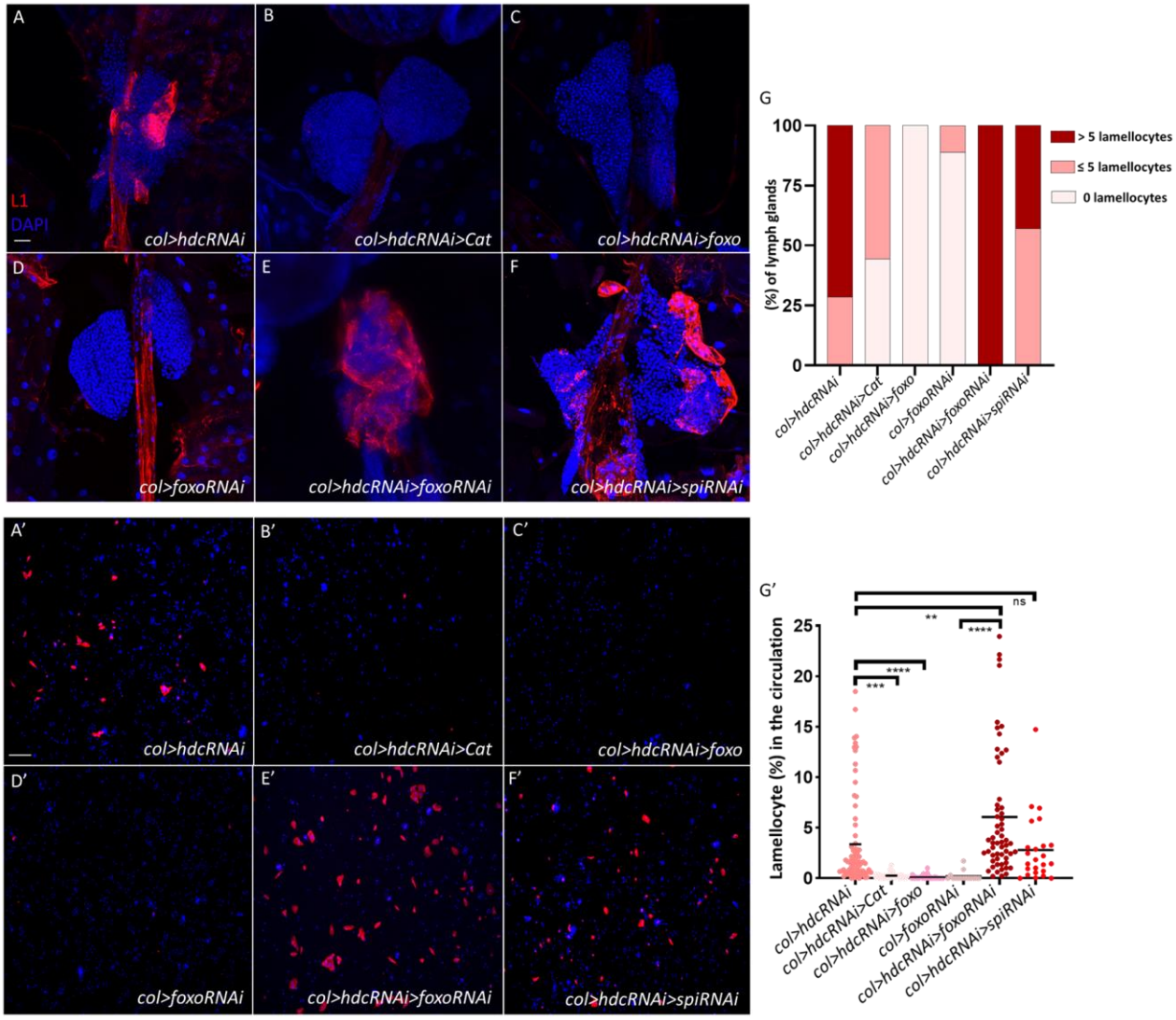

Fig 19. *hdc* mutant lamellocyte phenotype is affected by ROS levels in the niche. (A-C) Overexpressing *Cat* (*Pcol85-Gal4, UAS-hdcRNAi/UAS-Cat*) (n = 9) (B) and *foxo* (*Pcol85-Gal4, UAS-hdcRNAi/UAS-foxo*) (n = 10) (C) rescue lamellocyte differentiation in the lymph glands of *col>hdcRNAi* (*Pcol85-Gal4, UAS-hdcRNAi/+*) larvae (n = 7) (A). (D-E) Silencing *foxo* alone in the niche does not lead to lamellocyte differentiation in the lymph gland (*Pcol85-Gal4/+; UAS-foxoRNAi/+*) (n = 9) (D), while silencing it together with *hdc* enhances *hdc* mutant lamellocyte phenotype in the lymph gland (*Pcol85-Gal4, UAS-hdcRNAi/+; UAS-foxoRNAi/+*) (n = 10) (E). (F) Silencing *spi* does not affect lamellocyte differentiation in *col>hdcRNAi* lymph glands (*Pcol85-Gal4, UAS-hdcRNAi/UAS-spiRNAi*) (n = 7) (blue: nuclei, red: lamellocytes). n refers to the number of lymph glands analyzed. Scale bar: 20 μm. (G) A bar graph showing the percentage of lymph glands from the genotypes in the panels (A-F) categorized into lymph glands with 0 lamellocytes, lymph glands with 5 or fewer lamellocytes, and lymph glands containing more than 5 lamellocytes. (A'-C') Overexpressing *Cat* (*Pcol85-Gal4, UAS-hdcRNAi/UAS-Cat*) (0.25% (n = 40)) (B') or *foxo* (*Pcol85-Gal4, UAS-hdcRNAi/UAS-foxo*) (0.08% (n = 51)) (C') rescue lamellocyte release into the circulation in response to *hdc* silencing (*Pcol85-Gal4, UAS-hdcRNAi/+*) (2% (n = 69)) (A'). (D'-E') Silencing *foxo* alone in the niche does not lead to lamellocyte appearance in the circulation (*Pcol85-Gal4/+;*

UAS-foxoRNAi/+) (0.19% (n = 15)) (D'), while silencing it together with *hdc* increases significantly the number of lamellocytes present in the circulation of *col>hdcRNAi* animals (*Pcol85-Gal4,UAS-hdcRNAi/+; UAS-foxoRNAi/+*) (4.8% (n = 54)) (E') (F'). Silencing *spi* in the niche does not affect lamellocyte numbers in *col>hdcRNAi* larvae circulation (*Pcol85-Gal4,UAS-hdcRNAi/UAS-spiRNAi*) (2.8% (n = 24) (blue: nuclei, red: lamellocytes). n refers to the number of larvae analyzed. Scale bar: 20 μm. (G') A Scatter dot plot quantifying lamellocyte numbers in larvae from the genotypes in the panels (A'-F'). Each dot in the graph represents a single larva. Data were analyzed using ANOVA with Tukey's test for multiple comparisons, ** $p \leq 0.01$, *** $p \leq 0.001$, **** $p \leq 0.0001$, ns: non-significant.

4.2. Characterizing the role of Hdc in the medullary zone

4.2.1. *hdc* expression disappears from the anterior lobes of the lymph gland in response to immune induction

Previously, our colleagues have shown that *hdc* has a unique expression pattern in the lymph gland during development **(Fig 20A-20A'')** (Varga et al. 2019). In the second instar larva, *hdc* is expressed in most cells of the anterior lobes. However, *hdc* expression starts to disappear from the edges of the anterior lobes during as the CZ starts to form at the beginning of third instar larval stage, until it ceases totally by the end of the third larval stage when progenitors begin to differentiate, and the lymph gland prepares to disintegrate and release its content into the circulation. These observations intrigued us to investigate *hdc* expression in the lymph gland after immune induction with the *Leptopilina boulardi* parasitic wasp. Because the anterior lobes of the lymph gland were shown to disperse 20 hours following wasp induction (Louradour et al. 2017), we looked at lymph glands 16 hours post wasp infestation (hpi). Indeed, *hdc* expression was completely reduced in the anterior lobes of the lymph gland at this timepoint **(Fig 20B-20C" and quantified in 20D).** This change in the pattern of *hdc* expression during development and after immune induction suggests that *hdc* expression needs to be turned down in progenitors to allow their differentiation. This observation also implies that Hdc, independent from its non-cell-autonomous role in the niche, may play a cell-autonomous role in the MZ progenitors in suppressing their premature differentiation.

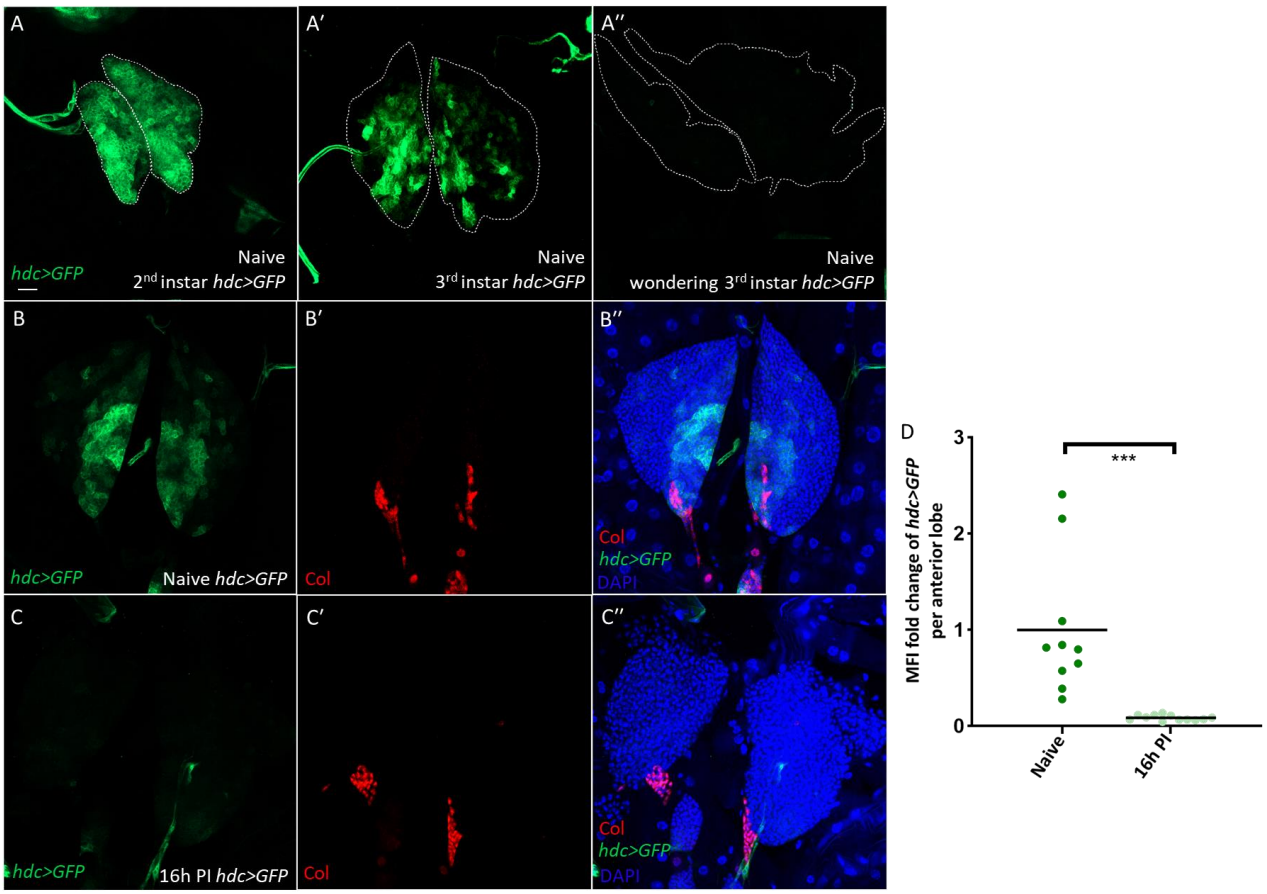

Fig 20. *hdc* expression during development and following immune induction. (A-A") *hdc>GFP* expression decreases in the anterior lobes of the lymph gland during development until it vanishes completely in late third stage wondering larvae (*UAS-mCD8::GFP; hdc^{19}-Gal4*) (green: *hdc*). (B-C") *hdc>GFP* expression disappears from the anterior lobes of the lymph gland 16 hpi) (C-C") in comparison to naive control lymph glands (*UAS-mCD8::GFP; hdc^{19}-Gal4*) (number of lobes = 10) (B-B") (blue: nuclei, green: *hdc*, red: Col). Scale bar: 20 µm. (D) A scatter dot plot showing the fold change decrease (average = -12.5 folds) in MFI of *hdc>GFP* in the anterior lymph gland lobes of wasp infested (16 hpi) larvae compared to the control (*UAS-mCD8::GFP; hdc^{19}-Gal4*). Each dot in the graph represents one anterior lobe. Data were analyzed using two-tailed unpaired Student's t-test, *** $p \leq 0.001$.

4.2.2. *hdc* knockdown in the MZ but not the IZ leads to lamellocyte differentiation at the expense of crystal cells

To examine the possibility of a cell-autonomous function of Hdc in the MZ progenitors, we silenced *hdc* using the MZ-specific driver *domeMESO*-Gal4 and investigated progenitor differentiation in these larvae. We observed lamellocyte differentiation in the lymph gland, as well as the appearance of these cells in the circulation **(Fig 21A, 21B, 21E and 21F, and quantified in 21D and 21H)**,

suggesting that Hdc is required cell-autonomously in the progenitors to suppress their premature differentiation.

Notably, when we silenced *hdc* using *CHIZ-Gal4* in the IZ intermediate progenitors, which are more differentiated than MZ progenitors (Spratford et al. 2021), lamellocytes did not differentiate **(Fig 21C and 21G and quantified in 21D and 21H)**. This aligns with our co-expression experiments, in which we found that *hdc* shows opposing expression to *Hml:DsRed* **(Fig 21I-I')**, and highlights that *hdc* functions in MZ but not in IZ progenitors as a suppressor of differentiation. Furthermore, although we did not observe a difference in the area occupied by P1 positive plasmatocytes in *domeMESO>hdcRNAi* lymph glands **(S1A and S1B Fig, quantified in S1D)**, we found a significant decrease in the crystal cell index as compared to the control **(S1E and S1F Fig, quantified in S1H)**, suggesting that the differentiation of progenitors into lamellocytes reduces the rate of their differentiation into crystal cells.

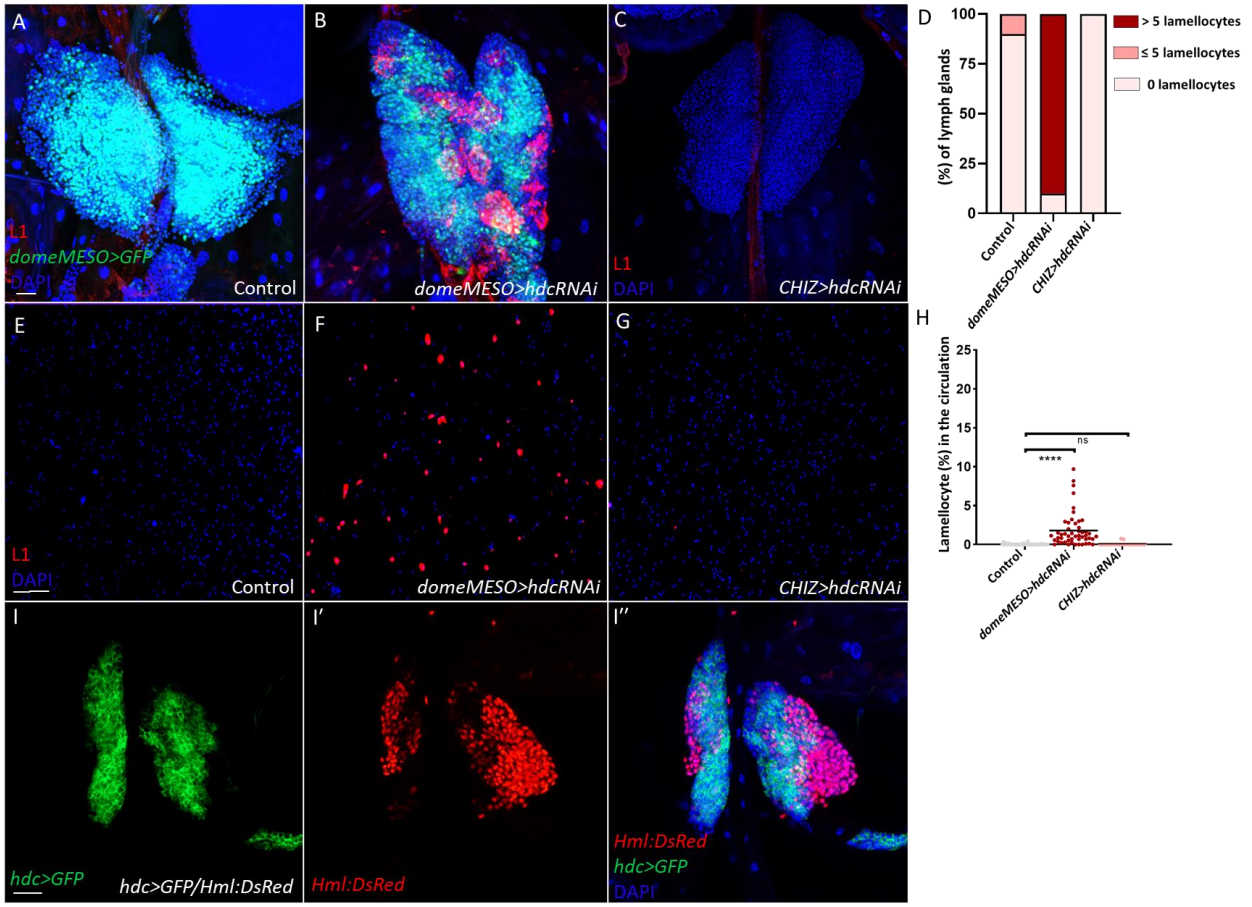

Fig 21. A new role for Hdc in the MZ. (A-C) Silencing *hdc* in the MZ leads to lamellocyte differentiation in the lymph gland (*UAS-hdcRNAi/+; domeMESO-GAL4,UAS-2xEGFP/+*) (n = 10) (B), while lamellocytes are not detected in the control (*domeMESO-GAL4,UAS-2xEGFP/+*) (n = 10) (A), or when *hdc* is silenced

using the *CHIZ-Gal4* specific for the IZ (*CHIZ-Gal4*/*UAS-hdcRNAi*) (n = 8) (C) (blue: nuclei, green: MZ, red: lamellocytes). n refers to the number of lymph glands analyzed. Scale bar: 20 μm. (D) A bar graph showing the percentage of lymph glands from the genotypes presented in panels (A-C) categorized into lymph glands with 0 lamellocytes, lymph glands with 5 or fewer lamellocytes, and lymph glands containing more than 5 lamellocytes. (E-G) Silencing *hdc* in the MZ leads to the appearance of lamellocytes in the circulation (*UAS-hdcRNAi/+; domeMESO-GAL4, UAS-2xEGFP/+*) (1.8% (n = 50)) (F), which are normally not present in the control (*domeMESO-GAL4, UAS-2xEGFP/+*) (0.04% (n = 33)) (E), or when *hdc* is silenced using the *CHIZ-Gal4* specific for the IZ (*CHIZ-Gal4*/*UAS-hdcRNAi*) (0.06% (n = 22)) (G) (blue: nuclei, red: lamellocytes). n refers to the number of larvae analyzed. Scale bar: 20 μm. (H) A scatter dot plot showing the percentage of lamellocytes in the circulation of larvae from the genotypes presented in panels (E-G). Each dot in the graph represents one single larva. Data were analyzed using ANOVA with Tukey's test for multiple comparisons, **** $p \leq 0.0001$, ns: non-significant. (I-I'') *hdc>GFP* shows complementary expression to the CZ marker *Hml:DsRed* (*UAS-mCD8::GFP; hdc^{19}-Gal4/Hml:DsRed)* (n = 8) (blue: nuclei, green: *hdc*, red: CZ). n refers to the number of lymph glands analyzed. Scale bar: 20 μm.

Collectively, these findings propose a novel, cell-autonomous function for Hdc in MZ progenitors but not the IZ progenitors, to support their maintenance. When Hdc is depleted in MZ cells, progenitors differentiate into lamellocytes instead of crystal cells.

4.2.3. Depleting Hdc leads to ROS accumulation in the lymph gland

After identifying a new cell-autonomous role for Hdc in the MZ progenitors, we sought to understand the mechanism behind their differentiation into lamellocytes. Since we found that ROS accumulates in the niche in response to *hdc* silencing, we wanted to examine whether knocking down of *hdc* in the MZ induces a similar phenotype. To assay this, we investigated *gstD-GFP* expression in larvae where *hdc* was silenced with the MZ-specific *domeMESO-Gal4* driver. A clear induction of *gstD-GFP* was observed in the anterior lobes of *domeMESO>hdcRNAi* lymph glands **(Fig 22A and 22B, quantified in 22C)**. The same was observed in the lymph glands of homozygous *hdc$^{\Delta 8}$* null larvae carrying the *gstD-GFP* reporter **(Fig 22D and 22E, quantified in 22F)**, suggesting that Hdc depletion in the progenitors leads to ROS buildup. However, unlike in the niche, we did not observe an induction in *Thor-LacZ* reporter upon depleting Hdc in the MZ **(S1I and S1J Fig, quantified in S1K)**, suggesting a different response of the progenitors to Hdc depletion as opposed to PSC cells.

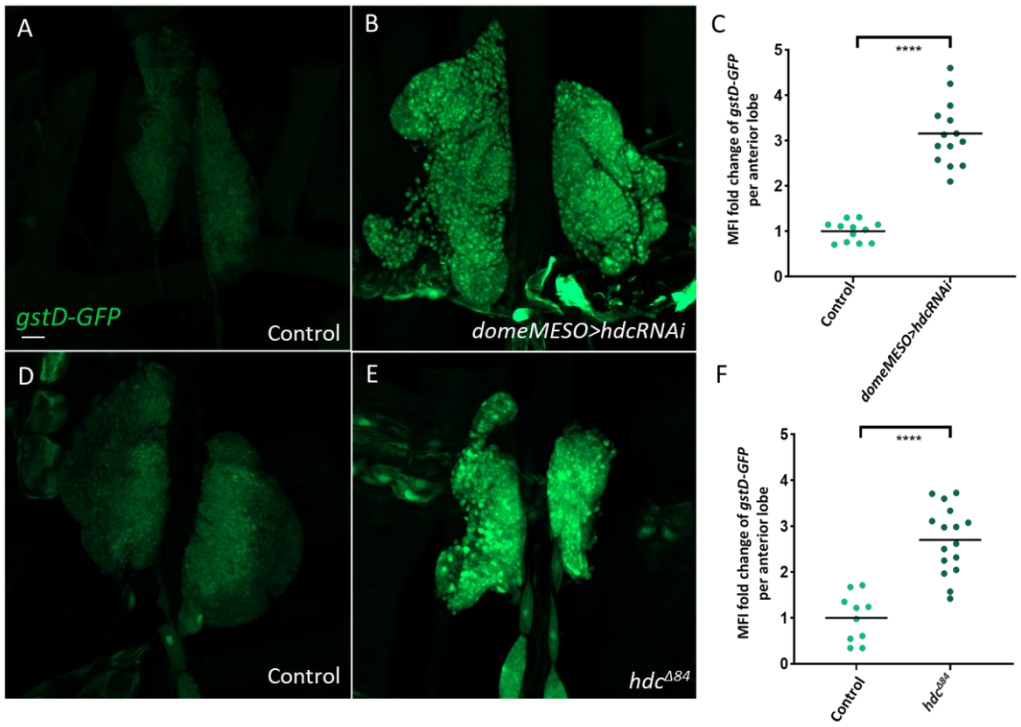

Fig 22. The induction of *gstD-GFP* by *hdc* loss-of-function. (A-B) Silencing of *hdc* in the MZ leads to higher levels of ROS in the anterior lobes of the lymph gland as visualized by the *gstD-GFP* reporter (*UAS-hdcRNAi/gstD-GFP; domeMESO-GAL4/+*) (number of lobes = 14) (B) in comparison to the control (*gstD-GFP/+; domeMESO-GAL4/+*) (number of lobes = 12) (A) (green: ROS). Scale bar: 20 μm. (C) A scatter dot plot showing the fold change increase (average = 3.1 folds) in the MFI of *gstD-GFP* per anterior lobe of *domeMESO>hdcRNAi* (*UAS-hdcRNAi/gstD-GFP; domeMESO-GAL4/+*) larvae in comparison to the control (*gstD-GFP/+; domeMESO-GAL4/+*). Each dot in the graph represents one anterior lobe. Data were analyzed using two-tailed unpaired student's t-test, **** $p \leq 0.0001$. (D-E) $hdc^{\Delta 84}$ null mutant shows higher levels of ROS in the anterior lobes (*gstD-GFP;* $hdc^{\Delta 84}$) (number of lobes = 16) (E) in comparison to the control (*gstD-GFP*) (number of lobes = 10) (D) (green: ROS). Scale bar: 20 μm. (F) A scatter dot plot showing the fold change increase (average = 2.7 folds) in the MFI of *gstD-GFP* per anterior lobe of $hdc^{\Delta 84}$ mutant larvae (*gstD-GFP;* $hdc^{\Delta 84}$) in comparison to the control (*gstD-GFP*). Each dot in the graph represents one anterior lobe. Data were analyzed using two-tailed unpaired student's t-test, **** $p \leq 0.0001$.

To determine whether elevated ROS levels in the progenitors are the reason behind their early differentiation upon Hdc depletion, we overexpressed the ROS scavenging enzyme Catalase, and found that this suppresses lamellocyte differentiation in *domeMESO>hdcRNAi* larvae **(Fig 23A, 23B, 23A', 23B', and quantified in 23D and 23D')**. This suggests that similarly to the niche, ROS functions as a signaling molecule in the MZ in response to *hdc* silencing. Notably, overexpression of *foxo* in the MZ also significantly decreases the number of lamellocytes in the lymph gland and in the circulation in *domeMESO>hdcRNAi* larvae **(Figs 23C and 23C', quantified in 23D and 23D')**. This is probably because *foxo* overexpression directs progenitor differentiation into plasmatocytes

and crystal cells, as reported in the literature and replicated in our experiments **(S3C and S3G Fig, quantified in S3D and S3H)**, which might shift progenitors from differentiating into lamellocytes.

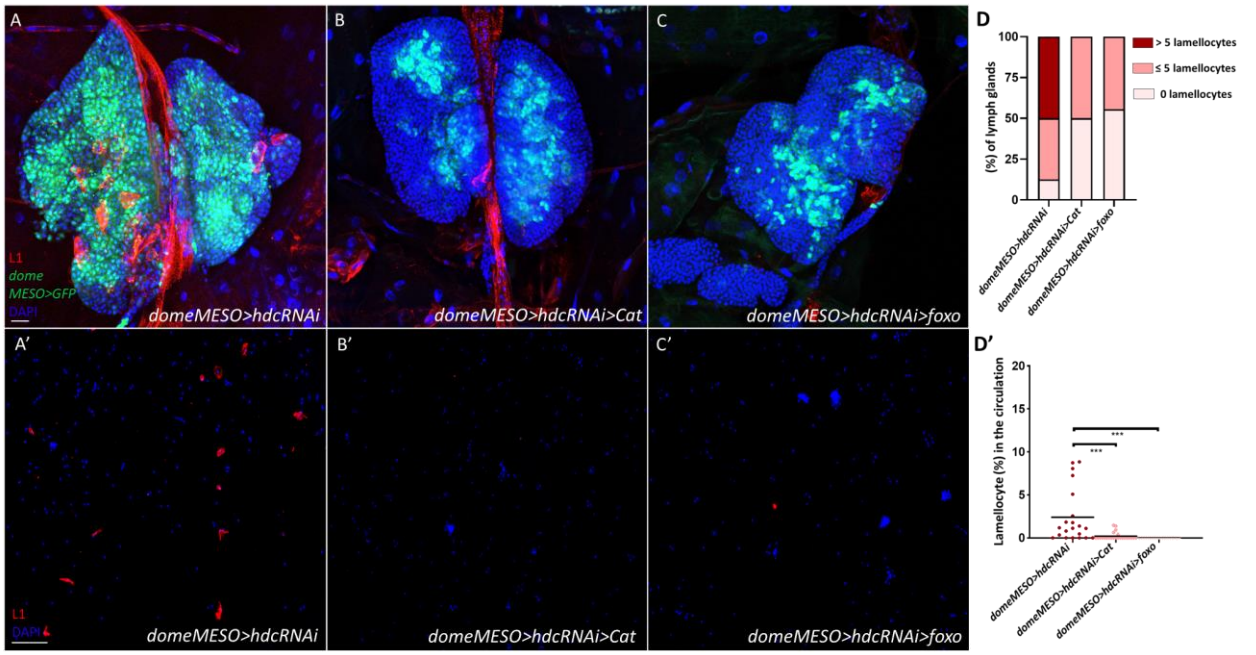

Fig 23. Lamellocyte differentiation in response to *hdc* silencing in the MZ is rescued by scavenging ROS. (A-C) Overexpression of *Cat* (*UAS-hdcRNAi/UAS-Cat; domeMESO-GAL4, UAS-2xEGFP/+*) (n = 8) (B) or *foxo* (*UAS-hdcRNAi/UAS-foxo; domeMESO-GAL4, UAS-2xEGFP/+*) (n = 9) (C) rescues lamellocyte differentiation in the lymph gland of *domeMESO>hdcRNAi* larvae (*UAS-hdcRNAi/+; domeMESO-GAL4, UAS-2xEGFP/+*) (n = 8) (A) (blue: nuclei, green: MZ, red: lamellocytes). n refers to the number of lymph glands analyzed. Scale bar: 20 μm. (D) A bar graph showing the percentage of lymph glands from the genotypes presented in panels (A-C) categorized into lymph glands with 0 lamellocytes, lymph glands with 5 or fewer lamellocytes, and lymph glands containing more than 5 lamellocytes. (A'-C') Overexpression of *Cat* (*UAS-hdcRNAi/UAS-Cat; domeMESO-GAL4, UAS-2xEGFP/+*) (0.2% (n = 24)) (B') or *foxo* (*UAS-hdcRNAi/UAS-foxo; domeMESO-GAL4, UAS-2xEGFP/+*) (0% (n = 22)) (C') reduces lamellocyte numbers in the circulation of *domeMESO>hdcRNAi* larvae (*UAS-hdcRNAi/+; domeMESO-GAL4,UAS-2xEGFP/+*) (2.4% (n = 21)) (A') (blue: nuclei, red: lamellocytes). n refers to the number of larvae analyzed. Scale bar: 20 μm. (D') A scatter dot plot showing the percentage of lamellocytes in the circulation of larvae from the genotypes presented in panels (A'-C'). Each dot in the graph represents one single larva. Data were analyzed using ANOVA with Tukey's test for multiple comparisons, *** $p \leq 0.001$.

All the above suggests that similarly to the niche, ROS acts as a signaling molecule in the MZ upon *hdc* silencing, which triggers lamellocyte differentiation. This agrees with previous literature showing that ROS functions as a cell-autonomous signal in the progenitors to induce their differentiation (Owusu-Ansah & Banerjee 2009).

4.2.4. Hdc functions upstream to distinct signaling pathways in the MZ than in the PSC

Since we found earlier that Hdc negatively regulates the insulin/mTOR pathway in the niche, we explored whether Hdc may play a similar role in the MZ. First, we silenced *unk* alone or together with *hdc* in the MZ and investigated lamellocyte differentiation in the lymph gland and circulation of the larvae. Unexpectedly, we observed that lamellocyte differentiation is not significantly affected by silencing *unk* alone in the MZ **(Fig 24A, 24B, 24A', and 24B', quantified in 24I, and 24I')**. Furthermore, *unk* silencing does not boost lamellocyte differentiation in *domeMESO>hdcRNAi* larvae **(Fig 24C and 24C', quantified in 24I, and 24I')**. Added to that, inhibition of the insulin/mTOR pathway by silencing of *Akt* and *raptor* in MZ fail to rescue *hdc* loss-of-function phenotype **(Fig 24D, 24E, 24D', and 24E', quantified in 24I, and 24I')**, excluding the insulin/mTOR pathway engagement downstream to *hdc* in the MZ.

An earlier work revealed that the activity of the EGFR pathway in the MZ is indispensable for progenitor immune response to wasp parasitization (Louradour et al. 2017). Another study has found that elevated ROS levels in the MZ promote progenitor differentiation by activating the JNK pathway and decreasing the adhesion molecule E-cadherin (E-cad) levels in progenitors (Owusu-Ansah & Banerjee 2009). Therefore, we investigated if these pathways are involved in lamellocyte differentiation in response to *hdc* knockdown in the MZ. We discovered that blocking the EGFR and JNK pathways by expressing a dominant negative version of EGFR or Bsk (the only known JNK in *Drosophila*), respectively, rescues the *hdcRNAi*-induced lamellocyte differentiation **(Fig 24F, 24G, 24F', and 24G', quantified in 24I, and 24I')**. Similar results were observed when the adherens junction protein E-cad was overexpressed in the progenitors **(Fig 24H and 24H', and quantified in 24I, and 24I')**.

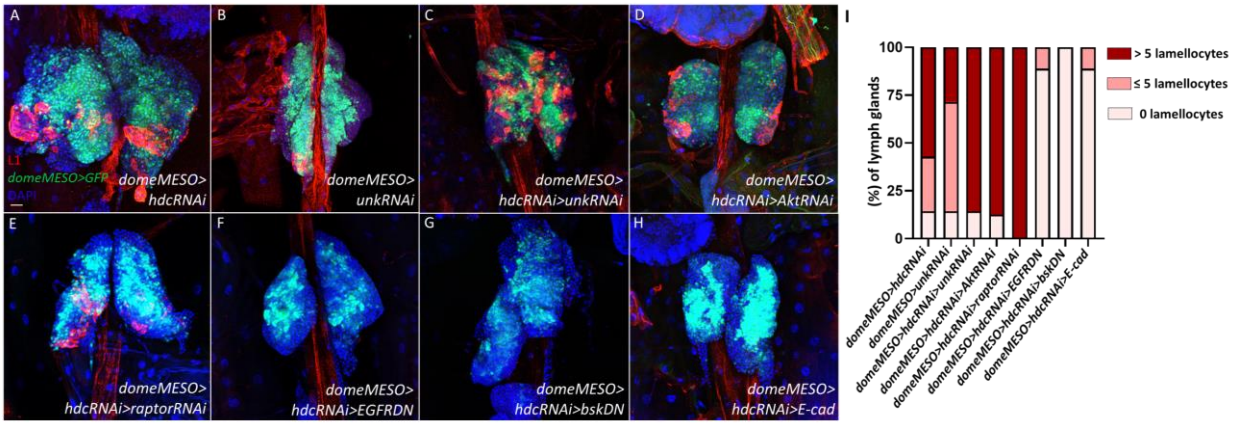

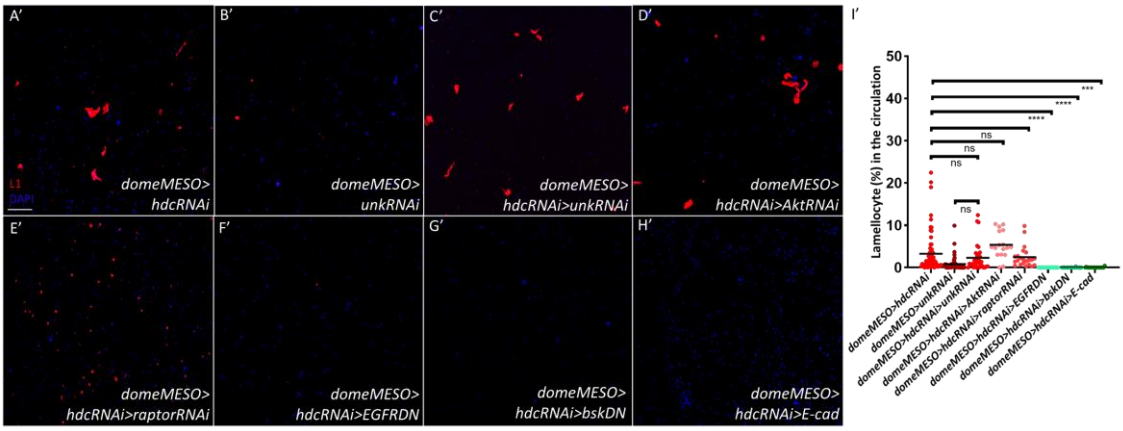

Fig 24. Hdc functions upstream to distinct pathways in the MZ. (A-C) Unlike silencing *hdc* in the MZ (*UAS-hdcRNAi/+; domeMESO-GAL4, UAS-2xEGFP/+*) (n =7) (A), silencing *unk* does not lead to significant lamellocyte differentiation in the lymph gland (*UAS-unkRNAi/+; domeMESO-GAL4, UAS-2xEGFP/+*) (n = 7) (B), and silencing *unk* and *hdc* together does not enhance *hdc* phenotype (*UAS-hdcRNAi/UAS-unkRNAi; domeMESO-GAL4, UAS-2xEGFP/+*) (n = 7) (C). (D-H) Silencing of *Akt* (*UAS-hdcRNAi/+; domeMESO-GAL4,UAS-2xEGFP/UAS-AktRNAi*) (n = 8) (D) *or raptor* (*UAS-hdcRNAi/+; domeMESO-GAL4,UAS-2xEGFP/UAS-raptorRNAi*) (n = 7) (E) has no suppressor effect, while expression of a dominant negative version of *EGFR* (*UAS-hdcRNAi/UAS-EGFR.DN; domeMESO-GAL4,UAS-2xEGFP/UAS-EGFR.DN*) (n = 9) (F), or *bsk* (*UAS-hdcRNAi/+; domeMESO-GAL4,UAS-2xEGFP/UAS-bsk53R*) (n = 7) (G), or overexpression of *E-cad* (*UAS-hdcRNAi/+; domeMESO-GAL4,UAS-2xEGFP/UAS-E-cad*) (n = 9) (H) rescue domeMESO>*hdcRNAi* phenotype in the lymph gland (blue: nuclei, green: MZ, red: lamellocytes). n refers to the number of lymph glands analyzed. Scale bar: 20 μm. (I) A bar graph showing the percentage of lymph glands from the genotypes presented in panels (A-H) categorized into lymph glands with 0 lamellocytes, lymph glands with 5 or fewer lamellocytes, and lymph glands containing more than 5 lamellocytes. (A'-C') Unlike silencing *hdc* in the MZ (*UAS-hdcRNAi/+; domeMESO-GAL4, UAS-2xEGFP/+*) (3.268 (n = 66)) (A'), silencing *unk* does not cause lamellocyte appearance in the circulation (*UAS-unkRNAi/+; domeMESO-GAL4,UAS-2xEGFP/+*) (0.8% (n = 59)) (B'), and silencing *unk* and *hdc* together does not significantly enhance lamellocyte numbers in domeMESO>*hdcRNAi larvae* (2.3% (n = 34)) (C'). (D'-H') Silencing *Akt* (*UAS-hdcRNAi/+; domeMESO-GAL4,UAS-2xEGFP/UAS-AktRNAi*) (5.3% (n = 17)) (D') *or raptor* (*UAS-hdcRNAi/+; domeMESO-GAL4,UAS-2xEGFP/UAS-raptorRNAi*) (2.4% (n = 22)) (E') does not suppress the phenotype of *domeMESO>hdcRNAi* larvae, while expressing a dominant negative version of EGFR (*UAS-hdcRNAi/UAS-EGFR.DN; domeMESO-GAL4,UAS-2xEGFP/UAS-EGFR.DN*) (0% (n = 26)) (F'), or *bsk* (*UAS-hdcRNAi/+; domeMESO-GAL4,UAS-2xEGFP/UAS-bsk53R*) (0.01% (n = 26)) (G'), as well as overexpression of *E-cad* (*UAS-hdcRNAi/+; domeMESO-GAL4,UAS-2xEGFP/UAS-E-cad*) (0.03% (n = 19)) (H') have a significant suppressor effect (blue: nuclei, red: lamellocytes). n refers to the number of larvae analyzed. Scale bar: 20 μm. (I') A scatter dot plot showing percentage of lamellocytes in the circulation of larvae from the genotypes presented in panels (A'-H'). Each dot in the graph represents one single larva. Data were analyzed using ANOVA with Tukey's test for multiple comparisons, *** $p \leq 0.001$, ns: non-significant.

Notably, inhibiting the EGFR and JNK pathways or overexpressing E-cad in the PSC did not affect lamellocyte differentiation in *col>hdcRNAi* larvae **(Fig 25A-25D and Fig 25A'-25D', quantified**

in Fig 25E and Fig 25E'), indicating that unique pathways are activated upon silencing *hdc* in the MZ than in the PSC.

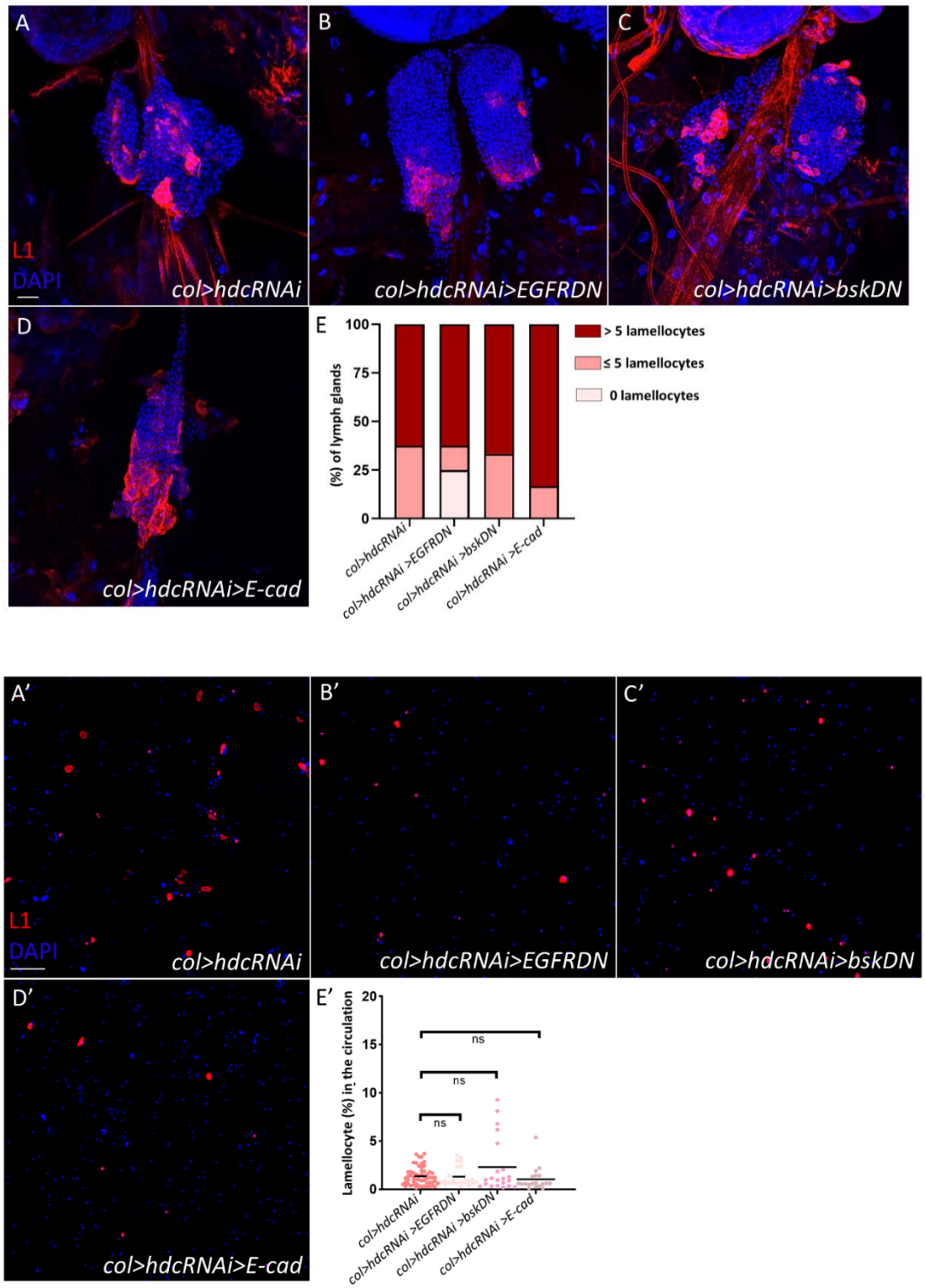

Fig 25. The interaction between Hdc and the EGFR, JNK and E-cad signaling in the PSC. (A'-D') Expressing a dominant negative version of EGFR (*Pcol85-Gal4, UAS-hdcRNAi/UAS-EGFR.DN; UAS-EGFR.DN/+*) ((n = 8)) (B'), or *bsk* (*Pcol85-Gal4, UAS-hdcRNAi/+; UAS-bsk53R/+*) (n = 9) (C'), or overexpressing *E-cad* (*Pcol85-Gal4, UAS-hdcRNAi/+; UAS-E-cad/+*) (n = 6) (D') does not affect lamellocyte differentiation in the lymph glands of col>*hdcRNAi* larvae (*Pcol85-Gal4, UAS-hdcRNAi/+*) (n = 8) (A') (blue: nuclei, red: lamellocytes). n refers to the number of lymph glands analyzed. Scale bar: 20 μm. (E') A bar graph showing the percentage of lymph glands from the genotypes presented in panels (A'-D') categorized into lymph glands with 0 lamellocytes, lymph glands with 5 or fewer lamellocytes, and lymph glands containing more than 5 lamellocytes. (A-D) Expressing a dominant negative version of EGFR (*Pcol85-Gal4, UAS-hdcRNAi/UAS-EGFR.DN; UAS-EGFR.DN/+*) (1.3% (n = 25)) (B), or *bsk* (*Pcol85-Gal4, UAS-hdcRNAi/+; UAS-bsk53R/+*) (2.3% (n = 21)) (C), or overexpressing *E-cad* (*Pcol85-Gal4, UAS-hdcRNAi/+; UAS-E-cad/+*) (1% (n = 19)) (D) does not affect lamellocyte differentiation in the circulation of col>*hdcRNAi* larvae (*Pcol85-Gal4, UAS-hdcRNAi/+*) (1.3% (n = 57)) (A) (blue: nuclei, red: lamellocytes). n refers to the number of larvae analyzed. Scale bar: 20 μm. (E) A scatter dot plot showing lamellocyte numbers in larvae from the genotypes presented in panels (A-D). Each dot in the graph represents a single larva. Data were analyzed using ANOVA with Tukey's test for multiple comparisons, ns: non-significant.

4.3. Screening for new interacting partners of Hdc

As mentioned earlier, Unk and Raptor are the only two proteins described to interact with Hdc in *Drosophila* (N. Li et al. 2019). For this reason, one of our aims was to search for novel interactors of Hdc using LC-MS/MS. Since the *hdc* gene was shown to encode for two isoforms, a long one and a short one, through bypassing the translational termination at an internal UAA stop codon (Steneberg & Samakovlis 2001), we created three HA-tagged UAS transgenes encoding for the short isoform only (*UAS-hdcRA_STOP*), the short and long isoforms both by including the full cDNA of the *hdc* gene containing the internal stop codon (*UAS-hdcRC_STOP*), and a third one coding for the long one only by deleting the internal stop codon present in the full cDNA of the *hdc* gene (*UAS-hdcRC_NOSTOP*).

When we expressed these transgenes using Actin driver to test their functionality, only the short isoform could be detected to be expressed from *UAS-hdcRA_STOP* and *UAS-hdcRC_STOP* transgenes in extracts from whole third instar stage larvae **(Fig 26A)**. For this reason, we continued with *UAS-hdcRA_STOP*, the transgene coding for the short isoform only. Since *hdc* null allele $hdc^{\Delta 84}$ and the enhancer trap hdc^{19} are pupal lethal in homozygous conditions and in combination with each other (Varga et al. 2019), we tested whether the expression of the HA tagged short isoform of Hdc can rescue this lethality. Certainly, we found that expressing the short isoform was enough to rescue the lethality of the $hdc^{\Delta 84}/hdc^{19}$ combination with 100% penetrance **(Data not**

shown). Moreover, expressing the short isoform was sufficient to rescue the lamellocyte differentiation observed in these larvae as well **(Fig 26B)**, suggesting that the short isoform of Hdc is adequate for proper Hdc function in the lymph gland.

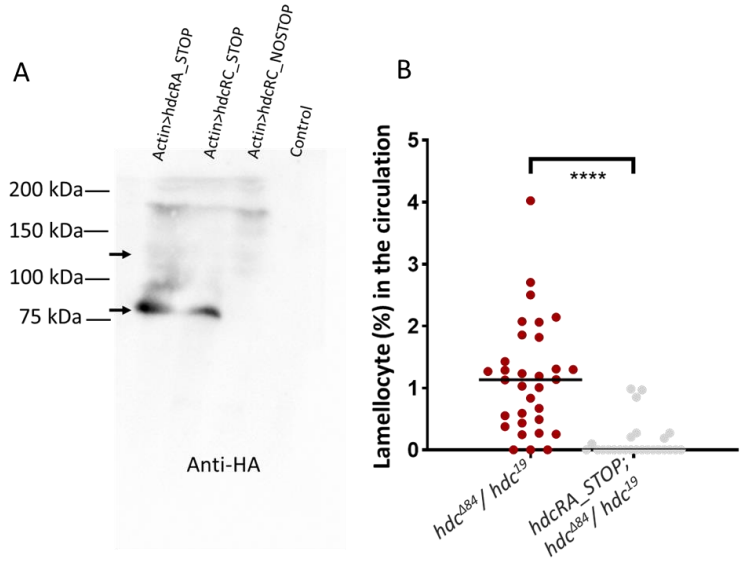

Fig 26. Screening for new Hdc interacting partners. (A) a western blot showing the HA-tagged Hdc protein in larvae from the genotypes *UAS-hdcRA_STOP/Actin-Gal4, UAS-mCherry*, *UAS-hdcRC_STOP/Actin-Gal4, UAS-mCherry, UAS-hdcRC_NOSTOP/Actin-Gal4, UAS-mCherry* in addition to the negative control *+/Actin-Gal4, UAS-mCherry*. Arrows refer to the expected sizes of the short HA tagged Hdc isoform (~70kDa) and the long one (~130 kDa). (B) A scatter dot plot showing the percentage of lamellocytes in the circulation of larvae from the genotypes $hdc^{\Delta 84}/hdc^{19}$*-Gal4* (1.1% n = 32) and *UAS-hdcRA_STOP/+;* $hdc^{\Delta 84}/hdc^{19}$*-Gal4* (0.15% n = 25). n refers to the number of larvae analyzed. Each dot in the graph represents one single larva. Data were analyzed using two-tailed unpaired Student's t-test, **** $p \leq 0.0001$.

After validating the functionality of the *UAS-hdcRA_STOP* transgene, we used it to search for new interactors of Hdc using liquid chromatography-tandem mass spectrometry (LC-MS/MS) analysis, where HA-tagged Hdc proteins were immunopercipitated using anti-HA beads, and the proteins bound to the beads were identified using mass spectrometry. After scoring the candidate proteins by their peptide count (number of peptides that were identified from each protein/number of total peptides in the experiment) and coverage (number of amino acids of a candidate protein covered in the experiment/total number of amino acids in the protein), we got a list of around 468 top candidates **(S3 Table)**. Notably, RNA processing, ribosome binding, translation initiation, and protein folding were among the most enriched GO terms in the gene ontology (GO) analysis of the predicted molecular functions of these proteins **(Table 1)**.

Table 1. The gene ontology terms enriched in the list of top 468 Hdc candidate partners. Data were analyzed using STRING functional enrichment analysis (https://string-db.org/).

GO-term	term description	observed gene count	background gene count	strength	false discovery rate
GO:0003735	Structural constituent of ribosome	92	173	1.22	9.89E-69
GO:0005198	Structural molecule activity	113	575	0.78	5.57E-48
GO:0003723	RNA binding	115	652	0.74	6.83E-45
GO:1901363	Heterocyclic compound binding	207	2800	0.36	8.89E-31
GO:0097159	Organic cyclic compound binding	207	2825	0.35	2.45E-30
GO:0003676	Nucleic acid binding	147	1794	0.4	1.17E-23
GO:0005488	Binding	292	5541	0.21	2.77E-23
GO:0003729	mRNA binding	30	233	0.6	0.000000287
GO:0019843	rRNA binding	13	39	1.01	0.00000132
GO:0000166	Nucleotide binding	66	958	0.33	0.00000352
GO:0043021	Ribonucleoprotein complex binding	15	67	0.84	0.00000638
GO:0008135	Translation factor activity, RNA binding	15	70	0.82	0.00000975
GO:0036094	Small molecule binding	70	1087	0.3	0.000011
GO:0017111	Nucleoside-triphosphatase activity	30	289	0.51	0.0000131
GO:0032555	Purine ribonucleotide binding	57	810	0.34	0.0000131
GO:0035639	Purine ribonucleoside triphosphate binding	55	787	0.33	0.0000221
GO:0044877	Protein-containing complex binding	33	356	0.46	0.000026
GO:0043168	Anion binding	64	1003	0.29	0.0000398
GO:0045182	Translation regulator activity	16	100	0.69	0.0000655
GO:0003743	Translation initiation factor activity	11	48	0.85	0.00016
GO:0043022	Ribosome binding	9	30	0.97	0.00021
GO:0051082	Unfolded protein binding	13	81	0.69	0.00058
GO:0008312	7S RNA binding	5	6	1.41	0.0009
GO:0016887	ATP hydrolysis activity	17	143	0.56	0.0009
GO:0097367	Carbohydrate derivative binding	59	1009	0.26	0.001

Since we were interested mostly in new interacting partners of Hdc involved in hematopoiesis, we searched the top LC-MS/MS candidates in *Drosophila* blood cell regulation literature and selected only 7 candidates that were mentioned previously to be related to *Drosophila* hematopoiesis (**S3 Table, highlighted in yellow)** (Avet-Rochex et al. 2010; Evans et al. 2021). These are Calmodulin (Cam), eukaryotic translation initiation factor 5B (eIF5B), Chaperonin containing TCP1 subunit 1 (CCT1), eukaryotic translation release factor 3 (eRF3), Heat shock protein cognate 4 (Hsc70-4), Regulatory particle non-ATPase 11 (Rpn11), and Adaptor protein complex 2 alpha subunit (AP-2a). To test whether the genes coding for these proteins interact genetically with *hdc*, we silenced

them alone or together with *hdc* in the PSC using *col* driver and checked whether this enhanced or suppressed *col>hdcRNAi* lamellocyte phenotype **(Fig 27A)**. Notably, even though silencing none of these genes enhances lamellocyte differentiation in *col>hdcRNAi* larvae significantly, silencing 4 of them alone (*eIF5B*, *CCT1*, *eRF3*, and *Hsc70-4*) leads to the appearance of lamellocytes in the circulation of naive larvae, suggesting that they have a role in progenitor maintenance in the lymph gland.

Moreover, silencing *Cam* suppresses lamellocyte differentiation in *col>hdcRNAi* larvae **(Fig 27A)**, suggesting that Cam might interact with Hdc and be required for its activity. To validate this interaction, we co-expressed Hdc-nYFP (Hdc protein tagged with the N-terminal fragment of the YFP) and Cam-cYFP (Cam tagged with the C-terminal fragment of the YFP), Hdc-nYFP and Unk-cYFP (positive control), and Hdc-nYFP and PCID2-cYFP (negative control) in S2R+ *Drosophila* cell line, and assayed for YFP fluorescence. Interestingly, while we did not see a YFP signal in the negative control **(Fig 27B)**, we could detect a signal in the positive control and in case of expressing Hdc-nYFP and Cam-cYFP **(Fig 27C-27D)**, indicating that Hdc interacts with Cam.

To validate whether there is a physical interaction between Hdc and Cam, we co-expressed Hdc-His (Hdc protein tagged with Histidine), and Cam-GST (Cam tagged with glutathione S-transferase affinity tag), or Hdc-His and GST alone (negative control) and used glutathione beads to precipitate Cam-GST. Using antibodies specific for GST and His, we examined the presence of both proteins on the beads. Although we could verify that Cam-GST proteins were attached to the beads **(Fig 27E first panel)**, suggesting that the experimental procedure was successful, we could not detect Hdc-His on the beads **(Fig 27E, second panel)**, proposing that Hdc and Cam might be interacting indirectly through other mediator proteins.

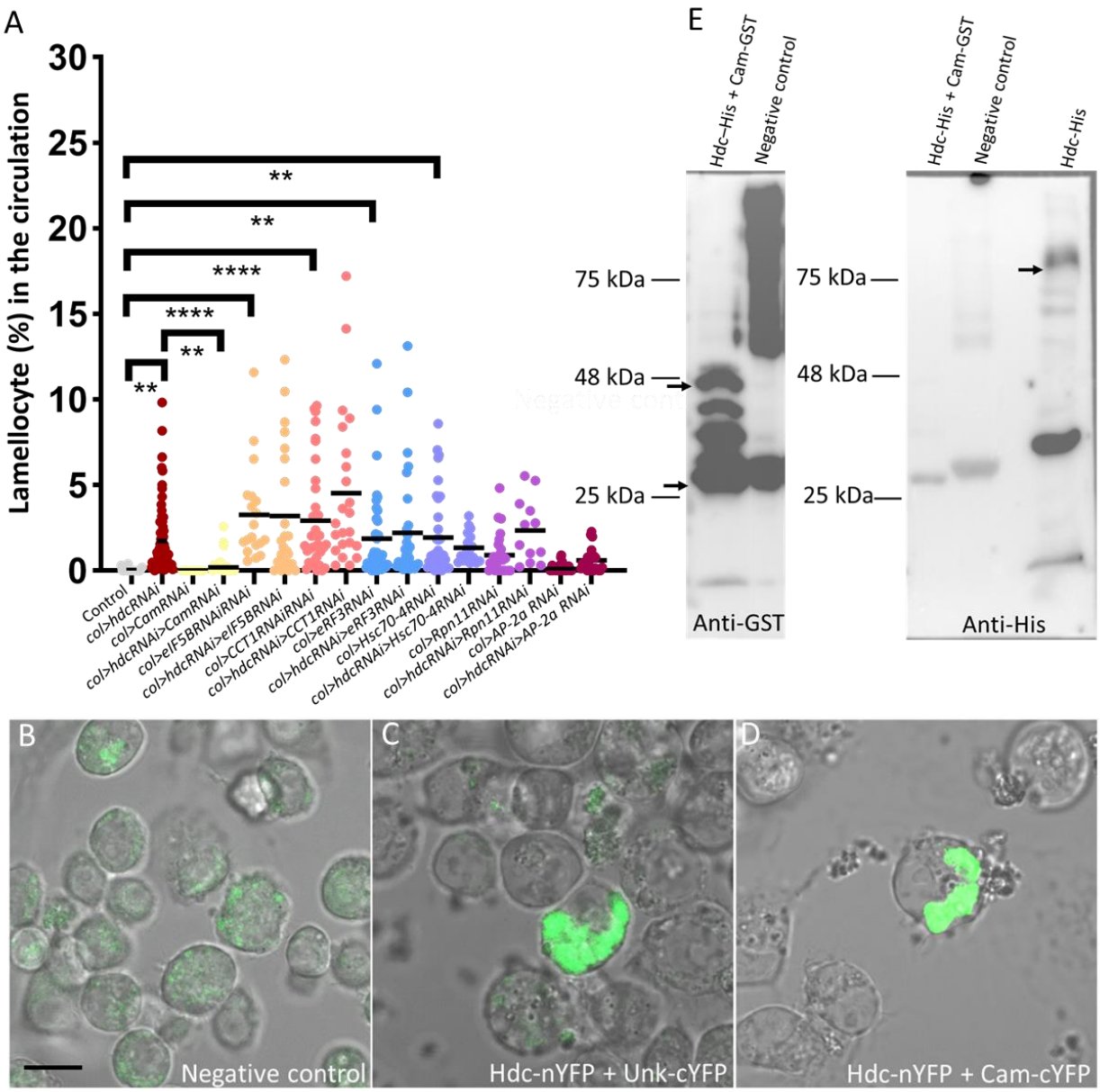

Fig 27. Validation of potential Hdc interactors. (A) A scatter dot plot showing percentage of lamellocytes in the circulation of larvae from the genotypes: (*Pcol85-Gal4/+*) (0.03% (n = 55)), (*Pcol85-Gal4,UAS-hdcRNAi/+)* (1.7% (n = 78)), (*Pcol85-Gal4/+; UAS-CamRNAi/+)* (0% (n = 13)), (*Pcol85-Gal4,UAS-hdcRNAi/+; UAS-CamRNAi/+)* (0.19% (n = 58)), (*Pcol85-Gal4/+; UAS-eIF5BRNAi/+)* (3.2% (n = 19)), (*Pcol85-Gal4,UAS-hdcRNAi/+; UAS-eIF5BRNAi/+)* (3.1% (n = 23)), (*Pcol85-Gal4/+; UAS-CCT1RNAi/+)* (2.9% (n = 37)), (*Pcol85-Gal4,UAS-hdcRNAi/+; UAS-CCT1RNAi/+)* (4.5% (n = 23)), (*Pcol85-Gal4/+; UAS-eRF3RNAi/+)* (1.8% (n = 38)), (*Pcol85-Gal4,UAS-hdcRNAi/+; UAS-eRF3RNAi/+)* (2.2% (n = 30)), (*Pcol85-Gal4/+; UAS-HSC70-4RNAi/+)* (1.9% (n = 36)), (*Pcol85-Gal4,UAS-hdcRNAi/+; UAS-HSC70-4RNAi/+)* (1.3% (n = 17)), (*Pcol85-Gal4/+; UAS-Rpn11RNAi/+)* (0.9% (n = 33)), (*Pcol85-Gal4,UAS-hdcRNAi/+; UAS-Rpn11RNAi/+)* (2.3% (n = 12)), (*Pcol85-Gal4/+; UAS-AP-2aRNAi/+)* (0.1% (n = 35)), and (*Pcol85-Gal4,UAS-hdcRNAi/+; UAS-AP-2aRNAi/+)* (0.6% (n = 24)). n refers to the number

of larvae analyzed. Each dot in the graph represents one single larva. Data were analyzed using ANOVA with Tukey's test for multiple comparisons, ** $p \leq 0.01$, **** $p \leq 0.0001$. (B-D) S2R+ cells co-transfected with hdc-nYFP and unk-cYFP (C) or hdc-nYFP and Cam-cYFP (D) show a positive YFP signal unlike cells co-transfected with hdc-nYFP and PCID2-cYFP (B, negative control) (green: YFP). Scale bar, 100 μm. (E) A western blot detecting GST and His in pull-down samples of Hdc-His and Cam-GST or Hdc-His and GST alone (negative control), in addition to validating the expression of Hdc-His in the IVTT reaction. Arrows refer to the expected sizes of Cam-GST (42 kDa), GST (26 kDa) and Hdc-His (70.8 kDa).

5. Discussion

Despite the differences at the structural level between the *Drosophila* lymph gland and mammalian hematopoietic compartments, the signaling pathways responsible for controlling hemocyte progenitor maintenance are remarkably similar to those found in mammals **(Fig 11)** (Banerjee et al. 2019; Kharrat et al. 2022). The lymph gland with its hematopoietic niche (PSC) sending signals to hemocyte progenitors in the MZ, to regulate their differentiation into effector hemocytes in the CZ, provides an excellent model to understand the role of these important signaling pathways. Studies aiming to better understand hemocyte differentiation within the lymph gland are highly facilitated by transgenic constructs that allow for context-specific manipulation of signaling pathways and analyzing the resulting phenotype (Lebestky et al. 2003; Crozatier et al. 2004; Jung et al. 2005; Krzemień et al. 2007; Oyallon et al. 2016).

One of the aims of the work presented in this thesis was to further investigate the previously reported non-cell-autonomous function of Hdc in the hematopoietic niche. Although it was documented that PSC-specific silencing of *hdc* leads to the differentiation of lamellocytes that are typically not present in naive larvae (Varga et al. 2019), the precise mechanism underlying the phenotype was not previously understood. Here we show that Hdc is required in the PSC to prevent the overactivation of the insulin/mTOR pathway. This is underlined by the observation that using the PSC specific driver *col* to silence Unk, a previously described partner of Hdc involved in the regulation of the insulin/mTOR pathway (Avet-Rochex et al. 2014; N. Li et al. 2019) led to lamellocyte differentiation, and that silencing it together with *hdc* significantly increased lamellocyte numbers **(Figs 15A-15D, 16A-16D and quantified in 15J and 16J)**. Moreover, inhibition of the insulin/mTOR pathway by knocking down the insulin pathway kinase Akt (Tsuchiya et al. 2014), or the mTORC1 complex member Raptor (N. Li et al. 2019) rescued the effect of Hdc depletion **(Figs 15G, 15H, 16G, and 16H, and quantified in 15J and 16J)**, while *hdc* overexpression alleviated the phenotype caused by insulin/mTOR pathway overactivation **(Figs 15I and 16I, and quantified in 15J and 16J)**. These results are in line with previous observations suggesting that Hdc and Unk bind to the mTOR complex through Raptor to inhibit its activity in the imaginal discs (N. Li et al. 2019), and are consistent with prior studies revealing that the continuous activation of the insulin/mTOR pathway in the niche triggers lamellocyte differentiation in the lymph gland **(Figs 15E, 15F, 16F and 16E, and quantified in 15J and 16J)**. (Benmimoun et al. 2012; Kaur et al. 2019).

Interestingly, although it was reported that activation of the insulin/mTOR pathway increases PSC size **(Fig 17A–17C and quantified in 17H)** (Benmimoun et al. 2012; Y. Tokusumi et al. 2012; Kaur et al. 2019), the elevation of niche cell number was not observed in *hdc* mutant larvae or in case of PSC-specific silencing of *hdc* **(Fig 17D and quantified in 17H)** (Varga et al. 2019). A plausible resolution of this contradiction is that cell death caused by *hdc* compensates for the increase of niche cell number. Our observations that overexpression of the apoptosis inhibitor *p35* in *col>hdcRNAi* increased the number of PSC cells significantly, and that knocking down *hdc* reduced the PSC size to normal in larvae were the insulin pathway is activated in the niche (*col>PtenRNAi*) support this hypothesis **(Fig 17E-17G, and quantified in 17H)**, and also agree with studies showing that *hdc* loss-of-function causes apoptosis in the adult progenitor cells (APCs), as well as in stem cells of the testis and the intestines (Resende et al. 2013, 2017; Giannios & Casanova 2021).

The continuous activation of the insulin/mTOR pathway increases ribogenesis and protein synthesis, which in turn leads to cellular stress hallmarked by elevated ROS levels (Kaur et al. 2019; Giannios & Casanova 2021). We found that two markers of oxidative stress, *gstD-GFP* and *Thor-lacZ* become active in the PSC when *hdc* is silenced **(Fig 18A-18B' and 18D-E' and quantified in 18C and 18F)**. The alleviation of the hematopoietic phenotype resulting from *hdc* silencing in the niche through the overexpression of *Cat* and *foxo* **(Fig 19A-19C and 19A'-19C' and quantified in 19G and 19G')** suggests that ROS play a key role in lamellocyte differentiation when *hdc* function is compromised. These results also suggest that *foxo* is upregulated in response to cellular stress in the niche of *col>hdcRNAi* larvae (as indicated by the elevation of *Thor-lacZ*, a direct reporter of *foxo*) **(Fig 18D-E' and quantified in 18F)**, and that this endogenous upregulation seems to partially compensates lamellocyte differentiation, as we observed that knocking down *foxo* results in higher lamellocyte numbers in these larvae **(Fig 19D-19E and 19D'-19E' and quantified in 19G and 19G')**. Collectively, all these results are in accordance with previous publications showing that higher ROS levels in the niche trigger progenitor differentiation in the lymph gland (Sinenko et al. 2012; Kaur et al. 2019).

We also showed that *hdc* expression is downregulated in the anterior lobes of the lymph gland in response to immune induction by parasitic wasp **(Fig 20B-20C" and quantified in 20D)**. This observation, supported by the former findings of my colleagues that *hdc* expression is downregulated in the anterior lobes at the end of larval stages when progenitors prepare to

differentiate (Varga et al. 2019), agrees with early reports stating that *hdc* expression ceases in the imaginal cells when they differentiate into adult tissues (Weaver & White 1995). These observations also brought to our attention a possible cell-autonomous inhibitory role for Hdc in the MZ progenitors. Notably, we found that knocking down *hdc* specifically in the MZ progenitors promotes their differentiation into lamellocytes while reducing the number of crystal cells in the lymph gland, suggesting that progenitors prioritize lamellocyte fate over differentiation into crystal cells **(Figs 21A, 21B, 21E, 21F, S1E and S1F and quantified in 21D and 21H and S1H)**, as previously described (Krzemien et al. 2010).

Although silencing *hdc* in both the PSC and MZ leads to higher ROS levels **(Figs 18A-18B', 22A and 22B and quantified in 18C and 22C)**, we found that both zones respond differently to Hdc depletion. For example, the *Thor-lacZ* reporter, which is activated when *hdc* function is lost in the niche, does not respond to MZ specific *hdc* silencing **(S1I and S1J Fig, quantified in S1K)**. Moreover, we found that downstream to *hdc*, distinct signaling pathways are involved in the phenotype in the MZ than in the PSC **(Fig 28)**. For instance, *hdc* knockdown phenotype is not mediated by the insulin/mTOR pathway in the MZ, but rather by the activity of the EGFR and JNK pathways, and the levels of the cell adhesion molecule E-cad **(Fig 24F-H and 24F'-24H', quantified in 24I, and 24I')**. These results further support the involvement of ROS in response to *hdc* loss in the progenitors, as elevated ROS levels in these cells were described to result in premature differentiation through activating the JNK pathway and lowering the levels of E-cad junctions. Our results also suggest a previously unknown direct regulatory role of the EGFR pathway downstream to ROS in the MZ (Owusu-Ansah & Banerjee 2009).

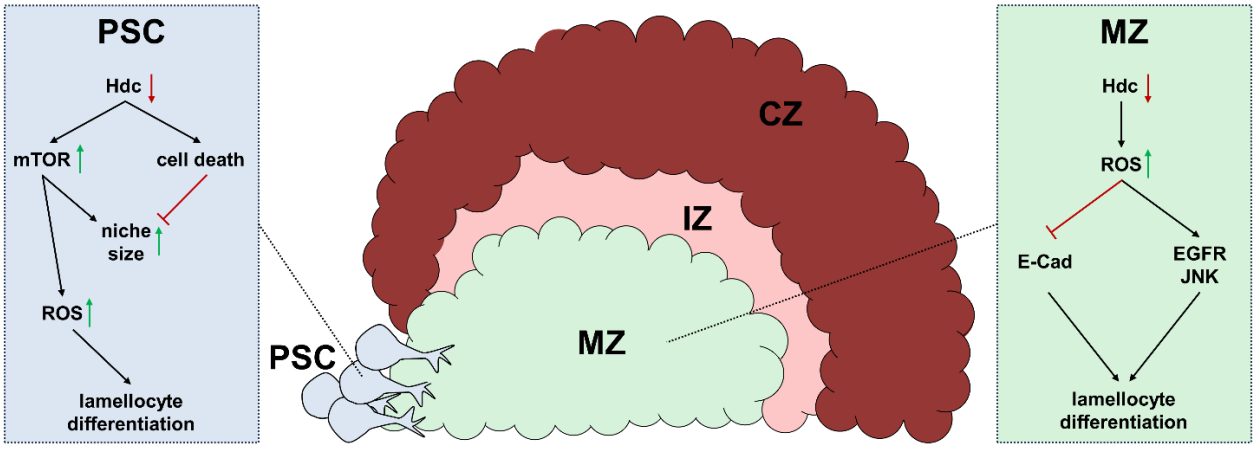

Fig 28. A graphical summary of the dual effect of Hdc depletion in the lymph gland. In the hematopoietic niche, silencing *hdc* leads to overactivation of the insulin/mTOR pathway. The consequent elevation of ROS levels results in impaired progenitor maintenance and differentiation of lamellocytes. The increase in PSC size as a result of insulin/mTOR activation is compensated by cell death caused by *hdc* loss-of-function. Although *hdc* silencing also leads to the elevation of ROS levels in the medullary zone of the lymph gland, the insulin/mTOR is not involved in the resulting phenotype. Instead, high levels of ROS degrade cell-cell connections and induce the activity of the EGFR and JNK pathways leading to lamellocyte differentiation.

In addition to unveiling the signaling pathways through which Hdc functions in the lymph gland, we aimed to identify new Hdc interactors. Interestingly, when testing the functionality of our newly created HA-tagged Hdc transgene isoforms, we found that the short Hdc isoform is able to rescue both the lethality **(Data not shown)** and the hematopoietic phenotype of *hdc* mutant **(Fig 26A)**. This suggests that unlike in the trachea, where the long isoform of Hdc is necessary for the inhibition of excessive tracheal branching (Steneberg & Samakovlis 2001), in the lymph gland, the short isoform is sufficient to inhibit blood cell progenitor differentiation. Therefore, in our experiments, we used the HS-tagged short Hdc isoform in LC-MS/MS for partner identification.

Notably, the top LC-MS/MS candidates seemed to be involved in general cellular functions, such as RNA processing, ensuring proper transcription, translation, and protein folding **(Table 1)**, which hints that Hdc may be a chaperon that assists in the appropriate function of other cellular proteins. This might explain why its depletion shows pleiotropic phenotypes, such as triggering apoptosis or progenitor differentiation that we can observe in the lymph gland, imaginal discs, and stem cells niches in the intestines and testicles (Resende et al. 2013, 2017; Giannios & Casanova 2021).

By validating the interaction of Hdc with the top LC-MS/MS candidates with genetic interactions, Split-YFP, and pull-down assay, we found that Cam might interact with Hdc indirectly **(Fig 27A-E)**. As Cam was described previously in human cell lines to positively regulate the activity of the insulin/mTOR pathway (R.-J. Li et al. 2016), one explanation for our results is that Cam plays a similar role in *Drosophila*, and that its interaction with Hdc might be mediated through the mTORC1 complex. Moreover, our genetic screen showed that silencing *eIF5B*, *CCT1*, *eRF3*, and *Hsc70-4* in the niche lead to lamellocyte differentiation **(Fig 27A)**, a phenotype not described earlier for any of these genes. This opens possibilities for future studies to investigate in detail the role of each of these factors in hemocyte progenitor maintenance in *Drosophila*, and to research their human homologues in blood cell disorders or leukemias. We hope that our results will be

beneficial not only for understanding how blood cell differentiation is regulated in *Drosophila*, but also for unveiling how parallel signaling mechanisms operate in humans.

6. Summary

The hematopoietic organ of the *Drosophila* larva, the lymph gland, is a simplified representation of mammalian hematopoietic compartments, with the presence of hemocyte (blood cell) progenitors in the medullary zone (MZ), differentiated hemocytes in the cortical zone (CZ), and a hematopoietic niche called the posterior signaling centre (PSC) that signals to the progenitors to control their differentiation. In the CZ of the lymph gland and in the circulation, one can distinguish two types of mature hemocytes: phagocytic plasmatocytes and melanizing crystal cells. Following immune induction, a third type of hemocytes, lamellocytes, appear in the circulation and in the lymph gland, and encapsulate larger sized invaders, such as the parasitic wasp egg.

Our previous work has demonstrated that the imaginal cell factor Headcase (Hdc) is required in the hematopoietic niche to suppress progenitor differentiation into lamellocytes in the lymph gland. Here, through extensive genetic interaction experiments, we have demonstrated that Hdc exerts this function by negatively regulating the insulin/mTOR pathway in the niche. When Hdc is depleted in the niche, the overactivation of this pathway triggers reactive oxygen species (ROS) accumulation, which promotes lamellocyte differentiation in the lymph gland, and their consequent appearance in the hemolymph. This is supported by our observations that scavenging ROS from the niche of alleviates the phenotype, while interfering with the stress protective machinery, boosts lamellocyte differentiation.

Although overactivation of insulin/mTOR signaling was described to cause an increase in PSC cell number, we do not observe this phenotype in *hdc* larvae. According to the results presented here, Hdc depletion causes cell death in the niche independently from the insulin/mTOR pathway, thereby concealing mTOR overactivation and resulting in a niche size indistinguishable from the control.

Moreover, we have described here a novel cell-autonomous role for Hdc in suppressing progenitor differentiation in the MZ. We found that even though the insulin/mTOR pathway is not involved in the *hdc* phenotype in the MZ, similarly to the niche, knocking down *hdc* in MZ progenitors leads to ROS elevation, which affects cell-cell adhesion and induces the activity of the EGFR and JNK pathways leading to premature progenitor loss.

Besides understanding Hdc function in the lymph gland, we aimed to isolate new Hdc interacting partners. We used HA-tagged Hdc transgenic protein in LC-MS/MS to search for possible interactors. We identified a genetic interaction and an indirect physical interaction between Hdc

and Calmodulin (Cam), a calcium binding protein that was described previously to be required for the activity of the insulin/mTOR pathway in human cell lines, which suggests that Cam may play a similar role in the hematopoiesis in *Drosophila*. Moreover, through our genetic interaction screens, we have identified a novel role for 4 genes (*eIF5B*, *CCT1*, *eRF3*, and *Hsc70-4*) in suppressing lamellocyte fate in the niche. This opens new ways for further research into the function of each of these genes in blood cell differentiation in *Drosophila*.

The important role of Hdc in progenitor maintenance in the lymph gland is further corroborated by our observations showing that *hdc* expression decreases in the anterior lobes of the lymph gland in response to immune induction by parasitic wasp, and at the end of larval stages as progenitors prepare to differentiate. Considering this and previous data demonstrating that *hdc* expression is lost in the imaginal cells as they start to differentiate into adult tissues, we conclude that Hdc may play a general suppressive role in the maintenance of progenitors and imaginal cells of the larva. Given that the function of the top LC-MS/MS candidate interactors of Hdc is to enable basic cellular tasks, such as translation, and protein folding, Hdc is likely a chaperon that facilitates proper cellular function. This is also underlined by our finding that *hdc* loss-of-function leads to cellular stress, resulting in various consequences, such as triggering precursor cell differentiation.

We hope that our findings help to shed light on the regulation of blood cell development in *Drosophila*, as well as parallel mechanisms implicated in HSC differentiation and hematopoietic disorders in humans.

7. Összefoglaló

A *Drosophila* lárva vérsejtképző szerve a központi nyirokszerv (lymph gland), kiváló modellként szolgál az emlős hematopoietikus kompartmentumok működésének megértéséhez. A nyirokszerv medulláris zónájában (MZ) progenitor sejtek, a kortikális zónájában (CZ) differenciált hemociták (vérsejtek) találhatók. A szerv úgynevezett poszterior szignalizációs központja (PSC) vérsejtképző niche-ként működik, mely jelátviteli utakon keresztül szabályozza a progenitorok differenciálódását. A CZ-ban, illetve a lárva keringésében kétféle érett hemocitát különböztethetünk meg: fagocita plazmatocitákat és melanizációra képes kristálysejteket. Az immunindukciót követően egy harmadik típusú vérsejt, a lamellocita jelenik meg a keringésben és a nyirokszervben. A lamellociták feladata, hogy a nagyobb méretű betolakodókat a tokképzés folyamata során elpusztítsák.

Korábbi munkánk során kimutattuk, hogy a vérsejtképző niche-ben, valamint az imaginális szövetekben aktív Headcase (Hdc) fehérje szükséges a nyirokszervben található progenitor sejtek fenntartásához, a lamellocita differenciálódás gátlásához. A dolgozatban bemutatott részletes genetikai interakciós kísérletek rávilágítottak, hogy a fehérje ezt a feladatát a niche-ben az inzulin/mTOR útvonal negatív szabályozásán keresztül fejti ki. A *hdc* funkcióvesztése esetén ennek az szignalizációs útvonalnak a túlaktiválódása reaktív oxigéngyökök (ROS) felhalmozódását váltja ki, melynek következtében a központi nyirokszervben lamellociták differenciálódnak, majd innen a lárva keringésébe lépnek. Erre utalnak azon megfigyeléseink is, melyek szerint a ROS szint niche-ben történő csökkentése mérsékli, míg a sejtszintű stressz fokozása elősegíti a lamellociták differenciálódását.

Bár az inzulin/mTOR jelátvitel túlaktiválása a szakirodalom szerint a PSC sejtek számának növekedését okozza, ez a fenotípus nem volt megfigyelhető a *hdc* mutáns lárvákban. Az általunk bemutatott eredmények szerint ennek az az oka, hogy a *hdc* depléciója az inzulin/mTOR jelátviteli útvonaltól függetlenül sejthalált okoz, így elfedve az útvonal aktivitásának hatását.

Munkánk arra is rávilágított, hogy a Hdc sejtautonóm módon is szerepet játszik a MZ progenitorok differenciálódásának gátlásában. Annak ellenére, hogy kísérleteink szerint az inzulin/mTOR útvonal nem vesz részt ebben a folyamatban, a niche-ben megfigyeltekhez hasonlóan a *hdc* csendesítése az MZ progenitor sejtjeiben is a ROS szint emelkedését okozza, ami befolyásolja a

sejtek adhézióját és indukálja az EGFR és JNK jelátviteli útvonalak aktivitását. Ezek a folyamatok végül a progenitor állapot elvesztéséhez vezetnek.

A Hdc működésének megértése mellett további célunk volt, hogy a fehérje új kölcsönható partnereit azonosítsuk. Ehhez HA-jelölt transzgenikus Hdc fehérjével végeztünk proteomikai vizsgálatokat LC-MS/MS segítségével. Ezen kísérletek során igazoltuk a Hdc és a Calmodulin (Cam) genetikai, illetve indirekt fizikai interakcióját. Mivel a Cam-ról kimutatták, hogy emberi sejtvonalakban szükséges az inzulin/mTOR útvonal aktivitásához, eredményeink arra utalnak, hogy a fehérje hasonló szerepet játszhat az ecetmuslica vérsejtképzése során is. További genetikai interakciós vizsgálatok során 4 olyan gént (*eIF5B*, *CCT1*, *eRF3* és *Hsc70-4*) azonosítottunk, melyek a niche-ben a lamellocita differenciálódás gátlásában vesznek részt. Ezen eredményeink új lehetőségeket teremtenek az ecetmuslica vérsejt-differenciálódásában szerepet játszó folyamatok további vizsgálatához.

Azt, hogy a Hdc fontos szerepet játszik a központi nyirokszerv progenitor sejtjeinek fenntartásában, tovább erősítik azon megfigyeléseink, melyek szerint a *hdc* expresszója a nyirokszerv elsődleges lebenyében lecsökken darázs parazitózis hatására, illetve a lárva állapot végén, amikor a progenitorok differenciálódni kezdenek. Ezen megfigyeléseink, illetve azok az irodalmi adatok, melyek szerint a *hdc* expresszió megszűnik az imaginális sejtekben azok felnőtt szövetekké történő differenciálódása során, arra engednek következtetni, hogy a Hdc általános represszor szerepet játszhat a lárva progenitor sejtjeinek fenntartásában. Mivel az LC-MS/MS kísérletek során azonosított Hdc kölcsönható partner jelöltek legfontosabb funkciója az alapvető sejtfeladatok, például a transzláció és a fehérje érés (folding) elősegítése, a Hdc feltehetőleg egy chaperon fehérje feladatait látja el, elősegítve a sejtek megfelelő működését. Ezt valószínűsíti az a felfedezésünk is, hogy a *hdc* funkcióvesztése sejtszintű stresszhez vezet, ami számos következményeinek egyikeként vérsejt progenitor differenciálódást vált ki.

Azt reméljük, hogy a dolgozatban bemutatott eredményeink segítik a vérsejtek differenciálódási folyamatainak megértését, és hozzájárulnak az emberi vérképzőszervi rendellenességekben szerepet játszó mechanizmusok megismeréséhez is.

8. Acknowledgment

I would like to thank my supervisor Dr. Viktor Honti for accepting me into his group, for giving me the opportunity to be involved in the great field of developmental genetics, and for all his advice and guidance throughout my PhD years. I would also like to thank all current and former members of the Drosophila Blood Cell Differentiation Group - especially Erika, Enikő, Niki, Ishrak, Blanka, Móni, Melinda, and Andi for all their assistance and for making the long PhD journey feel very short.

I am thankful to my mentor Dr. Ernő Kiss for his advice and support during my PhD years.

I am very grateful for the kindness of Dr. Gábor Csordás and his generosity in sharing his knowledge and expertise with me.

I am also grateful to the Innate Immunity Group members - especially Dr. István Andó, Dr. Éva Kurucz, Dr. Gyöngyi Cinege, and Olga Kovalcsik, for providing us with reagents and assistance.

I am appreciative to Dr. Ildikó Maruzs-Kristó and the Drosophila Nuclear Actin Laboratory for helping in the Split-YFP and pull-down experiments, in addition to Dr. Rita Sinka, Dr. Ferenc Jankovics and Dr. Enikő Kúthy-Sutus for their help in cloning the hdc constructs. I am thankful to Aladár Pettkó-Szandtner for the LC/MS analysis, and László Sipos from the Drosophila Embryo Injection Service in the BRC. To all other labs, facilities, and members of the Institute of Genetics, led by Dr. Miklós Erdélyi, and the entire BRC, thanks so much for providing such a supportive environment for research.

I would like to thank Dr. Csaba Vizler and Dr. László Henn for taking their time to read my thesis and for all their constructive comments and suggestions.

For all people surrounding me in Hungary who became like family to me away from home, I am so thankful for all of you.

To mom and grandma, the most selfless, I wouldn't be here today without you.

To my father, who left us very early, I hope I am making you proud.

Funding:

This work was supported by the National Research, Development and Innovation Office OTKA K-131484 (VH) and the 2022-2.1.1-NL-2022-00008 (National Laboratory of Biotechnology) grants.

9. References

Abel, T., Michelson, A.M. & Maniatis, T., 1993. A Drosophila GATA family member that binds to Adh regulatory sequences is expressed in the developing fat body. Development, 119, 623–633, The Company of Biologists Ltd.

Akada, H., Akada, S., Hutchison, R.E., Sakamoto, K., Wagner, K.U. & Mohi, G., 2014. Critical Role of Jak2 in the Maintenance and Function of Adult Hematopoietic Stem Cells. Stem Cells, 32, 1878, NIH Public Access. doi:10.1002/STEM.1711

Alfonso, T.B. & Jones, B.W., 2002. gcm2 promotes glial cell differentiation and is required with glial cells missing for macrophage development in Drosophila. Dev Biol, 248, 369–383, Elsevier.

Anderl, I., Vesala, L., Ihalainen, T.O., Vanha-aho, L.M., Andó, I., Rämet, M. & Hultmark, D., 2016. Transdifferentiation and Proliferation in Two Distinct Hemocyte Lineages in Drosophila melanogaster Larvae after Wasp Infection. PLoS Pathog, 12, e1005746, Public Library of Science. doi:10.1371/JOURNAL.PPAT.1005746

Avet-Rochex, A., Boyer, K., Polesello, C., Gobert, V., Osman, D., Roch, F., Augé, B., et al., 2010. An in vivo RNA interference screen identifies gene networks controlling Drosophila melanogasterblood cell homeostasis. BMC Dev Biol, 10, 1–15, BioMed Central.

Avet-Rochex, A., Carvajal, N., Christoforou, C.P., Yeung, K., Maierbrugger, K.T., Hobbs, C., Lalli, G., et al., 2014. Unkempt Is Negatively Regulated by mTOR and Uncouples Neuronal Differentiation from Growth Control. PLoS Genet, 10, PLOS. doi:10.1371/JOURNAL.PGEN.1004624

Babcock, D.T., Brock, A.R., Fish, G.S., Wang, Y., Perrin, L., Krasnow, M.A. & Galko, M.J., 2008. Circulating blood cells function as a surveillance system for damaged tissue in Drosophila larvae. Proceedings of the National Academy of Sciences, 105, 10017–10022, National Acad Sciences.

Banerjee, U., Girard, J.R., Goins, L.M. & Spratford, C.M., 2019. Drosophila as a Genetic Model for Hematopoiesis. Genetics, 211, 367–417, Oxford Academic. doi:10.1534/GENETICS.118.300223

Benmimoun, B., Polesello, C., Haenlin, M. & Waltzer, L., 2015. The EBF transcription factor Collier directly promotes Drosophila blood cell progenitor maintenance independently of the niche. Proc Natl Acad Sci U S A, 112, 9052–9057, National Academy of Sciences. doi:10.1073/PNAS.1423967112/SUPPL_FILE/PNAS.201423967SI.PDF

Benmimoun, B., Polesello, C., Waltzer, L. & Haenlin, M., 2012. Dual role for Insulin/TOR signaling in the control of hematopoietic progenitor maintenance in Drosophila. Development, 139, 1713–1717, Development. doi:10.1242/DEV.080259

Bernardoni, R., Vivancos, V. & Giangrande, A., 1997. glide/gcmIs expressed and required in the scavenger cell lineage. Dev Biol, 191, 118–130, Elsevier.

Bhardwaj, G., Murdoch, B., Wu, D., Baker, D.P., Williams, K.P., Chadwick, K., Ling, L.E., et al., 2001. Sonic hedgehog induces the proliferation of primitive human hematopoietic cells via BMP regulation. Nature Immunology 2001 2:2, 2, 172–180, Nature Publishing Group. doi:10.1038/84282

Bhatia, M., Bonnet, D., Wu, D., Murdoch, B., Wrana, J., Gallacher, L. & Dick, J.E., 1999. Bone Morphogenetic Proteins Regulate the Developmental Program of Human Hematopoietic Stem Cells. Journal of Experimental Medicine, 189, 1139–1148, The Rockefeller University Press. doi:10.1084/JEM.189.7.1139

Binggeli, O., Neyen, C., Poidevin, M. & Lemaitre, B., 2014. Prophenoloxidase Activation Is Required for Survival to Microbial Infections in Drosophila. PLoS Pathog, 10, Public Library of Science. doi:10.1371/JOURNAL.PPAT.1004067

Blanco-Obregon, D., Katz, M.J., Durrieu, L., Gándara, L. & Wappner, P., 2020. Context-specific functions of Notch in Drosophila blood cell progenitors. Dev Biol, 462, 101–115, Academic Press. doi:10.1016/J.YDBIO.2020.03.018

Bor, V. Van De, Zimniak, G., Papone, L., Cerezo, D., Malbouyres, M., Juan, T., Ruggiero, F., et al., 2015. Companion blood cells control ovarian stem cell niche microenvironment and homeostasis. Cell Rep, 13, 546–560, Elsevier.

Bosch, P.S., Makhijani, K., Herboso, L., Gold, K.S., Baginsky, R., Woodcock, K.J., Alexander, B., et al., 2019. Adult Drosophila lack hematopoiesis but rely on a blood cell reservoir at the respiratory epithelia to relay infection signals to surrounding tissues. Dev Cell, 51, 787–803, Elsevier.

Boulet, M., Renaud, Y., Lapraz, F., Benmimoun, B., Vandel, L. & Waltzer, L., 2021. Characterization of the Drosophila adult hematopoietic system reveals a rare cell population with differentiation and proliferation potential. Front Cell Dev Biol, 9, 739357, Frontiers.

Bretscher, A.J., Honti, V., Binggeli, O., Burri, O., Poidevin, M., Kurucz, É., Zsámboki, J., et al., 2015. The Nimrod transmembrane receptor Eater is required for hemocyte attachment to the sessile compartment in Drosophila melanogaster. Biol Open, 4, 355–363, Company of Biologists Ltd. doi:10.1242/BIO.201410595/-/DC1

Brückner, K., Kockel, L., Duchek, P., Luque, C.M., Rørth, P. & Perrimon, N., 2004. The PDGF/VEGF receptor controls blood cell survival in Drosophila. Dev Cell, 7, 73–84, Elsevier.

Cattenoz, P.B., Sakr, R., Pavlidaki, A., Delaporte, C., Riba, A., Molina, N., Hariharan, N., et al., 2020. Temporal specificity and heterogeneity of Drosophila immune cells. EMBO J, 39, e104486.

Cerenius, L., Lee, B.L. & Söderhäll, K., 2008. The proPO-system: pros and cons for its role in invertebrate immunity. Trends Immunol, 29, 263–271, Elsevier.

Charroux, B. & Royet, J., 2009. Elimination of plasmatocytes by targeted apoptosis reveals their role in multiple aspects of the Drosophila immune response. Proceedings of the National Academy of Sciences, 106, 9797–9802, National Acad Sciences.

Cho, B., Spratford, C.M., Yoon, S., Cha, N., Banerjee, U. & Shim, J., 2018. Systemic control of immune cell development by integrated carbon dioxide and hypoxia chemosensation in Drosophila. Nature Communications 2018 9:1, 9, 1–12, Nature Publishing Group. doi:10.1038/s41467-018-04990-3

Cho, B., Yoon, S.H., Lee, D., Koranteng, F., Tattikota, S.G., Cha, N., Shin, M., et al., 2020. Single-cell transcriptome maps of myeloid blood cell lineages in Drosophila. Nat Commun, 11, Nature Publishing Group. doi:10.1038/S41467-020-18135-Y

Cooper, E.L., 1976. Evolution of blood cells. Ann Immunol (Paris), Vol. 127, pp. 817–825.

Crozatier, M., Ubeda, J.M., Vincent, A. & Meister, M., 2004. Cellular Immune Response to Parasitization in Drosophila Requires the EBF Orthologue Collier. PLoS Biol, 2, e196, Public Library of Science. doi:10.1371/JOURNAL.PBIO.0020196

Csordás, G., Gábor, E. & Honti, V., 2021. There and back again: The mechanisms of differentiation and transdifferentiation in Drosophila blood cells. Dev Biol, 469, 135–143, Academic Press. doi:10.1016/J.YDBIO.2020.10.006

Cumano, A. & Godin, I., 2007. Ontogeny of the hematopoietic system. Annu. Rev. Immunol., 25, 745–785, Annual Reviews.

Defaye, A., Evans, I., Crozatier, M., Wood, W., Lemaitre, B. & Leulier, F., 2009. Genetic ablation of Drosophila phagocytes reveals their contribution to both development and resistance to bacterial infection. J Innate Immun, 1, 322–334, S. Karger AG Basel, Switzerland.

Destalminil-Letourneau, M., Morin-Poulard, I., Tian, Y., Vanzo, N. & Crozatier, M., 2021. The vascular niche controls drosophila hematopoiesis via fibroblast growth factor signaling. Elife, 10, 1–21, eLife Sciences Publications Ltd. doi:10.7554/ELIFE.64672

Dey, N.S., Ramesh, P., Chugh, M., Mandal, S. & Mandal, L., 2016. Dpp dependent hematopoietic stem cells give rise to Hh dependent blood progenitors in larval lymph gland of Drosophila. Elife, 5, eLife Sciences Publications Ltd. doi:10.7554/ELIFE.18295

Dowejko, A., Bauer, R., Bauer, K., Müller-Richter, U.D.A. & Reichert, T.E., 2012. The human HECA interacts with cyclins and CDKs to antagonize Wnt-mediated proliferation and chemoresistance of head and neck cancer cells. Exp Cell Res, 318, 489–499, Academic Press. doi:10.1016/J.YEXCR.2011.11.004

Dowejko, A., Bauer, R.J., Müller-Richter, U.D.A. & Reichert, T.E., 2009. The human homolog of the Drosophila headcase protein slows down cell division of head and neck cancer cells. Carcinogenesis, 30, 1678–1685, Oxford Academic. doi:10.1093/CARCIN/BGP189

Dudzic, J.P., Kondo, S., Ueda, R., Bergman, C.M. & Lemaitre, B., 2015. Drosophila innate immunity: regional and functional specialization of prophenoloxidases. BMC Biol, 13, BioMed Central. doi:10.1186/S12915-015-0193-6

Duncan, A.W., Rattis, F.M., DiMascio, L.N., Congdon, K.L., Pazianos, G., Zhao, C., Yoon, K., et al., 2005. Integration of Notch and Wnt signaling in hematopoietic stem cell maintenance. Nature Immunology 2005 6:3, 6, 314–322, Nature Publishing Group. doi:10.1038/ni1164

Duvic, B., Hoffmann, J.A., Meister, M. & Royet, J., 2002. Notch signaling controls lineage specification during Drosophila larval hematopoiesis. Curr Biol, 12, 1923–1927, Curr Biol. doi:10.1016/S0960-9822(02)01297-6

Dzierzak, E. & Speck, N.A., 2008. Of lineage and legacy: the development of mammalian hematopoietic stem cells. Nat Immunol, 9, 129–136, Nature Publishing Group US New York.

Elrod-Erickson, M., Mishra, S. & Schneider, D., 2000. Interactions between the cellular and humoral immune responses in Drosophila. Current Biology, 10, 781–784, Cell Press. doi:10.1016/S0960-9822(00)00569-8

Evans, C.J., Hartenstein, V. & Banerjee, U., 2003. Thicker Than Blood: Conserved Mechanisms in Drosophila and Vertebrate Hematopoiesis. Dev Cell, 5, 673–690, Elsevier. doi:10.1016/S1534-5807(03)00335-6

Evans, C.J., Liu, T. & Banerjee, U., 2014. Drosophila hematopoiesis: markers and methods for molecular genetic analysis. Methods, 68, 242–251, Elsevier.

Evans, C.J., Olson, J.M., Mondal, B.C., Kandimalla, P., Abbasi, A., Abdusamad, M.M., Acosta, O., et al., 2021. A functional genomics screen identifying blood cell development genes in Drosophila by undergraduates participating in a course-based research experience. G3, 11, jkaa028, Oxford University Press.

Fessler, J.H. & Fessler, L.I., 1989. Drosophila extracellular matrix. Annu Rev Cell Biol, 5, 309–339, Annual Reviews 4139 El Camino Way, PO Box 10139, Palo Alto, CA 94303-0139, USA.

Finkel, T. & Holbrook, N.J., 2000. Oxidants, oxidative stress and the biology of ageing. Nature 2000 408:6809, 408, 239–247, Nature Publishing Group. doi:10.1038/35041687

Fu, Y., Huang, X., Zhang, P., Leemput, J. van de & Han, Z., 2020. Single-cell RNA sequencing identifies novel cell types in Drosophila blood. Journal of Genetics and Genomics, 47, 175–186, Elsevier.

Fujiwara, Y., Chang, A.N., Williams, A.M. & Orkin, S.H., 2004. Functional overlap of GATA-1 and GATA-2 in primitive hematopoietic development. Blood, 103, 583–585, American Society of Hematology.

Gajewski, K.M., Sorrentino, R.P., Lee, J.H., Zhang, Q., Russell, M. & Schulz, R.A., 2007. Identification of a crystal cell-specific enhancer of the black cells prophenoloxidase gene in drosophila. Genesis, 45, 200–207, Wiley Online Library.

Galko, M.J. & Krasnow, M.A., 2004. Cellular and genetic analysis of wound healing in Drosophila larvae. PLoS Biol, 2, e239, Public Library of Science San Francisco, USA.

Gao, H., Wu, X. & Fossett, N., 2009. Upregulation of the Drosophila Friend of GATA Gene u-shaped by JAK/STAT Signaling Maintains Lymph Gland Prohemocyte Potency . Mol Cell Biol, 29, 6086–6096, American Society for Microbiology. doi:10.1128/MCB.00244-09/ASSET/67F1A6F1-FF95-48BC-89A5-E31E984867A2/ASSETS/GRAPHIC/ZMB0220983460009.JPEG

Gao, H., Wu, X. & Fossett, N., 2013. Drosophila E-Cadherin Functions in Hematopoietic Progenitors to Maintain Multipotency and Block Differentiation. PLoS One, 8, Public Library of Science. doi:10.1371/JOURNAL.PONE.0074684

Gao, H., Wu, X., Simon, L.T. & Fossett, N., 2014. Antioxidants Maintain E-Cadherin Levels to Limit Drosophila Prohemocyte Differentiation. PLoS One, 9, e107768, Public Library of Science. doi:10.1371/JOURNAL.PONE.0107768

Geutskens, S.B., Andrews, W.D., Stalborch, A.M.D. Van, Brussen, K., Holtrop-De Haan, S.E., Parnavelas, J.G., Hordijk, P.L., et al., 2012. Control of human hematopoietic stem/progenitor cell migration by the extracellular matrix protein Slit3. Lab Invest, 92, 1129–1139, Lab Invest. doi:10.1038/LABINVEST.2012.81

Ghosh, S., Singh, A., Mandal, S. & Mandal, L., 2015. Active Hematopoietic Hubs in Drosophila Adults Generate Hemocytes and Contribute to Immune Response. Dev Cell, 33, 478, Elsevier. doi:10.1016/J.DEVCEL.2015.03.014

Giannios, P. & Casanova, J., 2021. Systemic and local effect of the Drosophila headcase gene and its role in stress protection of Adult Progenitor Cells. PLoS Genet, 17, PLOS. doi:10.1371/JOURNAL.PGEN.1009362

Girard, J.R., Goins, L.M., Vuu, D.M., Sharpley, M.S., Spratford, C.M., Mantri, S.R. & Banerjee, U., 2021. Paths and pathways that generate cell-type heterogeneity and developmental progression in hematopoiesis. Elife, 10, eLife Sciences Publications, Ltd. doi:10.7554/ELIFE.67516

Gohl, C., Banovic, D., Grevelhörster, A. & Bogdan, S., 2010. WAVE forms hetero-and homo-oligomeric complexes at integrin junctions in Drosophila visualized by bimolecular fluorescence complementation. Journal of Biological Chemistry, 285, 40171–40179, ASBMB.

Goto, A., Kadowaki, T. & Kitagawa, Y., 2003. Drosophila hemolectin gene is expressed in embryonic and larval hemocytes and its knock down causes bleeding defects. Dev Biol, 264, 582–591, Dev Biol. doi:10.1016/J.YDBIO.2003.06.001

Grigorian, M., Mandal, L. & Hartenstein, V., 2011. Hematopoiesis at the Onset of Metamorphosis: Terminal Differentiation and Dissociation of the Drosophila Lymph Gland. Dev Genes Evol, 221, 121, NIH Public Access. doi:10.1007/S00427-011-0364-6

Guan, S., Price, J.C., Prusiner, S.B., Ghaemmaghami, S. & Burlingame, A.L., 2011. A data processing pipeline for mammalian proteome dynamics studies using stable isotope metabolic labeling. Molecular & Cellular Proteomics, 10, ASBMB.

Ho, K.Y.L., Khadilkar, R.J., Carr, R.L. & Tanentzapf, G., 2021. A gap-junction-mediated, calcium-signaling network controls blood progenitor fate decisions in hematopoiesis. Curr Biol, 31, 4697-4712.e6, Curr Biol. doi:10.1016/J.CUB.2021.08.027

Hoebe, K., Janssen, E. & Beutler, B., 2004. The interface between innate and adaptive immunity. Nat Immunol, 5, 971–974. doi:10.1038/ni1004-971

Holz, A., Bossinger, B., Strasser, T., Janning, W. & Klapper, R., 2003. The two origins of hemocytes in Drosophila. Development, 130, 4955–4962, Development. doi:10.1242/DEV.00702

Honti, V., Csordás, G., Kurucz, É., Márkus, R. & Andó, I., 2014. The cell-mediated immunity of Drosophila melanogaster: hemocyte lineages, immune compartments, microanatomy and regulation. Dev Comp Immunol, 42, 47–56, Dev Comp Immunol. doi:10.1016/J.DCI.2013.06.005

Honti, V., Csordás, G., Márkus, R., Kurucz, É., Jankovics, F. & Andó, I., 2010. Cell lineage tracing reveals the plasticity of the hemocyte lineages and of the hematopoietic compartments in Drosophila melanogaster. Mol Immunol, 47, 1997–2004, Pergamon. doi:10.1016/J.MOLIMM.2010.04.017

Honti, V., Kurucz, É., Csordás, G., Laurinyecz, B., Márkus, R. & Andó, I., 2009. In vivo detection of lamellocytes in Drosophila melanogaster. Immunol Lett, 126, 83–84, Elsevier. doi:10.1016/J.IMLET.2009.08.004

Hosokawa, K., Arai, F., Yoshihara, H., Takubo, K., Ito, K., Matsuoka, S. & Suda, T., 2006. Reactive Oxygen Species Control Hematopoietic Stem Cell-Niche Interaction through the Regulation of N-Cadherin. Blood, 108, 86–86, American Society of Hematology. doi:10.1182/BLOOD.V108.11.86.86

Hubner, N.C., Bird, A.W., Cox, J., Splettstoesser, B., Bandilla, P., Poser, I., Hyman, A., et al., 2010. Quantitative proteomics combined with BAC TransgeneOmics reveals in vivo protein interactions. Journal of Cell Biology, 189, 739–754, The Rockefeller University Press.

Irving, P., Ubeda, J.M., Doucet, D., Troxler, L., Lagueux, M., Zachary, D., Hoffmann, J.A., et al., 2005. New insights into Drosophila larval haemocyte functions through genome-wide analysis. Cell Microbiol, 7, 335–350, John Wiley & Sons, Ltd. doi:10.1111/J.1462-5822.2004.00462.X

Ito, K., Hirao, A., Arai, F., Matsuoka, S., Takubo, K., Hamaguchi, I., Nomiyama, K., et al., 2004. Regulation of oxidative stress by ATM is required for self-renewal of haematopoietic stem cells. Nature, 431, 997–1002, Nature. doi:10.1038/NATURE02989

Jagannathan-Bogdan, M. & Zon, L.I., 2013. Hematopoiesis. Development, 140, 2463, Company of Biologists. doi:10.1242/DEV.083147

Jiravanichpaisal, P., Lee, B.L. & Söderhäll, K., 2006. Cell-mediated immunity in arthropods: hematopoiesis, coagulation, melanization and opsonization. Immunobiology, 211, 213–236, Elsevier.

Jung, S.H., Evans, C.J., Uemura, C. & Banerjee, U., 2005. The Drosophila lymph gland as a developmental model of hematopoiesis. Development, 132, 2521–2533, Development. doi:10.1242/DEV.01837

Jünger, M.A., Rintelen, F., Stocker, H., Wasserman, J.D., Végh, M., Radimerski, T., Greenberg, M.E., et al., 2003. The Drosophila Forkhead transcription factor FOXO mediates the reduction in cell number associated with reduced insulin signaling. J Biol, 2, 20, BioMed Central. doi:10.1186/1475-4924-2-20

Karanu, F.N., Murdoch, B., Gallacher, L., Wu, D.M., Koremoto, M., Sakano, S. & Bhatia, M., 2000. The Notch Ligand Jagged-1 Represents a Novel Growth Factor of Human Hematopoietic Stem Cells. Journal of Experimental Medicine, 192, 1365–1372, The Rockefeller University Press. doi:10.1084/JEM.192.9.1365

Kaur, H., Sharma, S.K., Mandal, S. & Mandal, L., 2019. Lar maintains the homeostasis of the hematopoietic organ in Drosophila by regulating insulin signaling in the niche. Development, 146, Company of Biologists. doi:10.1242/DEV.178202

Kharrat, B., Csordás, G. & Honti, V., 2022. Peeling Back the Layers of Lymph Gland Structure and Regulation. International Journal of Molecular Sciences 2022, Vol. 23, Page 7767, 23, 7767, Multidisciplinary Digital Publishing Institute. doi:10.3390/IJMS23147767

Kleppe, M., Spitzer, M.H., Li, S., Hill, C.E., Dong, L., Papalexi, E., Groote, S. De, et al., 2017. Jak1 Integrates Cytokine Sensing to Regulate Hematopoietic Stem Cell Function and Stress Hematopoiesis. Cell Stem Cell, 21, 489-501.e7, Cell Stem Cell. doi:10.1016/J.STEM.2017.08.011

Kocks, C., Cho, J.H., Nehme, N., Ulvila, J., Pearson, A.M., Meister, M., Strom, C., et al., 2005. Eater, a transmembrane protein mediating phagocytosis of bacterial pathogens in Drosophila. Cell, 123, 335–346, Elsevier B.V. doi:10.1016/J.CELL.2005.08.034/ATTACHMENT/8A3E936E-214F-43C5-8504-14DBE35B25B8/MMC1.PDF

Krautz, R., Arefin, B. & Theopold, U., 2014. Damage signals in the insect immune response. Front Plant Sci, 5, 342, Frontiers.

Krzemien, J., Crozatier, M. & Vincent, A., 2010. Ontogeny of the Drosophila larval hematopoietic organ, hemocyte homeostasis and the dedicated cellular immune response to parasitism. International Journal of Developmental Biology, 54, 1117–1125, UPV/EHU Press.

Krzemień, J., Dubois, L., Makki, R., Meister, M., Vincent, A. & Crozatier, M., 2007. Control of blood cell homeostasis in Drosophila larvae by the posterior signalling centre. Nature, 446, 325–328, Nature. doi:10.1038/NATURE05650

Krzemien, J., Oyallon, J., Crozatier, M. & Vincent, A., 2010. Hematopoietic progenitors and hemocyte lineages in the Drosophila lymph gland. Dev Biol, 346, 310–319, Dev Biol. doi:10.1016/J.YDBIO.2010.08.003

Kurucz, É., Márkus, R., Zsámboki, J., Folkl-Medzihradszky, K., Darula, Z., Vilmos, P., Udvardy, A., et al., 2007. Nimrod, a Putative Phagocytosis Receptor with EGF Repeats in Drosophila Plasmatocytes. Current Biology, 17, 649–654, Elsevier. doi:10.1016/J.CUB.2007.02.041/ATTACHMENT/6F55F587-F3BA-4895-8CEB-70149627BE55/MMC2.PDF

Kurucz, É., Váczi, B., Márkus, R., Laurinyecz, B., Vilmos, P., Zsámboki, J., Csorba, K., et al., 2007. Definition of Drosophila hemocyte subsets by cell-type specific antigens. Acta Biol Hung, 58, 95–111, Akadémiai Kiadó.

Kúthy-Sutus, E., Kharrat, B., Gábor, E., Csordás, G., Sinka, R. & Honti, V., 2023. A Novel Method for Primary Blood Cell Culturing and Selection in Drosophila melanogaster. Cells, 12, 24, MDPI. doi:10.3390/CELLS12010024/S1

Lanot, R., Zachary, D., Holder, F. & Meister, M., 2001. Postembryonic Hematopoiesis in Drosophila. Dev Biol, 230, 243–257, Academic Press. doi:10.1006/DBIO.2000.0123

Lebestky, T., Chang, T., Hartenstein, V. & Banerjee, U., 2000. Specification of Drosophila hematopoietic lineage by conserved transcription factors. Science, 288, 146–149, Science. doi:10.1126/SCIENCE.288.5463.146

Lebestky, T., Jung, S.H. & Banerjee, U., 2003. A Serrate-expressing signaling center controls Drosophila hematopoiesis. Genes Dev, 17, 348, Cold Spring Harbor Laboratory Press. doi:10.1101/GAD.1052803

Leitão, A.B. & Sucena, É., 2015. Drosophila sessile hemocyte clusters are true hematopoietic tissues that regulate larval blood cell differentiation. Elife, 4, 1–38, Elife. doi:10.7554/ELIFE.06166

Letourneau, M., Lapraz, F., Sharma, A., Vanzo, N., Waltzer, L. & Crozatier, M., 2016. Drosophila hematopoiesis under normal conditions and in response to immune stress. FEBS Lett, 590, 4034–4051, FEBS Lett. doi:10.1002/1873-3468.12327

Li, N., Liu, Q., Xiong, Y. & Yu, J., 2019. Headcase and Unkempt Regulate Tissue Growth and Cell Cycle Progression in Response to Nutrient Restriction. Cell Rep, 26, 733, NIH Public Access. doi:10.1016/J.CELREP.2018.12.086

Li, R.-J., Xu, J., Fu, C., Zhang, J., Zheng, Y.G., Jia, H. & Liu, J.O., 2016. Regulation of mTORC1 by lysosomal calcium and calmodulin. Elife, 5, e19360, eLife Sciences Publications, Ltd.

Li, Y. & Andrade, J., 2017. DEApp: an interactive web interface for differential expression analysis of next generation sequence data. Source Code Biol Med, 12, 1–4, BioMed Central.

Liguori, F., Mascolo, E. & Vernì, F., 2021. The genetics of diabetes: What we can learn from Drosophila. Int J Mol Sci, 22, 11295, MDPI.

Lipinszki, Z., Vernyik, V., Farago, N., Sari, T., Puskas, L.G., Blattner, F.R., Posfai, G., et al., 2018. Enhancing the translational capacity of E. coli by resolving the codon bias. ACS Synth Biol, 7, 2656–2664, ACS Publications.

Loncle, N. & Williams, D.W., 2012. An Interaction Screen Identifies headcase as a Regulator of Large-Scale Pruning. The Journal of Neuroscience, 32, 17086, Society for Neuroscience. doi:10.1523/JNEUROSCI.1391-12.2012

Louradour, I., Sharma, A., Morin-Poulard, I., Letourneau, M., Vincent, A., Crozatier, M. & Vanzo, N., 2017. Reactive oxygen species-dependent Toll/NF-κB activation in the Drosophila hematopoietic niche confers resistance to wasp parasitism. Elife, 6, e25496, eLife Sciences Publications, Ltd.

Madhwal, S., Shin, M., Kapoor, A., Goyal, M., Joshi, M.K., Rehman, P.M.U., Gor, K., et al., 2020. Metabolic control of cellular immune-competency by odors in drosophila. Elife, 9, 1–93, eLife Sciences Publications Ltd. doi:10.7554/ELIFE.60376

Makhijani, K., Alexander, B., Rao, D., Petraki, S., Herboso, L., Kukar, K., Batool, I., et al., 2017. Regulation of Drosophila hematopoietic sites by Activin-β from active sensory neurons. Nat Commun, 8, 15990, Nature Publishing Group UK London.

Makhijani, K., Alexander, B., Tanaka, T., Rulifson, E. & Brückner, K., 2011. The peripheral nervous system supports blood cell homing and survival in the Drosophila larva. Development, 138, 5379–5391, Company of Biologists. doi:10.1242/DEV.067322/-/DC1

Mandal, L., Banerjee, U. & Hartenstein, V., 2004. Evidence for a fruit fly hemangioblast and similarities between lymph-gland hematopoiesis in fruit fly and mammal aorta-gonadal-mesonephros mesoderm. Nat Genet, 36, 1019–1023, Nature Publishing Group US New York.

Mandal, L., Martinez-Agosto, J.A., Evans, C.J., Hartenstein, V. & Banerjee, U., 2007. A Hedgehog- and Antennapedia-dependent niche maintains Drosophila haematopoietic precursors. Nature, 446, 320–324, Nature Publishing Group. doi:10.1038/NATURE05585

Márkus, R., Laurinyecz, B., Kurucz, É., Honti, V., Bajusz, I., Sipos, B., Somogyi, K., et al., 2009. Sessile hemocytes as a hematopoietic compartment in Drosophila melanogaster. Proceedings of the National Academy of Sciences, 106, 4805–4809, National Acad Sciences.

Martinek, N., Shahab, J., Saathoff, M. & Ringuette, M., 2008. Haemocyte-derived SPARC is required for collagen-IV-dependent stability of basal laminae in Drosophila embryos. J Cell Sci, 121, 1671–1680, Company of Biologists.

Medvinsky, A. & Dzierzak, E., 1996. Definitive hematopoiesis is autonomously initiated by the AGM region. Cell, 86, 897–906, Elsevier.

Millar, D.A. & Ratcliffe, N.A., 1989. The evolution of blood cells: facts and enigmas. Endeavour, 13, 72–77, Elsevier.

Mondal, B.C., Mukherjee, T., Mandal, L., Evans, C.J., Sinenko, S.A., Martinez-Agosto, J.A. & Banerjee, U., 2011. Interaction between differentiating cell and niche-derived signals in hematopoietic progenitor maintenance. Cell, 147, 1589, NIH Public Access. doi:10.1016/J.CELL.2011.11.041

Morin-Poulard, I., Sharma, A., Louradour, I., Vanzo, N., Vincent, A. & Crozatier, M., 2016. Vascular control of the Drosophila haematopoietic microenvironment by Slit/Robo signalling. Nat Commun, 7, Nature Publishing Group. doi:10.1038/NCOMMS11634

Nagahata, Y., Masuda, K., Nishimura, Y., Ikawa, T., Kawaoka, S., Kitawaki, T., Nannya, Y., et al., 2022. Tracing the evolutionary history of blood cells to the unicellular ancestor of animals. Blood, The Journal of the American Society of Hematology, 140, 2611–2625, American Society of Hematology Washington, DC.

Nam, H., Jang, I., You, H., Lee, K. & Lee, W., 2012. Genetic evidence of a redox-dependent systemic wound response via Hayan protease-phenoloxidase system in Drosophila. EMBO J, 31, 1253–1265, John Wiley & Sons, Ltd Chichester, UK.

Nappi, A.J., Vass, E., Frey, F. & Carton, Y., 1995. Superoxide anion generation in Drosophila during melanotic encapsulation of parasites. Eur J Cell Biol, 68, 450–456.

Nelson, R.E., Fessler, L.I., Takagi, Y., Blumberg, B., Keene, D.R., Olson, P.F., Parker, C.G., et al., 1994. Peroxidasin: a novel enzyme-matrix protein of Drosophila development. EMBO J, 13, 3438–3447, EMBO J. doi:10.1002/J.1460-2075.1994.TB06649.X

Nemoto, S. & Finkel, T., 2002. Redox regulation of forkhead proteins through a p66shc-dependent signaling pathway. Science, 295, 2450–2452, Science. doi:10.1126/SCIENCE.1069004

Neyen, C., Binggeli, O., Roversi, P., Bertin, L., Sleiman, M.B. & Lemaitre, B., 2015. The Black cells phenotype is caused by a point mutation in the Drosophila pro-phenoloxidase 1 gene that triggers melanization and hematopoietic defects. Dev Comp Immunol, 50, 166–174, Elsevier.

Orkin, S.H. & Zon, L.I., 2008. Hematopoiesis: an evolving paradigm for stem cell biology. Cell, 132, 631–644, Elsevier.

Owusu-Ansah, E. & Banerjee, U., 2009. Reactive Oxygen Species prime Drosophila haematopoietic progenitors for differentiation. Nature, 461, 537, NIH Public Access. doi:10.1038/NATURE08313

Oyallon, J., Vanzo, N., Krzemień, J., Morin-Poulard, I., Vincent, A. & Crozatier, M., 2016. Two Independent Functions of Collier/Early B Cell Factor in the Control of Drosophila Blood Cell Homeostasis. PLoS One, 11, e0148978, Public Library of Science. doi:10.1371/JOURNAL.PONE.0148978

Pastor-Pareja, J.C., Wu, M. & Xu, T., 2008. An innate immune response of blood cells to tumors and tissue damage in Drosophila. Dis Model Mech, 1, 144–154, The Company of Biologists Limited.

Pennetier, D., Oyallon, J., Morin-Poulard, I., Dejean, S., Vincent, A. & Crozatier, M., 2012. Size control of the Drosophila hematopoietic niche by bone morphogenetic protein signaling reveals parallels with mammals. Proc Natl Acad Sci U S A, 109, 3389–3394, National Academy of Sciences. doi:10.1073/PNAS.1109407109/-/DCSUPPLEMENTAL

Port, F., Chen, H.-M., Lee, T., & Bullock, S. L. (2014). Optimized CRISPR/Cas tools for efficient germline and somatic genome engineering in Drosophila. Proceedings of the National Academy of Sciences, 111(29), E2967–E2976.

Presley, C.A., Lee, A.W., Kastl, B., Igbinosa, I., Yamada, Y., Fishman, G.I., Gutstein, D.E., et al., 2005. Bone marrow connexin-43 expression is critical for hematopoietic regeneration after chemotherapy. Cell Commun Adhes, 12, 307–317, Taylor & Francis.

Puig, O., Marr, M.T., Ruhf, M.L. & Tjian, R., 2003. Control of cell number by Drosophila FOXO: downstream and feedback regulation of the insulin receptor pathway. Genes Dev, 17, 2006–2020, Genes Dev. doi:10.1101/GAD.1098703

Regan, J.C., Brandão, A.S., Leitão, A.B., Mantas Dias, A.R., Sucena, É., Jacinto, A. & Zaidman-Rémy, A., 2013. Steroid hormone signaling is essential to regulate innate immune cells and fight bacterial infection in Drosophila. PLoS Pathog, 9, e1003720, Public Library of Science San Francisco, USA.

Rehorn, K.-P., Thelen, H., Michelson, A.M. & Reuter, R., 1996. A molecular aspect of hematopoiesis and endoderm development common to vertebrates and Drosophila. Development, 122, 4023–4031, The Company of Biologists Ltd.

Resende, L.P.F., Boyle, M., Tran, D., Fellner, T. & Jones, D.L., 2013. Headcase Promotes Cell Survival and Niche Maintenance in the Drosophila Testis. PLoS One, 8, e68026, Public Library of Science. doi:10.1371/JOURNAL.PONE.0068026

Resende, L.P.F., Truong, M.E., Gomez, A. & Jones, D.L., 2017. Intestinal stem cell ablation reveals differential requirements for survival in response to chemical challenge. Dev Biol, 424, 10–17, Elsevier.

Reya, T., Duncan, A.W., Ailles, L., Domen, J., Scherer, D.C., Willert, K., Hintz, L., et al., 2003. A role for Wnt signalling in self-renewal of haematopoietic stem cells. Nature 2003 423:6938, 423, 409–414, Nature Publishing Group. doi:10.1038/nature01593

Rizki, M.T.M., 1957. Alterations in the haemocyte population of Drosophila melanogaster. J Morphol, 100, 437–458. doi:10.1002/JMOR.1051000303

Rizki, T.M., 1978. circulatory system and associated cells and tissues. Genetics and biology of Drosophila.

Rizki, T.M. & Rizki, R.M., 1992. Lamellocyte differentiation in Drosophila larvae parasitized by Leptopilina. Dev Comp Immunol, 16, 103–110, Pergamon. doi:10.1016/0145-305X(92)90011-Z

Rosendaal, M., Mayen, A., Koning, A. De, Dunina-Barkovskaya, T., Krenacs, T. & Ploemacher, R., 1997. Does transmembrane communication through gap junctions enable stem cells to overcome stromal inhibition? Leukemia, 11, 1281–1289, Nature Publishing Group.

Rugendorff, A., Younossi-Hartenstein, A. & Hartenstein, V., 1994. Embryonic origin and differentiation of the Drosophila heart. Rouxs Arch Dev Biol, 203, 266–280, Rouxs Arch Dev Biol. doi:10.1007/BF00360522

Russo, J., Dupas, S., Frey, F., Carton, Y. & Brehelin, M., 1996. Insect immunity: early events in the encapsulation process of parasitoid (Leptopilina boulardi) eggs in resistant and susceptible strains of Drosophila. Parasitology, 112, 135–142, Cambridge University Press.

Sam, S., Leise, W. & Hoshizaki, D.K., 1996. The serpent gene is necessary for progression through the early stages of fat-body development. Mech Dev, 60, 197–205, Elsevier.

Sanchez-Sanchez, B.J., Urbano, J.M., Comber, K., Dragu, A., Wood, W., Stramer, B. & Martín-Bermudo, M.D., 2017. Drosophila embryonic hemocytes produce laminins to strengthen migratory response. Cell Rep, 21, 1461–1470, Elsevier.

Schofield, R., 1978. The relationship between the spleen colony-forming cell and the haemopoietic stem cell. Blood Cells, 4, 7–25.

Shatoury, H.H. El, 1955. The structure of the lymph glands of Drosophila larvae. Wilhelm Roux Arch Entwickl Mech Org, 147, 489–495, Wilhelm Roux Arch Entwickl Mech Org. doi:10.1007/BF00576000

Shim, J., Mukherjee, T. & Banerjee, U., 2012. Direct sensing of systemic and nutritional signals by hematopoietic progenitors in Drosophila. Nat Cell Biol, 14, 394, NIH Public Access. doi:10.1038/NCB2453

Shim, J., Mukherjee, T., Mondal, B.C., Liu, T., Young, G.C., Wijewarnasuriya, D.P. & Banerjee, U., 2013. Olfactory control of blood progenitor maintenance. Cell, 155, 1141, NIH Public Access. doi:10.1016/J.CELL.2013.10.032

Shrestha, R. & Gateff, E., 1982. Ultrastructure and Cytochemistry of the Cell Types in the Larval Hematopoietic Organs and Hemolymph of Drosophila Melanogaster drosophila/hematopoiesis/blool cells/ultrastructure/cytochemistry. Dev Growth Differ, 24, 65–82. doi:10.1111/J.1440-169X.1982.00065.X

Sinenko, S.A., Mandal, L., Martinez-Agosto, J.A. & Banerjee, U., 2009. Dual role of Wingless signaling in stem-like hematopoietic precursor maintenance in Drosophila. Dev Cell, 16, 756, NIH Public Access. doi:10.1016/J.DEVCEL.2009.03.003

Sinenko, S.A., Shim, J. & Banerjee, U., 2012. Oxidative stress in the haematopoietic niche regulates the cellular immune response in Drosophila. EMBO Rep, 13, 83, European Molecular Biology Organization. doi:10.1038/EMBOR.2011.223

Smith, B.R., 1990. Regulation of hematopoiesis. Yale J Biol Med, 63, 371, Yale Journal of Biology and Medicine. Retrieved from /pmc/articles/PMC2589354/?report=abstract

Smith-Berdan, S., Nguyen, A., Hong, M.A. & Forsberg, E.C., 2015. ROBO4-Mediated Vascular Integrity Regulates the Directionality of Hematopoietic Stem Cell Trafficking. Stem Cell Reports, 4, 255, Elsevier. doi:10.1016/J.STEMCR.2014.12.013

Spahn, P., Huelsmann, S., Rehorn, K.-P., Mischke, S., Mayer, M., Casali, A. & Reuter, R., 2014. Multiple regulatory safeguards confine the expression of the GATA factor Serpent to the hemocyte primordium within the Drosophila mesoderm. Dev Biol, 386, 272–279, Elsevier.

Spratford, C.M., Goins, L.M., Chi, F., Girard, J.R., Macias, S.N., Ho, V.W. & Banerjee, U., 2021. Intermediate progenitor cells provide a transition between hematopoietic progenitors and their differentiated descendants. Development (Cambridge), 148, Company of Biologists Ltd. doi:10.1242/DEV.200216

Steneberg, P. & Samakovlis, C., 2001. A novel stop codon readthrough mechanism produces functional Headcase protein in Drosophila trachea. EMBO Rep, 2, 593–597, John Wiley & Sons, Ltd.

Stier, S., Cheng, T., Dombkowski, D., Carlesso, N. & Scadden, D.T., 2002. Notch1 activation increases hematopoietic stem cell self-renewal in vivo and favors lymphoid over myeloid lineage outcome. Blood, 99, 2369–2378, Content Repository Only! doi:10.1182/BLOOD.V99.7.2369

Stofanko, M., Kwon, S.Y. & Badenhorst, P., 2010. Lineage tracing of lamellocytes demonstrates Drosophila macrophage plasticity. PLoS One, 5, e14051, Public Library of Science San Francisco, USA.

Sullivan, W., Ashburner, M. & Hawley, R.S., 2000. Drosophila protocols., Cold Spring Harbor Laboratory Press.

Sutter, D. De & Buscema, M., 1977. Isolation of a highly pure archeocyte fraction from the fresh-water sponge Ephydatia fluviatilis. Wilehm Roux Arch Dev Biol, 183, 149–153, Springer.

Sutter, D. De & Vyver, G. Van De, 1977. Aggregative properties of different cell types of the fresh-water sponge Ephydatia fluviatilis isolated on ficoll gradients. Wilehm Roux Arch Dev Biol, 181, 151–161, Springer.

Sykiotis, G.P. & Bohmann, D., 2008. Keap1/Nrf2 signaling regulates oxidative stress tolerance and lifespan in Drosophila. Dev Cell, 14, 76, NIH Public Access. doi:10.1016/J.DEVCEL.2007.12.002

Szkalisity, A., Piccinini, F., Beleon, A., Balassa, T., Varga, I.G., Migh, E., Molnar, C., et al., 2021. Regression plane concept for analysing continuous cellular processes with machine learning. Nat Commun, 12, 2532, Nature Publishing Group UK London.

Tang, H., Kambris, Z., Lemaitre, B. & Hashimoto, C., 2006. Two proteases defining a melanization cascade in the immune system of Drosophila. Journal of Biological Chemistry, 281, 28097–28104, ASBMB.

Tao, Y. & Schulz, R.A., 2007. Heart development in Drosophila. Semin Cell Dev Biol, Vol. 18, pp. 3–15, Elsevier.

Tattikota, S.G., Cho, B., Liu, Y., Hu, Y., Barrera, V., Steinbaugh, M.J., Yoon, S.-H., et al., 2020. A single-cell survey of Drosophila blood. Elife, 9, e54818, eLife Sciences Publications, Ltd.

Teleman, A.A., Hietakangas, V., Sayadian, A.C. & Cohen, S.M., 2008. Nutritional Control of Protein Biosynthetic Capacity by Insulin via Myc in Drosophila. Cell Metab, 7, 21–32, Elsevier. doi:10.1016/j.cmet.2007.11.010

Tepass, U., Fessler, L.I., Aziz, A. & Hartenstein, V., 1994. Embryonic origin of hemocytes and their relationship to cell death in Drosophila. Development, 120, 1829–1837, Development. doi:10.1242/DEV.120.7.1829

Terriente-Felix, A., Li, J., Collins, S., Mulligan, A., Reekie, I., Bernard, F., Krejci, A., et al., 2013. Notch cooperates with Lozenge/Runx to lock haemocytes into a differentiation programme. Development (Cambridge), 140, 926–937, Development. doi:10.1242/DEV.086785/-/DC1

Tokusumi, T., Shoue, D.A., Tokusumi, Y., Stoller, J.R. & Schulz, R.A., 2009. New hemocyte-specific enhancer-reporter transgenes for the analysis of hematopoiesis in Drosophila. genesis, 47, 771–774, John Wiley & Sons, Ltd. doi:10.1002/DVG.20561

Tokusumi, T., Sorrentino, R.P., Russell, M., Ferrarese, R., Govind, S. & Schulz, R.A., 2009. Characterization of a Lamellocyte Transcriptional Enhancer Located within the misshapen Gene of Drosophila melanogaster. PLoS One, 4, Public Library of Science. doi:10.1371/JOURNAL.PONE.0006429

Tokusumi, Y., Tokusumi, T., Shoue, D.A. & Schulz, R.A., 2012. Gene Regulatory Networks Controlling Hematopoietic Progenitor Niche Cell Production and Differentiation in the Drosophila Lymph Gland. PLoS One, 7, e41604, Public Library of Science. doi:10.1371/JOURNAL.PONE.0041604

Tsuchiya, A., Kanno, T. & Nishizaki, T., 2014. PI3 kinase directly phosphorylates Akt1/2 at Ser473/474 in the insulin signal transduction pathway. J Endocrinol, 220, 49, Bioscientifica Ltd. doi:10.1530/JOE-13-0172

Vanha-Aho, L.-M., Anderl, I., Vesala, L., Hultmark, D., Valanne, S. & Rämet, M., 2015. Edin expression in the fat body is required in the defense against parasitic wasps in Drosophila melanogaster. PLoS Pathog, 11, e1004895, Public Library of Science San Francisco, CA USA.

Varga, G.I.B., Csordás, G., Cinege, G., Jankovics, F., Sinka, R., Kurucz, É., Andó, I., et al., 2019. Headcase is a Repressor of Lamellocyte Fate in Drosophila melanogaster. Genes (Basel), 10, Genes (Basel). doi:10.3390/GENES10030173

Vetvicka, V. & Sima, P., 2009. Origins and functions of annelide immune cells: the concise survey. Invertebrate Survival Journal, 6, 138–143.

Walhout, A.J.M., Temple, G.F., Brasch, M.A., Hartley, J.L., Lorson, M.A., Heuvel, S. van den & Vidal, M., 2000. [34] GATEWAY recombinational cloning: Application to the cloning of large numbers of open reading frames or ORFeomes. in Methods in enzymology, Vol. 328, pp. 575-IN7, Elsevier.

Weaver, T.A. & White, R.A.H., 1995. headcase, an imaginal specific gene required for adult morphogenesis in Drosophila melanogaster. Development, 121, 4149–4160, Development. doi:10.1242/DEV.121.12.4149

Williams, M.J., 2007. Drosophila hemopoiesis and cellular immunity. The Journal of Immunology, 178, 4711–4716, American Association of Immunologists.

Williams, M.J., Ando, I. & Hultmark, D., 2005. Drosophila melanogaster Rac2 is necessary for a proper cellular immune response. Genes to cells, 10, 813–823, Wiley Online Library.

Williams, M.J., Wiklund, M.-L., Wikman, S. & Hultmark, D., 2006. Rac1 signalling in the Drosophila larval cellular immune response. J Cell Sci, 119, 2015–2024, Company of Biologists.

Wood, W., Faria, C. & Jacinto, A., 2006. Distinct mechanisms regulate hemocyte chemotaxis during development and wound healing in Drosophila melanogaster. J Cell Biol, 173, 405–416, Rockefeller University Press.

Yilmaz, Ö.H., Valdez, R., Theisen, B.K., Guo, W., Ferguson, D.O., Wu, H. & Morrison, S.J., 2006. Pten dependence distinguishes haematopoietic stem cells from leukaemia-initiating cells. Nature 2006 441:7092, 441, 475–482, Nature Publishing Group. doi:10.1038/nature04703

Young, K., Eudy, E., Bell, R., Loberg, M.A., Stearns, T., Sharma, D., Velten, L., et al., 2021. Decline in IGF1 in the bone marrow microenvironment initiates hematopoietic stem cell aging. Cell Stem Cell, 28, 1473-1482.e7, Cell Stem Cell. doi:10.1016/J.STEM.2021.03.017

Yu, S., Luo, F. & Jin, L.H., 2021. Rab5 and Rab11 maintain hematopoietic homeostasis by restricting multiple signaling pathways in Drosophila. Elife, 10, 1–23, eLife Sciences Publications, Ltd. doi:10.7554/ELIFE.60870

Zettervall, C.J., Anderl, I., Williams, M.J., Palmer, R., Kurucz, E., Ando, I. & Hultmark, D., 2004. A directed screen for genes involved in Drosophila blood cell activation. Proc Natl Acad Sci U S A, 101, 14192–14197. doi:10.1073/PNAS.0403789101

Zhang, J., Grindley, J.C., Yin, T., Jayasinghe, S., He, X.C., Ross, J.T., Haug, J.S., et al., 2006. PTEN maintains haematopoietic stem cells and acts in lineage choice and leukaemia prevention. Nature 2006 441:7092, 441, 518–522, Nature Publishing Group. doi:10.1038/nature04747

Zhang, J., Niu, C., Ye, L., Huang, H., He, X., Tong, W.G., Ross, J., et al., 2003. Identification of the haematopoietic stem cell niche and control of the niche size. Nature 2003 425:6960, 425, 836–841, Nature Publishing Group. doi:10.1038/nature02041

10. Supplementary material

S1 Table. List of the *Drosophila* stocks used in this study.

Abbreviation	Genotype	Source
w	w^{1118}	BDSC_5905
col>	*w; Pcol85-Gal4/CyO, GFP; +*	(Krzemień et al., 2007)
col>hdcRNAi	*w; Pcol85-Gal4,UAS-hdcRNAi/CyO, GFP; +*	(Varga et al., 2019)
unkRNAi	*y, v, sc; UAS-unkRNAi; +*	BDSC_57026
PI3KCa	*y, w, UAS-Pi3K92E.CAAX; +; +*	BDSC_8294
PtenRNAi	*w; +; UAS-PtenRNAi*	BDSC_8550
AktRNAi	*y, v; +; UAS-AktRNAi*	BDSC_31701
raptorRNAi	*y, v; +; UAS-raptorRNAi*	BDSC_31528
col>PtenRNAi	*w; Pcol85-Gal4/CyO, GFP; UAS-PtenRNAi*	Generated by combining *Pcol85-Gal4* with *UAS-PtenRNAi*
hdc	*w; +; UAS-hdc.S*	A gift from Christos Samakovlis
col>GFP	*w; Pcol85-Gal4, UAS-2xEGFP/SM6b; +*	Generated by recombining *Pcol85-Gal4* with *UAS-2xEGFP* (BDSC_6874)

hdcRNAi	*w; UAS-hdcRNAi; +*	VDRC_v45069
col>hdcRNAi>GFP	*w; Pcol85-Gal4, UAS-hdcRNAi/CyO, GFP; UAS-2xEGFP*	Generated from combining *Pcol85-Gal4, UAS-hdcRNAi/CyO, GFP* with *y, w; +; UAS-EGFP* (BDSC_6658)
p35	*w; +; UAS-p35*	BDSC_5073
gstD-GFP	*w; gstD-GFP; +*	A gift from Lolitika Mandal (Sykiotis & Bohmann, 2008)
Thor-lacZ	*y, w; Thor-lacZ; +*	BDSC_9558
Cat	*w; UAS-Cat; +*	BDSC_24621
Foxo	*y, w; UAS-foxo; +*	BDSC_9575
foxoRNAi	*y, v; +; UAS-foxoRNAi*	BDSC_25997
UAS-spiRNAi	*w; UAS-spiRNAi; +*	VDRC_v103817
hdc^{19}	*w; +;* hdc^{19}*-Gal4/TM3, Kr::GFP*	(Varga et al., 2019)
hdc>GFP	*w; UAS-mCD8::GFP;* hdc^{19}*-Gal4/TM6, Tb*	Generated from combining hdc^{19} with *UAS-mCD8GFP* (A gift from József Mihály, BRC Szeged)
Hml:DsRed	*w; +; Hml:DsRed*	(Makhijani et al. 2011)
domeMESO>	*w; +; domeMESO-GAL4, UAS-2xEGFP/TM6*	(Oyallon et al., 2016)

CHIZ>	*w; dome^{MESO}-GAL4-AD, Hml$^{\Delta}$-GAL4-DBD (CHIZ-GAL4)/CyO, GFP; +*	A gift from Gregory D. Longmore. The *CyO* balancer was changed to *CyO, GFP* (Spratford et al., 2021)
gstD-GFP; domeMESO	*w; gstD-GFP; domeMESO-Gal4/Tm6, Tb*	Generated by combining *gstD-GFP* with *domeMESO-Gal4*
hdc$^{\Delta 84}$	*w; +; hdc $^{\Delta 84}$/TM3, Kr::GFP*	(Varga et al. 2019)
gstD-GFP; hdc$^{\Delta 84}$	*w; gstD-GFP; hdc$^{\Delta 84}$/TM6, Tb*	Generated by combining *gstD-GFP* with *hdc$^{\Delta 84}$*
domeMESO>hdcRNAi	*w; hdcRNAi/CyO, GFP; domeMESO-GAL4, UAS-2xEGFP/TM6, Tb*	Generated from combining *UAS-hdcRNAi* (VDRC_v45069) with domeMESO-GAL4, UAS-2xEGFP (Oyallon et al., 2016)
bskDN	*w; +; UAS-bskK53R*	BDSC_9311
EGFRDN	*y, w; UAS-Egfr.DN; UAS-Egfr.DN*	BDSC_5364
E-Cad	*w; +; UAS-E-cad*	A gift from Gregory D. Longmore.
hdcRA_STOP	*w; UAS-hdcRA_STOP/SM6b; +*	This study
hdcRC_STOP	*w; UAS-hdcRC_STOP/SM6b; +*	This study
hdcRC_NOSTOP	*w; UAS-hdcRC_NOSTOP/SM6b; +*	This study
hdcRA_STOP; hdc$^{\Delta 84}$	*w; UAS-hdcRA_STOP/Cyo, GFP; hdc$^{\Delta 84}$/TM6, Tb*	This study
CamRNAi	*y, sc, v, sev; +; UAS-CamRNAi*	BDSC_34609

eIF5BRNAi	*y, sc, v, sev; +; UAS-eIF5BRNAi/TM6, Tb*	BDSC_44418 (The *TM3* balancer was changed to *TM6, Tb*)
CCT1RNAi	*y, sc, v, sev; +; UAS-CCT1RNAi*	BDSC_32854
eRF3RNAi	*y, sc, v, sev; +; UAS-eRF3RNAi*	BDSC_36703
HSC70-4RNAi	*y, v; +; UAS-Hsc70-4RNAi*	BDSC_28709
Rpn11RNAi	*y, sc, v, sev; +; UAS-Rpn11*	BDSC_33662
AP-2aRNAi	*y, sc, v, sev; +; UAS-AP-2aRNAi*	BDSC_32866

S2 Table. List of the used primers.

hdccDNA_For	GGGGACAAGTTTGTACAAAAAAGCAGGCTTCACCATGGCTCCGCGTCGCAAC
hdccDNA_rev	GGGGACCACTTTGTACAAGAAAGCTGGGTCGCTTTCTGCGAGCGTCGGC
UnkcDNA_For	GGGGACAAGTTTGTACAAAAAAGCAGGCTTCACCATGTTGGCAAATGAAACG
UnkcDNA_rev	GGGGACCACTTTGTACAAGAAAGCTGGGTCGCTCCAGGTGTGGGTGGTT
CamcDNA_For	GGGGACAAGTTTGTACAAAAAAGCAGGCTTCACCATGGCCGATCAGCTGACA
CamcDNA_rev	GGGGACCACTTTGTACAAGAAAGCTGGGTCGCTCCACTTCGATGTCAT
HdccDNA_new_rev	GGGGACCACTTTGTACAAGAAAGCTGGGTTTTATGCGAGCGTCGGCAG
pDEST17-to-pHY22_For	CGCTGATATCGGATCGCCACCATGTCGTACTACCATCACCA
pDEST17-to-pHY22_rev	CTTAACAGTTGGATCCAAGAAAGCTGGGTT
pTHW_fwd	TGACGTAAGCTAGAGGATC
pTHW_rev	AGCAGCGTAATCTGGAAC
hdcRA_STOP_fwd	ACGTTCCAGATTACGCTGCTATGGCTCCGCGTCGCAAC
hdcRA_STOP_rev	AGATCCTCTAGCTTACGTCATTATGCGAGCGTCGGCAG
hdcRC_STOP_fwd	ACGTTCCAGATTACGCTGCTATGGCTCCGCGTCGCAAC
hdcRC_STOP_rev	AGATCCTCTAGCTTACGTCATTAGTTCATGTTGAGATAGTCGTTGAAGAGC
hdcRC_NOSTOP_1_fwd	ACGTTCCAGATTACGCTGCTATGGCTCCGCGTCGCAACAG
hdcRC_NOSTOP_1_rev	GGGCCTCATGTGCGAGCGTCGGCAGCCG
hdc_RCNOSTOP_2_fwd	GACGCTCGCACATGAGGCCCCGTTGGAG

hdc_RCNOSTOP_2_rev	AGATCCTCTAGCTTACGTCATTAGTTCATGTTGAGATAGTCGTTGAAGAG

S3 Table. List of the genes encoding for the 468 top candidate interactors of Hdc acquired through the LC-MS/MS analysis and ranked by their respective scores. The scores were calculated by multiplying the peptide count of candidate with the coverage percentage. The candidates that were tested further in genetic interactions are highlighted in yellow.

Gene symbol	Score
hdc	1730.134
RpL28	1696.67
Dmel\CG15019	1651.151
RpL23A	1636.532
RpL4	1604.386
RpL18	1578.489
up	1505.321
RpL14	1462.402
RpL13A	1370.045
RpL3	1359.627
RpS9	1354.426
RpL6	1347.981
RpL7	1335.222
RpL10	1263.076
RpL22	1247.572
RpL30	1235.954
RpL19	1204.481
Hsp27	1167.684
RpS23	1160.197
Srp14	1142.002
RpL13	1134.987
RpS2	1121.313
RpL37A	1116.731
RpL8	1116.478
RpL27	1091.222
RpL36	1073.335
RpL23	1071.072
RpL32	1032.063
RpS8	1014.509
RpS6	1007.496
RpL26	998.5103
RpL21	996.2187
RpS11	991.6272
RpL9	989.1591
RpS25	967.5059
RpS4	933.3681
RpL37a	928.4275
RpS16	901.4197
RpS18	867.4302
RpS14b	861.6721
RpL15	854.0318
RpS13	829.8351
His2B	828.2815
Non3	760.2471
RpL17	759.1937
RpS30	750.9231
RpL27A	741.7728
RpLP0	735.4474
RpS29	731.5581
RpS15Aa	716.4542
RpS7	695.8705
RpL10Ab	695.6046
alpha-KGDHC	663.2561
RpL24	658.9813
RpLP2	637.7768
RpS3A	610.6709
RpL5	609.9853
muc	609.1646
CG11184	599.1047
CG1542	595.1175
CG13096	563.7109
mRpL40	558.4555
RpL11	552.7656
His4	539.5831
Srp9	530.783
RpS26	521.2311
dbe	516.977
His1	499.4166
RpL35	490.7422
eIF1A	478.6132
CG12288	470.0734
Ns1	467.4745
RpLP1	466.6296
Dmel\CG14210	464.4272
RpL34b	453.4091
RpS27A	449.0473
RpS20	445.5355
RpS3	427.6742
Vito	418.4081
RpL29	407.5364
mRpL1	405.1374
Nol1Nt	394.0978
CALML5	390.894
DCD	390.5271
Dmel\CG32409	380.609
HmgZ	365.3393
Rlb1	353.1256
Sf3b2	341.3157
Nop56	337.5255
alphaTub84B	336.5386
RpL38	314.1621
His2A	313.0415
Dmel\CG8939	307.201
Dmel\CG18178	307.1447
snf	304.3477
RpL12	302.4545
AspRS	299.7304
nop5	289.1328
bic	286.6453
RpS24	281.2655
CG3817	273.7796
RpS19a	268.1625
SRPK	241.2573
CG11583	231.7085
cype	229.112
Dmel\CG12909	226.801
Srp68	225.1732

RpS27	218.7012
Hrb27C	203.7357
CG7637	201.3772
B52	200.7227
RpL31	192.9968
Clbn	192.3928
RpS15	191.4082
Cam	191.2068
RpS5a	184.5906
shrb	182.6746
Surf6	179.1539
Nacalpha	175.8808
CG3902	174.3182
mRpL33	171.9965
ear	168.3458
KRT1	165.8786
CG1234	165.6871
Rs1	162.5962
lost	160.8793
Act57B	157.137
Dmel\CG17127	156.2176
mRpL55	152.4782
Ip259	149.0496
RpS17	146.0631
KRT9	144.2144
Ccp84Ae	139.6851
CG6693	138.1003
CG9630	136.089
Gs2	129.9049
Idh	129.8388
Neb-cGP	128.359
Nop60B	126.0488
sta	123.5995
Nap1	122.8808
alt	121.0933
Srp19	120.4658
unk	119.6585
Lsd-1	113.4449
Trp1	112.834
Ccp84Ag	112.2718
cg4806	111.0347
Dmel\CG14419	110.7528
AP-2mu	109.9451
His3	109.2973
JUP	109.0114
mRpL48	107.1994
Mtch	104.7452
CG5958	104.677
Dmel\CG13047	103.9903
Srp72	103.2998
Hsc70-4	100.8199
Rpn10	100.6684
snama	99.56808
G	99.46903
sea	99.40974
mRpL24	99.11284
Dmel\CG18294	98.94138
eIF2beta	98.40253
Rho1	97.71792
KRT72	96.45542
ppan	96.1343
Adh	95.72784
Cpr64Ad	95.27521
Rack1	95.07616
Hts	93.45392
bip2	92.23564
aralar1	90.41981
Dmel\CG11835	90.38766
Dmel\CG12128	85.85836
Dmel\CG16753	84.91504
EG:BACR19J1.2	83.06326
Dmel\CG18428	79.89546
Dmel\CG11180	79.39983
Ost48	77.6237
Tctp	76.50253
hoip	75.8114
Tm1	75.33695
CG3098	74.97361
Fib	71.00049
Top1	70.51015
Mlc1	70.05491
Tsr	69.57114
Nipsnap	69.46938
Rpt1	67.71429
Ran	66.82622
eIF4A	66.47186
Dmel\CG11370	66.03753
Pepck	64.89557
eIF5B	64.86217
CG9480	62.19343
Rpt6	62.18066
SsRbeta	61.30253
Ras85D	59.49233
mRpS5	58.69231
ATPsyndelta	55.7333
825-Oak	55.31354
Dmel\CG1703	55.18881
pAbp	53.88874
Jafrac1	53.58967
Rlip	51.84079
smt3	51.83798
Mpcp2	51.72097
Pgd	50.59326
UQCR-C2	50.56215
CG4038	50.48842
Dmel\CG10565	49.21209
Dmel\CG14095	46.56486
RpS21	45.80823
Tapdelta	45.78889
TpnC73F	45.67921
Gs1	44.54226
Cyt-c1	42.7037
Cyp4d1	42.44076
MetRS	42.43901
Gp93	41.45557
Pdhb	41.43075
Dmel\CG7920	41.2702
l(2)37Cc	40.76571
DSG1	40.14106
CkIIalpha	39.52395
ACC	38.88101
AGO2	38.79604
cora	38.74511
Rpt3	37.67865
Hsp23	37.29007
Arf79F	36.9376
Not1	36.60633
SmD2	36.0249
ValRS	35.6827

mRpL19	35.63403
mRpL4	35.29152
Ccp84Ad	35.13475
ATPsynD	34.1234
ND-B14.5B	34.12055
Taf2	33.85584
TRAM	33.10969
CG17896	33.00475
ND75	32.86735
Sply	32.31945
mRpS30	32.17747
UQCR-6.4	32.13721
mRRF1	31.68778
Mi-2	31.41313
ALB	30.22393
l(2)44DEa	29.6836
CCT2	29.64828
mRpL37	29.43681
CG14558	29.19258
CRIF	29.00247
SmB	28.04668
Rpt4	27.35389
KRT13	26.45702
COX7A	26.37058
CG9302	26.2804
mRpL51	26.03559
ND-20	25.78503
mRpL36	25.4505
mRpL44	24.99098
Neurochondrin	24.67214
l(2)01289	24.25771
Tom20	23.77822
Zw	23.46535
GstD1	23.07091
Mfe2	22.41785
COX4	21.90352
CkIIbeta	21.8384
eIF2gamma	21.79358
HBA	21.5068
RpL7-like	21.34229
CG6087	20.87972
ND-42	20.1952
GNBP3	19.75732

DSP	19.58798
Mtpalpha	19.43257
FK506-bp2	19.03329
IleRS	19.0248
CG5001	18.5935
Tina-1	18.47058
Chc	18.30199
Gdh	18.18502
Dmel\CG12493	18.14654
beta'COP	17.9901
CCT6	17.76662
Sec61alpha	17.57761
CCT1	17.09694
scu	16.97663
eIF4G1	16.97404
CG2691	16.8596
Dmel\CG17593	16.49218
Rpn11	16.48841
eIF2Bdelta	16.38786
FABP5	16.36088
Imp	16.29294
mRpL11	16.23933
eIF3a	16.04626
mRpL38	16.02364
Pfk	15.81199
Spn	15.74752
rump	15.59978
mRpL22	15.4958
Dmel\CG7946	15.1283
Myo31DF	15.00068
alphaCOP	14.98599
chic	14.88374
Msp300	14.81874
mt:CoII	14.38908
Nopp140	14.33445
Cyp9b2	14.30269
Dp1	14.17789
Pebp1	14.06543
mRpL12	14.03451
Pdha	13.94512
RpS12	13.79986
Pep	13.6099
Fatp1	13.55982

HRNR	13.36948
spidey	12.5372
EfTuM	12.10812
BcDNA:RE26528	12.09092
CG12262	12.06122
Aldh7A1	11.93381
CycT	11.79281
Desat1	11.66563
GlyS	11.62351
l(1)G0156	11.49243
Dmel\CG17597	11.34319
Dmel\CG9775	11.30775
Non1	11.28572
AsnRS	11.26337
mRpL2	10.9505
CG31123	10.89693
Got1	10.79406
Dmel\CG34163	10.79406
SdhC	10.59293
GluProRS	10.56499
ND-ASHI	10.45884
CG14500	10.43653
eIF2alpha	10.26218
eEF1delta	9.721359
bsf	9.654315
Rpt5	9.429673
CG12203	9.341444
Idh3b	9.252052
Dmel\CG2790	9.091829
CG2145	8.999034
eRF3	8.939181
Dmel\CG14961	8.594242
Dak1	8.581613
Dmel\CG7728	8.548892
SNF4Agamma	8.443521
SF2	8.343235
Stt3B	8.313438
CG5033	8.268742
CG4364	8.222868
Sc2	8.157002
Kap-alpha3	8.045263
ND-39	8.045263
Dmel\CG14564	7.955099

CCT5	7.884357
ND-49	7.877653
CCT8	7.765913
Non2	7.763678
ND-B17.2	7.732391
Fim	7.678478
l(2)01289	7.642999
ThrRS	7.638234
Nc73EF	7.575956
L2HGDH	7.294371
Cyp12a4	7.235149
peng	7.140171
CG9004	7.125824
hfp	6.838473
Col4a1	6.508717
eIF3k	6.257426
TFAM	6.168035
Dmel\CG10932	6.168035
gammaCOP	6.100991
Pmp70	6.091217
Cat	6.078643
CG11563	6.033947
slgA	5.9967
Ccp84Af	5.876945
ScsbetaA	5.773221
SdhA	5.765772
rush	5.73225
Dmel\CG7470	5.682765
LManV	5.631684
Dmel\CG3106	5.497596
colt	5.363508
Adk3	5.262943
Ge-1	5.231312
Gpat4	5.095333
zda	5.061811

Top2	5.04505
sls	5.011426
Pabp2	5.005941
AP-2a	4.953796
Dmel\CG17514	4.894201
BG:DS09217.1	4.871853
CG11030	4.842056
eIF3l	4.536634
Adk2	4.397587
ND-30	4.380199
eIF3e	4.317624
CG30122-RB	4.290807
Dmel\CG2685	4.290807
Dhc64C	4.275908
Dmel\CG4662	4.257285
Nnp-1	4.246111
SmD3	4.223763
betaCOP	4.201415
GC1	4.171618
Karybeta3	4.098614
eIF4E1	4.022631
Cyp12c1	3.992834
Cyp28a5	3.977935
Rab1	3.922066
GIP	3.892631
Sec63	3.888544
Ldsdh1	3.81405
PRDX2	3.791577
eRF1	3.754456
Dmel\CG7518	3.463933
Tps1	3.463933
BEST:GH15838	3.419237
Vha44	3.419237
dre4	3.402476
Eap	3.396889

Sec24CD	3.221585
Swim	3.128713
rgn	3.124585
clu	3.084017
l(2)k09913	3.069119
vig2	3.039321
Sar1	3.020029
Rtf1	2.994626
jar	2.961104
Rpn12	2.860538
CG7185	2.815842
Dmel\CG4069	2.793494
UGP	2.741349
Dmel\CG8888	2.581188
CG4415	2.532768
Muc68Ca	2.363964
Ufl1	2.346535
Khc	2.234795
Agpat3	2.190099
Gfat2	2.175201
CG9246	2.145403
Fip1	1.832532
l(2)gl	1.787836
Spt5	1.653748
Fdh	1.653748
Dek	1.642574
yrt	1.642574
Rexo5	1.542009
mask	1.525705
coro	1.206789
EG:25E8.1	0.847728
DSC1	0.75983
upSET	0.335219
DS02252.3	0.119189

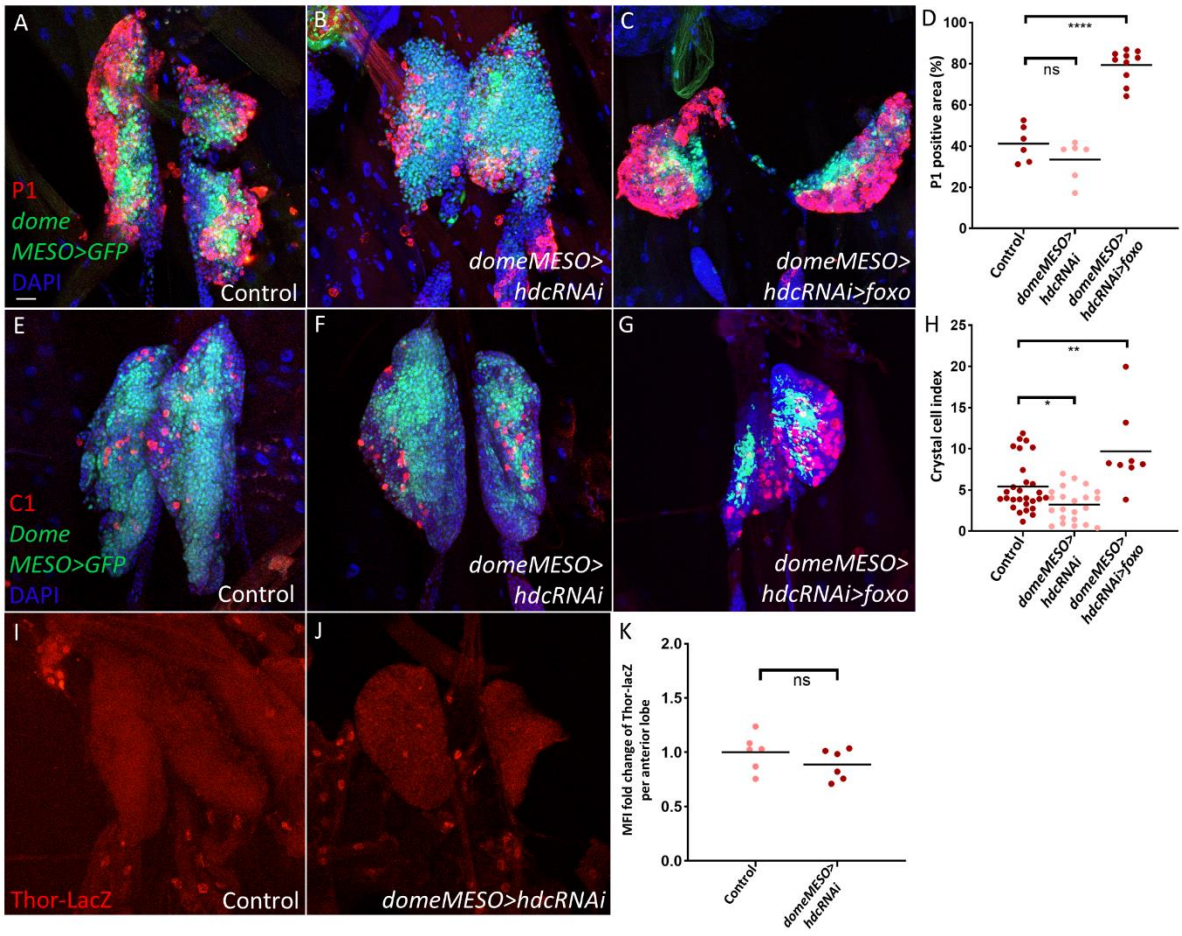

S1 Fig. The effect of *hdc* silencing in the MZ on plasmatocyte and crystal cell differentiation and *Thor-LacZ* reporter activity. (A-C) Silencing *hdc* in the MZ (*UAS-hdcRNAi/+; domeMESO-GAL4, UAS-2xEGFP/+*) does not affect P1 positive (plasmatocyte) area percentage per anterior lobe (average = 33%, number of lobes = 6) (B), while overexpressing *foxo* in *dome>hdcRNAi* larvae (*UAS-hdcRNAi/UAS-foxo; domeMESO-GAL4, UAS-2xEGFP/+*) significantly increases it (average = 79%, number of lobes = 10) (C) in comparison to the control (*domeMESO-GAL4, UAS-2xEGFP/+*) (average = 41%, number of lobes = 6) (A) (blue: nuclei, green: MZ, red: plasmatocytes). Scale bar: 20 μm. (D) A scatter dot plot showing P1 positive (plasmatocyte) area percentage per anterior lobe from the genotypes in the panels (A-C). Each dot in the graph represents one anterior lobe. Data were analyzed using ANOVA with Tukey's test for multiple comparisons, **** $p \leq 0.0001$, ns: non-significant. (E-G) Silencing *hdc* in the MZ (*UAS-hdcRNAi/+; domeMESO-GAL4, UAS-2xEGFP/+*) significantly reduces the crystal cell index (average = 3.2, number of lobes = 22) (F), while overexpressing *foxo* in *dome>hdcRNAi* larvae (*UAS-hdcRNAi/UAS-foxo; domeMESO-GAL4, UAS-2xEGFP/+*) significantly increases it (average = 9.7, number of lobes = 8) (G) in comparison to the control (*domeMESO-GAL4, UAS-2xEGFP/+*) (average = 5.4, number of lobes = 28) (E) (blue: nuclei, green: MZ, red: crystal cells). Scale bar: 20 μm. (H) A scatter dot plot quantifying crystal cell index from the genotypes in the panels (E-G). Each dot in the graph represents one anterior lobe. Data were analyzed using ANOVA with Tukey's test for multiple comparisons, * $p \leq 0.05$, ** $p \leq 0.01$. (I-J) Silencing *hdc* does not affect the transcription of *Thor* as detected by an anti-lacZ staining for the *Thor-lacZ* reporter

(*UAS-hdcRNAi/+; domeMESO-Gal4/Thor-lacZ*) (number of lobes = 6) (J) in comparison to the control (*domeMESO-Gal4/Thor-lacZ*) (number of lobes = 6) (I) (red: Thor-LacZ). Scale bar: 20 μm. (K) A Scatter dot plot showing fold change in MFI of Thor-LacZ per anterior lobe of (*UAS-hdcRNAi/+; domeMESO-Gal4/Thor-lacZ*) larvae (average = 0.8) compared to the control (*domeMESO-Gal4/Thor-lacZ*) (average = 1). Each dot in the graph represents one anterior lobe. Data were analyzed using two-tailed unpaired student's t-test, ns: non-significant.